Efficiency of Functional Brain Networks

Thesis
presented to the Faculty of Arts
of
the University of Zurich

for the degree of Doctor of Philosophy
by
Nicolas Langer
of Zurich, Switzerland

Zurich, 2012

Accepted in the spring semester 2012
on the recommendation of
Prof. Dr. Lutz Jäncke
Prof. Dr. Christoph Michel

Acknowledgements

Many people contributed to this work and I want to thank all of them. They have been of so much help at various stages of this doctoral thesis project.

My first thanks go to my mentor Prof. Dr. Lutz Jäncke, who firstly attracted my attention for neuroscience. Moreover he gave me the opportunity to learn different brain research methods, including electroencephalography (EEG) and magnetic resonance imaging (MRI). I am very grateful for having got the change to acquire practical and theoretical knowledge of these different methods and to work in the fascinating field of human brain research. I also thank Prof. Dr. Lutz Jäncke for his supportive scientific supervision, stimulating discussions, for his positive and constructive criticism of my ideas.

I wish to express my thanks to the members of my dissertation steering committee of the Neuroscience Center Zurich (ZNZ), Prof. Dr. Lutz Jäncke, Prof. Dr. Christoph Michel and Dr. Jürgen Hänggi.

I also want to thank all co-workers of the department of Neuropsychology at the University of Zurich for instrumental and emotional support. In particular Dr. des. Andreas Pedroni and Dr. Jürgen Hänggi for providing tremendous support at the application of the complex neuroimaging methods and the challenging discussions about different analysis strategies. Furthermore I would like to thank Prof. Dr. Christoph Michel for giving me insights in the newest EEG analysis techniques, learning from his EEG expertise and for his positive and constructive criticism of my work. I thank Dr. Roberto Pascual-Marqui for developing sLORETA, the data analysis as is would not have been possible without it.

My thanks also go to my collaborators during the different studies of my dissertation project. In experiment 1, I would express my thanks to Dr. Lorena Gianotti and Prof. Dr. Daria Knoch, who provided a lot of support. In experiment 2, in particular Claudia von Bastian, who implemented and supervised the working memory training and done all the extensive administrational work and Dr. Prof. Klaus Oberauer for the constructive collaboration.

This thesis would not have been completed without emotional support from my family and friends; especially I would like to thank Michèle Hubli for supporting me with a lot of love.

Original research articles included in this doctoral thesis

Experiment 1:

Langer, N., Pedroni, A., Gianotti, L.R.R., Hänggi, J., Knoch, D., Jäncke, L. (2011). Functional Brain Network Efficiency Predicts Intelligence. Human Brain Mapping. doi: 10.1002/hbm.21297.

Experiment 2:

Langer, N., von Bastian, C., Wirz, H., Oberauer, K., Jäncke, L. (2012). The Effects of Working Memory Training on Functional Brain Network Efficiency. (submitted).

Experiment 3:

Langer, N., Pedroni, A., Jäncke, L. (2012). The Problem of Thresholding in Small-World Network Analysis. (submitted)

Table of contents

I. Summary

Our perceptions, thoughts and experiences are the product of dynamic interactions occurring between functionally specialized regions of the brain. Thus, a complete understanding of such phenomena will by only possible once we understand how these interactions are organized and coordinated. The present thesis focuses on functional brain connectivity in the context of graph-theoretical network analysis to investigate so-called small-world networks. Recent studies have shown that functional and anatomical connections of the brain network are organized in a highly efficient small-world manner. A small-world organization of the brain network implies a high level of local neighborhood clustering combined with global efficiency or information transfer. Thus small-world networks explain how the brain minimizes wiring costs while simultaneously maximizing the efficiency information propagation. In the last then years, there's an increasing interest in modeling the human brain network, because they provide a simplified view on a complex system as the brain is. The fundamental motivations for graph theory as a method of brain network analysis are its relative simplicity, high degrees of generalizability and interpretability.

In the first experiment of this thesis, the main purpose was to identify whether individual differences in cognitive functions, such as intelligence, are associated with differences in small-world characteristics of functional networks based on resting-state electroencephalography (EEG) data. High-density resting state EEG was recorded in 74 healthy subjects to analyze graph-theoretical functional networks at an intracortical level. The results showed the more intelligent the subjects are the more the functional network in the alpha2 frequency spectrum

resembles a small-world network. Closer inspection of the hubs and nodes of the identified network revealed a parieto-frontal network that is associated with higher intelligence. This is the first study that substantiates the neural efficiency hypothesis as well as the parieto-frontal integration theory of intelligence in the context of functional brain network characteristics.

The aim of second experiment was to increase the intelligence and working memory performance by an intensive working memory training and shifting the underlying functional brain networks towards more small-world topology. A double-blinded study was conducted, where 66 young adults were trained, one half of the subjects practiced three working memory tasks and were compared to an active control group practicing task with low working memory demand. There were three main findings in this study. Firstly, training of working memory tasks increases the performance in these tasks and in near transfer effects, but not in psychometric intelligence performance. Secondly, theta frequency in the resting EEG plays an important role in working memory performance and could be increased by an intensive working memory training. Thirdly, the better the working memory performance the more the functional networks exhibit small world topology and working memory training shifts the networks towards more small-worldness.

In the third experiment, the usage of thresholds in graph-theoretical network analyses was analyzed. The common course of analysis is to compare small-world parameters between two groups using classical inferential statistics. This approach becomes problematic, when using connectivity measures of inter-subject correlations (i.e. structural MRI and DTI, when only using FA-values). Since for each voxel, there is only one data point, a measure of connectivity can

only be computed for a group. To empirically determine an adequate small-world network threshold and to generate the necessary dispersion of measures for classical inferential statistics, samples are generated by thresholding the networks on group level over a range of thresholds. There are mainly two problems with this approach. First, the number of thresholded networks is arbitrary. Second, the obtained thresholded networks are not independent samples. Potential consequences of this methodological issues were demonstrated in two examples. Consequently alternative approaches are presented potentially overcoming these methodological issues.

II. Zusammenfassung

Unsere Wahrnehmungen, Gedanken und Erfahrungen sind das Produkt dynamischer Interaktionen zwischen unterschiedlichen spezialisierten funktionellen Hirnregionen. Deshalb, ist ein vollständiges Verständnis solcher Phänomene nur möglich, wenn wir verstehen, wie diese Interaktionen organisiert und koordiniert sind. Die vorliegende Dissertation legte ihren Fokus auf neuronale Netzwerke im Kontext von graphentheoretischen Netzwerkanalysen, um so genannte Small-World Netzwerke zu untersuchen. Vorgängige Studien haben gezeigt, dass sowohl funktionelle wie auch strukturelle Verbindungen im Gehirn eine sehr effiziente Small-World Charakteristik aufweisen. Small-World Netzwerke sind gekennzeichnet durch eine hohe Effizienz der lokalen und globalen Informationsverarbeitung. Dies bedeutet, dass in den Netzwerken eine Segregation der Informationsverarbeitung stattfindet, welche durch Cluster repräsentiert wird. Gleichzeitig aber sind die Cluster untereinander effizient verknüpft, was eine effiziente Integration der Informatiosverarbeitung darstellt. In den letzten zehn Jahren entstand ein zunehmendes Interesse neuronale Netzwerke mittels Modellen darzustellen. Dies ist wohl darauf zurückzuführen, dass Modelle eine vereinfachte Sichtweise auf komplexe Systeme (Bsp. das Gehirn) ermöglichen. Die Hauptmotivation für graphenthoeretische Netzwerkanalysen sind die relative Einfachheit, der hohe Grad an Generalisierbarkeit und Interpretierbarkeit.

Im ersten Experiment der vorliegenden Dissertation wurden die neuronalen Mechanismen von individuellen Differenzen in der Intelligenzleistung untersucht. Das Ziel der Studie war es neuronale Netzwerkcharakteristiken zu indentifizieren

und ihre Beziehung zur Intelligenzleistung zu untersuchen. Dafür wurde der Ruhezustand des Gehirns von 74 gesunden Probanden mittels Elektroencephalographie (EEG) gemessen. Anschliessend wurden mittels graphentheoretischer Netzwerkanalyse im intrakortikalen Raum die Netzwerkeigenschaften untersucht. Es zeigte sich, dass die neuronalen Netzwerke im Alpha2 Frequenzbereich von intelligenteren Versuchspersonen erhöhte Small-World Eigenschaften aufweisen. Eine genauere Betrachtung der Hubs und Knoten innerhalb des Netzwerks zeigte, dass ein parieto-frontales Netzwerk mit erhöhter Intelligenz assoziiert werden kann. Dies ist die erste Studie, welche die neuronale Effizienz Hypothese, sowie die parieto-frontale Integrations-Theorie im Kontext von neuronalen Netzwerken bestätigt.

Das Ziel des zweiten Experiments war es die Intelligenz- und Arbeitsgedächtnisleistung mit einem intensiven Arbeitsgedächtnistraining zu erhöhen. Ausserdem sollten sich durch das Arbeitsgedächtnis die neuronalen Netzwerke so verändern, dass diese mehr Small-World Eigenschaften aufweisen. Es wurde eine doppelblinde Studie durchgeführt, in welcher 66 junge Erwachsene trainiert wurden. Die Hälfte der Versuchspersonen trainierten drei verschiedene Arbeitsgedächtnisaufgaben und wurden mit einer aktiven Kontrollgruppe verglichen, welche Aufgaben trainierten, die das Arbeitsgedächtnis nicht beanspruchten. Es gab drei Hauptbefunde in dieser Studie. Erstens zeigten die Versuchspersonen nach dem Arbeitsgedächtnistraining eine erhöhte Arbeitsgedächtnisleistung. Jedoch zeigte sich keine Verbesserung in der Intelligenzleistung. Weiter konnte gezeigt werden, dass das Theta-Frequenzband im Ruhe-EEG eine wichtige Rolle für die Arbeitsgedächtnisleistung spielt und durch ein intensives

Arbeitsgedächtnistraining erhöht werden kann. Zuletzt zeigte sich, je besser die Arbeitsgedächtnisleistung, desto mehr weisen die neuronalen Netzwerke Small-World Eigenschaften auf. Zudem verschiebt das Arbeitsgedächtnistraining die Organisation neuronaler Netzwerke in Richtung erhöhter Small-World Topologie.

Im dritten Experiment wurde die Verwendung von Schwellenwerten bei Netzwerkanalysen kritisch begutachtet. Im Allgemeinen werden mittels klassischer inferentieller Statistik die Small-World Parameter zwischen zwei Gruppen verglichen. Dieses Vorgehen kann problematisch werden, wenn man Konnektivitätsmesswerte verwendet, welche auf interindividuellen Korrelationen basieren (Bsp. bei strukturellen MRT und DTI, wenn nur die FA Werte verwendet werden). Da pro Voxel und Versuchsperson nur ein Datenpunkt zur Verfügung steht, kann die Konnektivität nur über die ganze Gruppe berechnet werden. Um statistisch einen adäquaten Small-World Schwellenwert zu bestimmen und um die für die klassische inferentielle Statistik benötigte Verteilung von Datenpunkten zu generieren, werden verschiedene Schwellenwerte auf die Netzwerke angewendet. Dieses Vorgehen beinhaltet zwei grundlegende Probleme: Erstens ist die Anzahl der Schwellenwerte arbiträr. Zweitens, sind die Netzwerke mit unterschiedlichen Schwellenwerten nicht unabhängig voneineder und können deshalb nicht als unabhängige Untersuchungseinheiten verwedent werden. Anhand von zwei Beispielen werden die möglichen Konsequenzen der Verwendung von multiplen Schwellenwerten und die Abhängigkeit der Netzwerke mit unterschiedlichen Schwellenwerten aufgezeigt. Zum Schluss werden alternative Analyseverfahren vorgestellt, welche diese methodischen Probleme bewältigen.

2. Brain Networks

2.1. Introduction

Our perceptions, thoughts and experiences are the product of dynamic interactions occurring between functionally specialized regions of the brain. Thus, a complete understanding of such phenomena will only be possible once we understand how these interactions are organized and coordinated. We know since the 19th century that the brain constitutes an effectively structural network (Cajal, 1995; Swanson, 2003). Since the 20th century it has been accepted in the broad scientific community that this structural network is the basis of dynamic emergence of coherent physiological activity, such as electrophysiologic oscillations, that can cross the spatially distinct brain areas that form a functional network (Fries, 2005; Singer, 1999). Therefore networks provide the physiological basis for information processing. In this thesis the focus is set on graph theoretical analysis to investigate functional small-world networks that could offer a powerful approach to quantify brain networks.

2.2. Brain Connectivity

In the highly evolved central nervous system, brain connectivity can be characterized at several scale. On a microscopic level synaptic connections link individual neurons, whereas fibre tracts connect brain regions at a macroscale level. A central property of every network is its connectivity. Neural networks

could be distinguished between different kinds of connectivity. In the following section the different modes of brain connectivity will be briefly presented.

2.2.1. Structural Connectivity

Structural or anatomical connectivity refers to the presence of physical connections between neurons or brain regions. Analyses of structural connectivity show that the cerebral cortex is comprised of clusters of densely and reciprocally coupled cortical areas that are globally interconnected (Sporns, 2010). Structural connections are relatively stable at shorter time scales (seconds to minutes). At longer time scales (hours to days), anatomical connections have the capacity to adapt to changing demands. This is well described in the brain plasticity literature (Imfeld, et al., 2009; Schlaug, et al., 2009; Scholz, et al., 2009) and was recently shown by one of our studies, which demonstrates morphological changes of the corticospinal tract due to limb immobilization after unilateral arm injury (Langer, et al., 2012). Anatomical connectivity could be analyzed with Diffusion Tensor Imaging and invasive tracing methods.

2.2.2. Functional Connectivity

Functional connectivity could be defined as statistical dependencies between spatially separated neurophysiological events among cortical regions (Friston, et al., 1993). Statistical dependencies may be estimated by measuring correlation or covariance, spectral coherence or phase-locking. These measures could be obtained on a microscopic level with intracortical microelectrodes arrays measuring spiking activity. In human brain studies investigating functional connectivity with electroencephalography (EEG), magnetoencephalography (MEG) or functional magnetic resonance imaging (fMRI), are generally used.

Mostly functional connectivity is calculated between all elements of a system, regardless of whether these elements are connected by direct structural links. Functional connectivity is highly time-dependent and can fluctuate on multiple time scales, some within tens or hundreds of milliseconds as measured with EEG. This functional coupling is present during the processing of cognitive tasks and it is even present during rest (Jann, et al., 2010; Laufs, 2008). The idea of functional connectivity goes back to the Hebbian learning that postulates "neurons that fire together wire together" (Hebb, 1949). The computational concept of functional connectivity has its origin in the analysis of multiunit recordings of discrete neuronal spikes, recorded simultaneously from different brain areas (Gerstein and Perkel, 1969). Temporal coherence among the activity of different neurons could be measured by cross-correlation of their spiking activity. This could be then interpreted as functional connectivity. But functional connectivity is not an invariant constitution. Functional connectivity can be changed in the course of learning (McIntosh, et al., 2003), stimulation-induced cortical reorganization (Rounis, et al., 2006), and neuroplasticity (Canals, et al., 2009). Studies of functional connectivity have demonstrated that functional brain networks exhibit small-world attributes. The small-world networks based on functional connectivity will be the main topic of this doctoral thesis. Interregional coupling as measured in the experiments of this thesis allow to investigate reconfigurations of functional interactions as a function of cognitive processes and adaption to environmental demands (Bassett, et al., 2006). In contrast to effective connectivity, functional connectivity does not make any explicit statement about directionality of the connection or the information flow.

2.2.3. Effective Connectivity

Effective connectivity specify the causal influence among neurons or neuronal populations (Friston, 1994). Probably the first evidence for effective connectivity was presented by Kaminski and Blinkowska, who described effective connectivity based on partial directed coherence measures and autoregressive models (Kaminski and Blinowska, 1991). Another possibility to demonstrate a causal influence is through systematic manipulation of the network. This could be done by lesion studies in animals, where a perturbation of a region can have influence on other regions. In human studies transcranial magnetic stimulation (TMS) or transcrial direct-current stimulation (tDCS) can manipulate the function of a brain area, which further can cause a reaction in an associated brain region and would prove the effective connectivity between the two regions. Another possibility to analyze causal influence is time series analysis. Since causes must precede effects in time, time series analysis are a powerful method in neuroscience to investigate effective connectivity. There are several approaches for extracting effective connectivity. Some require the assumption of models (i.e. Dynamic Causal Modeling, Structural Equation Modeling), whereas other techniques are rather "model-free", for example Granger causality. Recent discussions arise that using Granger causality in fMRI can be biased, since the time-resolution (sub sampling problem) and the filtering methods (hemodynamic response can mess up the dynamic interaction) in fMRI can elicit false result. For further details about this issue and different network modeling methods see (Smith, et al., 2011).

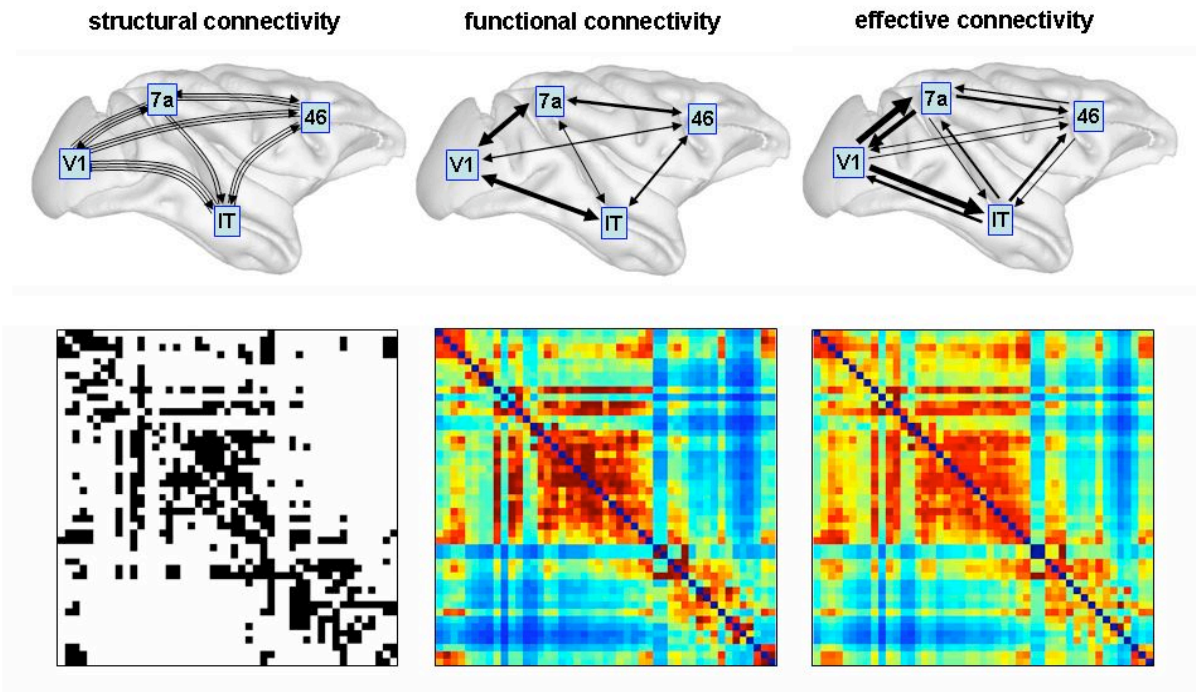

Figure 1. Displayed are the different connectivity forms of brain networks. The arrows in the illustrations in the top show fiber tracts in structural connectivity, correlations in functional connectivity and the information flow in effective connectivity between different brain regions in macaque cortex. Connectivity matrices at the bottom display binary structural connections (left), weighted symmetric functional connections (middle) and non-symmetric weighted information flow (right) (Sporns, 2010).

2.2.4. The Relationship between Structural and Functional Connectivity

When studying the brain networks, the questions arise how structural and functional connectivity is related to each other? In what ways does structure predicts function in the human brain? Does "structure" determines "function"? The structural networks seem to shape neural dynamics (Honey, et al., 2010). There are several studies, which have performed a combined analysis of structural and functional connectivity, which are reviewed in (Damoiseaux and Greicius, 2009). Most studies report high correlations between the strengths of structural and functional connectivity across the entire cerebral gray matter (Hagmann, et al., 2008; Honey, et al., 2009; Skudlarski, et al., 2008), although functional networks are likely to be denser than anatomical networks, as they

will typically contain numerous connections between anatomically unconnected regions (Damoiseaux and Greicius, 2009).

However, Honey and colleagues also advert that the amount of association between structural and functional connectivity is depending on spatial and time resolution of the neurophysiological data (Honey, et al., 2009). Moreover there are studies suggesting that changes in functional connectivity can occur in the course of spontaneous activity, even while structural connectivity remains unaltered (Honey, et al., 2007).

Taken together, these studies support the idea that the presence of structural connections are predictive of the presence and strength of functional connectivity, although further studies should provide a clearer understanding of the relationship between structure and function in the human brain.

2.3. Brain Graphs

2.3.1. Introduction

In the last ten years, there's an increasing interest in modeling the human brain network with brain graphs, because they provide a simplified view on a complex system as the brain is. A brain graph is a model of the brain as a number of nodes interconnected by a set of edges (Bullmore and Bassett, 2011). For example, the edge can represent functional or structural connections between cortical or subcortical regional nodes, based on analysis of human neuroimaging data. Recent studies have shown that the functional and anatomical connections of the brain network are organized in a highly efficient small-world manner (i.e. (Bullmore and Sporns, 2009; Sporns and Kotter, 2004; Stam and Reijneveld,

2007). A small-world organization of the brain network implies a high level of local neighborhood clustering (indexed by the clustering coefficient) combined with global efficiency of information transfer (indexed by the path length) (Bullmore and Sporns, 2009). Thus, the small-world networks explain how the brain minimizes wiring costs while simultaneously maximizing the efficiency of information propagation (Achard and Bullmore, 2007; Kaiser and Hilgetag, 2006; Sporns, et al., 2004). In order to mathematically describe small-world networks, graph-theoretical analysis techniques are generally used (Bullmore and Sporns, 2009), which are abstract representations of networks consisting of sets of nodes linked by edges.

"The origin of graph-theory goes back to the 18th century. Euler showed that it was impossible to traverse the city of Königsberg's seven bridges across the river Pregel exactly once and return to the starting point. To prove this conjecture, Euler represented the problem as a graph, and his original publication (Euler, 1736) is generally taken to be the origin of graph-theory" (Bullmore and Sporns, 2009). Later Erdös and Renyi discovered additional graph-theoretic concepts (Erdös and Rényi, 1959).

Small-world networks analyzed by graph-theory are not unique to the human brain, as it has been found in a wide range of complex systems and different scales. For example on a microscopic level in gene-gene interactions or the Caenorhabditis elegans, but also on macroscopic levels as the World Wide Web, the transport system or the ecosystem (Barabasi, 2009). However, graph-theory is based on a number of assumptions (e.g. nodes are independent and internally coherent). Such constraints and simplifications inevitably cause loss of

information, but they are accompanied with a high extent in generalizability and interpretability. Graph-theoretical analysis could probably be applied to almost any modality or scale of neuroscientific data (Bassett and Bullmore, 2009; Bullmore and Sporns, 2009; Sporns, 2010). Functional brain graphs have been created from EEG (Langer, et al., 2011; Stam, et al., 2007a), fMRI (Achard, et al., 2006; van den Heuvel, et al., 2009) and MEG (Deuker, et al., 2009; Stam, et al., 2009) data. Moreover, graph-theory on structural data has been shown with DTI (i.e. (Hagmann, et al., 2008) and anatomical MRI data (Hanggi, et al., 2011; He, et al., 2007). However, there are some caveats when using graph-theory on structural data, which are explained in the third experiment of the present thesis. This level of generalizability raises the possibility to compare the graph measures between structural and functional networks as they are described in the section 2.2.4. in this thesis.

The interpretability of neuroimaging data is or at least should be always the ultimate aim of each neuroscientific study. “The translation of modality-specific connectivity statistics to topological measures on brain graphs may help us to find more secure cognitive and clinical interpretations of neuroimaging systems“ (Bullmore and Bassett, 2011). Although this is a precarious statement, there are independent studies with different neuroimaging methods, which showed associations between higher cognitive performance and brain network efficiency (Langer, et al., 2011; Li, et al., 2009; van den Heuvel, et al., 2009).

2.3.2. What is a Node?

The constitution of a node within a brain network has to be specified by the

researcher and is depending on neuroimaging method, anatomical parcellation schemes, and connectivity measures (Rubinov and Sporns, 2010). The set of nodes has to be carefully selected and determines largely the connection and therefore also the interpretation of the brain networks (Butts, 2009).

For the instance of interpretability nodes should represent brain regions and are suppose to be inherently independent within the system. The relationship between two nodes is not meaningful when the nodes are too similar to each other. Think about smoothed voxel, which will have by definition similar data content, because the spatial smoothing filter induces similar activity to increase the signal to noise ratio (but also to induce a normal distribution in the data and to adjust the expected size of cluster). However, the spatial smoothing causes that the interaction between neighboring voxels are not only physiological but also artificially produced by the spatial smoothing. On other hand parcellation schemes that link heterogeneous brain regions into a single node might be meaningless as well.

On a microscopic level, each neuron can be considered as individual node, and the synapses would then build the edges as it was done in the Caenorhabditis elegans (Watts and Strogatz, 1998). The Caenorhabditis elegans is so far the only organism for which the brain graph is completely described (about 300 nodes and 7600 edges). On a macroscopic level, nodes are usually defined by anatomically defined template maps. An immense advantage of using an anatomical templates as Brodmann areas or the Automated Anatomical Labeling (AAL) atlas is that different networks of different studies, even functional and structural networks, could be directly compared. So fMRI, structural MRI, and DTI data most often use one of these template maps. The disadvantage of this

template maps is that the regions can vary extremely in the size (number of voxel within a nodes). Therefore, there emerge new approaches to define nodes, which deal with a data-driven approach to define the nodes (Zalesky, et al., 2010).

Most studies defined the electrodes as nodes for brain graphs based on data obtained with microelectrodes on cortical tissue, surface sensors in MEG, as well as scalp map electrodes recordings in EEG (Micheloyannis, et al., 2006b). This can cause strong correlations between neighboring electrodes due to volume conduction of electrical activity from a single source to multiply nearby electrodes on the scalp surface, which can confound the results of the graph-theoretical analysis (Stam, et al., 2007b). A better approach is to reconstruct the sources and define each source as a node, as it was done in this doctoral thesis and other studies (De Vico Fallani, et al., 2010; Palva, et al., 2010a; Palva, et al., 2010b). Thus, the volume conduction problem can be circumvented, but one should be careful, since some source reconstruction algorithms, such as beamformer, solve the inverse problem by estimating sources as statistically independent from each other, which is obviously not optimal for network analyses (Cheyne, et al., 2006).

2.3.3. What is an Edge?

An edge represents in neuroscience the connection between two brain regions or synapses on a microscopic level. Edges are distinguished on the basis of their weight and directionality. There could be binary links, which only describes the presence or absence of connections, while weighted links also contain information about connection strengths (Rubinov and Sporns, 2010). The weights in structural network may correspond to the size or density of

anatomical tracts, whereas weights in functional and effective networks could represent particular degrees of correlations or causal interactions. In functional connectivity statistic measures, an edge represents the extent to which two processes behave similarly over time, whereas in effective connectivity edges reflect statistics measures the extent to which one process can be predicted or explained by the other (Bullmore and Bassett, 2011). For effective networks directional edges are needed. Unfortunately, current neuroimaging methods are unable to directly detect anatomical or causal directionality, as tracts contain mostly reciprocal connections (Brodal and Walberg, 1982; Zarei, et al., 2007), which on the other hand provide some validity for the use of undirected networks.

In practice there is no unique answer to legitimate the choice of edges and they are highly dependent on the conditions of acquisition and preprocessing. There is an extensive literature about measuring the connectivity in fMRI, where mostly low-frequency <0.1 Hz are of particular interest. Since the focus of this thesis is on electrophysiological data and functional connectivity, the interested reader should refer to the extensive review (Smith, et al., 2011) for connectivity measures based on fMRI.

But also when using electrophysiological data many measures of associations could be used. One should always consider the advantages and disadvantages of the method chose for the analysis. Some measures are sensitive to associations between nodal times series, whereas wavelet correlations (Bullmore, et al., 2004) or coherence (De Vico Fallani, et al., 2010; Pascual-Marqui, 2007b) works in the frequency domain. In this thesis, we used a coherence measure, which operates in the frequency domain and takes the cross-spectrum and divided it by the product

of two corresponding auto power spectra. For further details please see (Langer, et al., 2011; Pascual-Marqui, 2007b) or the method section of experiment 1.

If the connectivity matrix is estimated, the next crucial question is, what type of graph should be analyzed. Most investigators use a correlation matrix, and then apply a particular or multiple thresholds to each element of the connectivity matrix. If the value within the element of the correlation matrix exceeds the threshold, the corresponding element of the correlation matrix is set to unity in binary networks or remains constant in weighted networks. Otherwise, if the value within the element fall below the threshold, the value is set to zero, which denoted no connection between the two nodes. The thresholding operation will define the edges in the connectivity matrix and have therefore strong influence on the network topology. There are two general approaches for thresholding. One can search for a single or (a kind of) optimal threshold and use this particular threshold to the connectivity matrix (Achard, et al., 2006; He, et al., 2007). On the other hand many thresholds at many different values can be chosen (Bassett, et al., 2008).

Applying increasing thresholds gradually will result in a monotonically, but not necessarily linearly, decreasing connection density of the graph. Threshold values are often arbitrarily determined and can bias the results of the graph-theoretical analysis as is described in experiment 3. However, there's a need of future developments to deal with the thresholding problems and also quantify the role of negative weights in brain networks.

2.3.4. Measures of Graphs

Once a brain network has been constructed the properties can be quantified by a

rich collection of metrics that has been developed to describe the network topology. As explained in section 2.3.1., a small-world organization denotes a high level of local neighborhood clustering combined with global efficiency of information transfer in comparison to random networks (Bullmore and Sporns, 2009). Consequently, the significance of small world topology should be established by comparison with simple random or ordered topologies but preserve basic characteristics of the original network. The most commonly used null-hypothesis network has a random topology but shares the size, density and binary degree distribution of the original network (Maslov and Sneppen, 2002; Rubinov and Sporns, 2010; Watts and Strogatz, 1998). A small world network is arranged between a random and a regular network. In regular networks each node is connected to its neighbor and thus has a high clustering coefficient but also a long path way, whereas random networks have a low clustering coefficient and a short characteristic path length (Figure 2). In the following section these different measures will be briefly described.

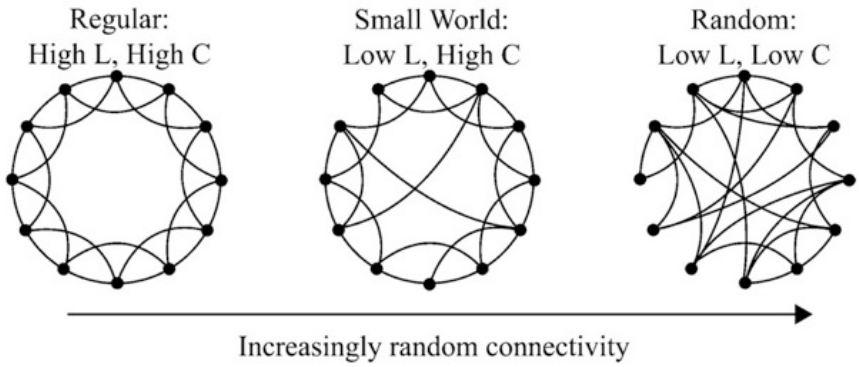

Figure 2. Displayed are a regular, a small-world and a random network. C stands for clustering coefficient and, whereas L stands for characteristic path length (Watts & Strogatz, 1998).

By the definition of small-world topology, there are segregated clusters present in the network. Thus suggesting a functional integration and segregation, which is very plausible in the model of how the human brain operates. Therefore this thesis will consequently distinguish between measures of functional integration and segregation. All used formulas for the applied measures are found in the Appendix of the thesis.

2.3.4.1. Measures of Functional Segregation

The most prominent measure of functional segregation is the "clustering coefficient", which is given by the ratio of the number of closed triplets to the total value of triplets and provides information about the level of local connectedness within a network (Watts and Strogatz, 1998). In other words, the cluster coefficient is the ratio between the number of connections between the direct neighbors of a node and the total number of possible connections between these neighbors. The mean clustering coefficient over the entire network hence reflects the quantity of the prevalence of clustering in the network.

A very similar measure to the clustering coefficient is the "transitivity", which is normalized collectively, whereas the clustering coefficient is normalized for each individual node separately (Newman, 2006). A more global measure of functional segregation is the "modularity" and is denoted to the subdivision of the networks into groups of nodes, with a maximum of possible within group connections and minimally possible between group connections (Girvan and Newman, 2002). In contrast to most other graph measures, the optimal modular structure is estimated, rather than computed exactly (Danon, et al., 2005).

2.3.4.2. Measures of Functional Integration

Functional integration could be understood as the ability to combine information

from segregated brain regions and the global efficiency of information transfer. The most commonly used measure of functional integration is the characteristic "path length" of a network and is given by the average number of connections that have to be crossed to travel from each node to every other node in the network (Watts and Strogatz, 1998).

Taken together, small-world organized networks are characterized by a clustering coefficient that is higher than the clustering coefficient of a randomly organized network, but still with a short characteristic path length that is similar to that of an equivalent random network (Humphries and Gurney, 2008; Humphries, et al., 2006; Watts and Strogatz, 1998). Formally, small-world networks show a ratio γ defined as clustering $\text{coefficient}_{real}$ / clustering $\text{coefficient}_{random}$ of >> 1 and a ratio λ defined as path length_{real} / path length_{random} of ~ 1 (Humphries and Gurney, 2008; Sporns and Zwi, 2004; Watts and Strogatz, 1998). A high γ reflects a high level of local neighborhood clustering within a network and a short travel distance λ expresses a high level of global communication efficiency within a network (Bullmore and Sporns, 2009; Sporns, et al., 2004; Watts and Strogatz, 1998).

2.3.4.3. Centrality Measures

Probably the simplest measure within graph theory is the "degree". The degree of a node is defined by the number of connections to that particular node. The sum of all degrees of all nodes in the network is equal to the total number of edges within the network, which is another measure of the network. (N*(N-1))/2 are the maximum number of edges that could exist, which means that each node is connected to all other nodes. The average of all degrees is used as a measure of

density, or the total "wiring cost" of the network (Rubinov and Sporns, 2010). Degree is often used to describe, which nodes within the network act as hub regions or play a key role within the network. However, there are additional centrality measures. For instance "closeness centrality", which is described as the inverse of the average shortest path length from one node to all other nodes in the network (Rubinov and Sporns, 2010). A similar measure is "betweenness centrality" and is denotes to the portion of all shortest paths in the network that pass through a given node (Sporns, 2010). Nodes with a high betweennness centrality serves as bridging nodes that connect disparate parts of the network.

2.3.5. Applications and Clinical Relevance

Although the concept of small-world networks in the human brain is novel, there's a formidable amount of studies, which investigated small-world networks in different domains, including age (Meunier, et al., 2009; Micheloyannis, et al., 2009), gender (Gong, et al., 2009), cognitive ability (Langer, et al., 2011; Li, et al., 2009; van den Heuvel, et al., 2009) and genetics (Smit, et al., 2008). To illustrate here the results would exceed the amount of space provided in this thesis. Taken together, the literature of the healthy population highlights that a higher cognitive performance is accompanied with increased small-world topology. However, network analyses are also increasingly used in clinical science. Many cognitive and emotional disorders are described as a dysconnectivity syndrome (Catani and ffytche, 2005), which is defined by an abnormal anatomical and/or functional connectivity between brain regions. In schizophrenia, for example, a disconnection between frontal and temporal cortices has been proposed (Friston and Frith, 1995). In fact there are several studies, which demonstrated a

disturbed brain network in schizophrenic patients (Bassett, et al., 2008; Micheloyannis, et al., 2006a; Rubinov, et al., 2009). A hyperconnectivity within the frontal cortices and a hypoconnectivity between the frontal and the rest of the brain was suggested in people suffering from autism (Courchesne and Pierce, 2005) and also could have been demonstrated by neuroimaging data (Murias, et al., 2007). Moreover, there are several studies investigating small-world network of neurological disorders as Alzheimer's disease (He, et al., 2008; Stam, 2010; Supekar, et al., 2008), stroke (de Vico Fallani, et al., 2009) and epilepsy (Horstmann, et al., 2010; Raj, et al., 2010). Together, these studies highlight the comprehensive clinical significance of brain network analysis of human neuroimaging data.

2.3.6. Conclusions

In the last ten years network analyses in the context of graph theory have rapidly growing in the field neuroscience. These approaches can provide fundamental insights into complex systems as the human brain by providing simple but powerful models of the brains structural and functional network. The study of brain connectivity has already opened new experimental and theoretical concepts in neuroscience. Connectivity plays a crucial role in neuroanatomy, electrophysiology, functional brain imaging and is the neural basis of cognition. However, like all other approaches in neuroscience, the results of brain network analysis are depending on premises. Future work will further increase the methodological development of brain network analyses in order to clarify and simplify the complexity of the human brain.

3. Neural Basis of Intelligence and Working Memory

In the present section, the main theories of the neural basis of intelligence and working memory will be presented with a specific focus on brain network analyses. In experiment 1 of this dissertation we investigated, if functional brain efficiency based on resting state EEG data can predict the performance in an intelligence task. The original idea of experiment 2 was to increase the working memory performance by an intensive working memory training and shifting the underlying functional brain networks towards more small-world topology. Since a previous study showed increased intelligence performance after a working memory training (Jaeggi, et al., 2008), we in addition intended to replicate this result and explain it by an overlapping brain network of the two cognitive constructs. However, we were not able to replicate the study (Jaeggi, et al., 2008), so we focused on working memory and the plasticity of the underlying brain networks.

3.1. Neural Correlates of Intelligence

Where in the brain is intelligence? This question has vexed researchers for at least the last two centuries. Already the phrenologists tried to find in the 19th century specific feature on the human skull, which were associated with intelligence. Later on, theories arisen that larger brains are smarter, but this could be only demonstrated across species and if the body weight is taken into account. This is described in the so-called encephalization quotient denoted to the ratio between the actual brain size and the predicted (by the body weight)

brain size. The human species has the biggest encephalization quotient within mammals (Kolb and Whishaw, 1998). But looking within a species such a relationship could not be sustained (Kolb and Whishaw, 1998). However, the study of intelligence has struggled under numerous challenges of definition. Probably the best, but not very useful definition is: "intelligence is that what intelligence tests measure" (Thorndike, 1921). A consensus panel of the American Psychological Association (APA) defined intelligence in this way: "Individuals differ from one another in their ability to understand complex ideas, to adapt effectively to the environment, to learn from experience, to engage in various forms of reasoning, to overcome obstacles by taking thought" (Neisser, et al., 1996). This definition implies a general intelligence factor, which was supported by the work of Spearman (Spearman, 1904). Studies investigating intelligence use tasks to measure intelligence, which are derived from the use of a single measure as the Raven's Progressive Matrices Test (Raven, 2003) or composite indices of intelligence such as the Wechsler Intelligence Scale (Wechsler, 1939).

Most studies of human intelligence have been conducted in the context of two influential theories: the neural efficiency hypothesis of intelligence (Neubauer and Fink, 2009) and the Parieto-Frontal Integration Theory of intelligence (P-FIT) (Jung and Haier, 2007). Studies supporting the neural efficiency hypothesis demonstrate that brighter individuals display lower (more efficient) brain activation while performing a cognitive task (Haier, et al., 1988). Therefore the neural efficiency hypothesis postulates that intelligence is not a function of how hard the brain works but rather how efficiently it works. The early studies on human intelligence confirmed this hypothesis (Haier, et al., 1992a; Haier, et al.,

1992b). Nevertheless later research has revealed oppositional findings (Gray, et al., 2003; Klimesch, et al., 1997a) or has identified some moderating variables as sex (Jausovec and Jausovec, 2009; Neubauer, et al., 2002), task type (Doppelmayr, et al., 2005) or brain areas. Males exhibit neural efficiency predominantly when they performed a figural-spatial task, while for females the expected negative relationship could only be found in a verbal matching task (Neubauer, et al., 2002). It has been shown, that neural efficiency arise commonly when tasks of subjectively low to moderate task difficulty was presented to the subjects (Doppelmayr, et al., 2005). Moreover, neural efficiency was observed in novel tasks or after sufficient practice allowing participants to develop strategies (Haier, et al., 1992b). As mentioned before, the neural efficiency was found primarily in frontal brain areas, whereas in parietal brain regions a positive correlation between performance and activity was observed (Jausovec and Jausovec, 2004; Rypma, et al., 2006).

The second fundamental theory in the context of intelligence is the so-called Parieto-Frontal Integration Theory (P-FIT) of intelligence. This theory is mainly based on brain imaging data obtained with positron emission tomography (PET) or functional magnetic resonance imaging (fMRI), but also supported by structural findings derived from voxel-based morphometry (Jung and Haier, 2007). The P-FIT of intelligence emphasizes that there is no focused intelligence centre in the brain, but that intelligence emerges from a network comprising frontal and parietal brain areas.

The P-FIT of intelligence describes how intelligence tasks are processed in the different regions of the brain, starting in the auditory and/or visual areas, since these are the main sensory systems how we perceive the world. Therefore

particular brain regions within the temporal and occipital lobes are critical to early processing of sensory information. The extrastriate cortex (BA 18 & BA 19) and fusiform gyrus (BA 37) are involved in recognition and subsequent imagery and / or elaboration of visual input (Jung, et al., 2009). As the auditory counterpart the Wernicke's area (BA 22) is involved in processing and / or elaboration of auditory information. Secondly, the theory assumes that this basic perceptual processing is then fed forward to the parietal cortex, predominantly the supramarginal (BA 40), superior parietal (BA 7) and angular gyri (BA 39), wherein structural symbolism, abstraction, and elaboration emerge (Jung, et al., 2009). The theory further assumes that the parietal cortex is effectively linked by white matter structures (i.e. arcuate fasciculus, superior longitudinal fasciculus) with frontal regions (BA's 6, 9, 10, 45-47), which serve to test various solutions to a given problem (Jung, et al., 2009). Once the best solution is arrived upon, the anterior cingulated (BA 32) is engaged to constrain response selection, as well as inhibiting other competing responses (Jung, et al., 2009). In the review of (Jung, et al., 2009) they present supporting evidence for the involvement of these regions during the performance of intelligence tasks. Although the P-FIT of intelligence suggests that variations in a distributed network exhibits the best prediction for individual differences, until the experiment 1 of this thesis, only three studies have related small-world network features to psychometric intelligence. Two recent brain imaging studies (one using fMRI (van den Heuvel, et al., 2009) and the other DTI (Li, et al., 2009)) demonstrated associations between psychometric intelligence and a particular brain network topology organized according to a small-world network. EEG has only been used once to study small-world characteristics in relation to intellectual abilities (Micheloyannis, et al., 2006b).

However, the findings of this study do not entirely fit with the results of the fMRI and DTI studies mentioned above. While the cause of this discrepancy is not yet clear, there are methodological issues of concern, such as the limited set of surface electrodes and unsolved problems with volume conductivity (see Method section of experiment 1). To circumvent these methodological issues, we re-addressed the question whether psychometric intelligence is related to a functional resting network resembling a small-world network architecture by using high-density EEG in association with a valid method to estimate the intracortical sources of surface EEG standardized low resolution brain electromagnetic tomography (sLORETA) (Pascual-Marqui, 2002).

Focusing on electrophysiological studies, several studies suggested that synchronized oscillatory activity in cell assemblies plays a key role in encoding, storage, and retrieval of information in the brain (Birbaumer, et al., 1990; Lisman and Idiart, 1995). In particular, the alpha frequency (8-12 Hz) was shown to correlate positively with indices of mental activity level, academic performance in high school students, performance on memory tasks, and with the performance in intelligence tests (Anokhin and Vogel, 1996; Golubeva, 1980; Klimesch, 1999). Alpha power emerges as a result of synchronous oscillations of synaptic potentials in large populations of neurons (mainly pyramidal cells) spread over the cortex (Michel, et al., 2009). Although the exact mechanisms of alpha rhythm generation and its functional meaning are not yet fully understood, there is mounting evidence that synchronized oscillatory activity in the cerebral cortex is essential for spatiotemporal information coordination and integration (Klimesch, 1999; Singer and Gray, 1995; Varela, et al., 2001; Womelsdorf, et al., 2007). Given that some studies also identified relationships between psychometric intelligence

and other frequency bands (e.g. theta, beta, gamma) (Jausovec and Jausovec, 2000; Klimesch, 1999; Thatcher, et al., 2007), we combined in experiment 1 our hypotheses with a data driven approach, in order to not constrict the analysis to a particular frequency band.

3.2. Neural Correlates of Working Memory

The first concept of working memory was used in the context of linking the brain to a computer by Miller, Galanter and Pribram (Miller, et al., 1960). There are several theories regarding how working memory functions. In this thesis the famous model of working memory by Baddeley and the model of Oberauer will be summarized below, since the working memory tasks and training of experiment 2 are based on the last named theory. The most popular working memory theory, which was based on the idea of a multicomponent model, was introduced by Baddeley and Hitch (Baddeley and Hitch, 1974). They postulate that two "slave systems" account for short-term maintenance of information, whereas a "central executive" is responsible for the supervision of information integration and for coordinating the slave systems (Baddeley, 2003; Baddeley and Hitch, 1974). The central executive is associated with the common term executive system, which is responsible to focus attention to relevant information, while suppressing irrelevant information. Moreover, the central executive serves as the "coordinator" between the two slave systems and other cognitive processes. The phonological loop, representing one of the two slave systems, stores phonological information and prevents its decay by continuously maintain the information by a rehearsal loop (Baddeley, 2003; Baddeley and Hitch, 1974).

The second slave system, called the visuo-spatial sketchpad, denotes to the storage of visual and spatial information's (Baddeley, 2003; Baddeley and Hitch, 1974). Mental maps, as well as visual perception are constructed and manipulated. A further distinction subdivided the visuo-spatial sketchpad to a visual and a spatial subsystem. Later on, Baddeley added a forth component to the model, the "episodic buffer", which memorized representations of the slave system (Baddeley, 2000). The name is based on the idea that the episodic buffer binds information into unitary transient episodic representations.

In contrast to the Baddeley's theory, which is build on theoretical concepts, the model of Oberauer is derived by a structural equation modeling approach (Oberauer, et al., 2000; Oberauer, et al., 2003). The model also considers three different facets of working memory, but they are differently described. One of the facets is storage and processing. "Storage is defined as the retention of briefly presented new information over a period of time in which the information is no longer present. Processing is specified as the transformation of information or the derivation of new information, in contrast to cognitive activities that maintain the information as given" (Oberauer, et al., 2003). The central executive of the model by Baddeley is also found in the Oberauer model, but labeled as executive processes. Oberauer denotes that "executive processes involves the monitoring of ongoing cognitive processes and actions, the selective activation of relevant representations and procedures, and the suppression of irrelevant, distracting ones" (Oberauer, et al., 2003). The last facet is defined as relational integration, for which he proposes "the coordination of information elements into structures. Working memory serves to build new relations between elements and to integrate relations into structures" (Oberauer, et al., 2003). The model of

Oberauer serves a basis for the working memory tasks and training in the second experiment of the present thesis. Working memory is a fundamental concept, since it has been shown that working memory is crucial for daily life skills, such as reading comprehension (deJonge and deJong, 1996) planning and problem-solving (Shah and Miyake, 1999) or to acquire knowledge and learn new skills (Pickering, 2006), whereas an impaired working memory is associated with neurological and psychiatric disorders (Baddeley, 2003).

From a neuroscientific point of view the involvement of fronto-parietal regions in working memory tasks has constantly been shown with different neuroscientific methods such the electroencephalogram (Meltzer, et al., 2008; Raghavachari, et al., 2006) functional magnetic imaging (Owen, et al., 2005), transcranial magnetic stimulation (Oliveri, et al., 2001). For a detailed description of the different brain areas associated with working memory please refer to the discussion of the second experiment in section 4.2.5. In summary, the frontal cortex was suggested to serves as the central executive, which focuses on relevant information and suppressing distracting ones. The secondary sensory areas and the parietal cortex deal with specific abstraction and elaboration of information's. Moreover the hippocampus and entorhinal cortex plays an important role in memory formation. Although most researches of working memory suggest that variations in a distributed network exhibits the best prediction for alterations in working memory performance, the neuroscientific investigation of working memory training effects in the context functional brain network analyses are rare. Moreover, there are no studies, which investigated the effects of an external environmental influence on the small-world characteristics based on EEG-data. Therefore we addressed the question in experiment 2, whether working memory

training could change the functional resting network, in particular the small-world topology. Previous EEG studies showed increased theta coherence in frontal and parietal regions during difficult working memory task (Sauseng, et al., 2005). Klimesch also emphasized that theta plays an important role during encoding (Klimesch, et al., 1996) and memory retrieval (Klimesch, et al., 2001). Patients with a working memory deficit like Alzheimer's disease or schizophrenia exhibit reduced fronto-parietal EEG coherence mainly in theta (Babiloni, et al., 2004b; Ford, et al., 2002; Hogan, et al., 2003; Winterer, et al., 2003). Therefore we expected changes in the theta band as a consequence of working memory training. Theta waves are usually in the 4-8 Hz frequency range and have been described in the cortical anterior midline, cingulated and limbic regions (hippocampus, entorhinal cortex and cingular areas), where they often display a participation in working memory tasks (Meltzer, et al., 2008; Onton, et al., 2005; Raghavachari, et al., 2006). The theta oscillations are considered to be the result of an interaction within neuronal networks mainly in the pyramidal cells of the hippocampus. Several EEG studies have indicated that a complex structure of feedback loops connecting the hippocampus with different cortical regions and the prefrontal cortex in particular may provide the anatomical basis of working memory performance (Asada, et al., 1999; Ishii, et al., 1999; Onton, et al., 2005; Uchida, et al., 2003; Wang, et al., 2005). Because working memory, as other higher cognitions, seems to be the product of dynamic interactions occurring between functionally specialized regions of the brain, a complete understanding of such phenomena is only possible by studying how these interactions are organized and coordinated. Therefore we investigated in experiment 2 the

functional brain networks underlying the neural correlates of working memory and their plasticity capacities induced by an intensive working memory training.

3.3. The Relationship between Intelligence and Working Memory

As already mentioned in the beginning of this chapter, the original idea of experiment 2 was to increase psychometric intelligence by an intensive working memory training. Such a transfer effect has been shown by the study of Jaeggi and colleagues (Jaeggi, et al., 2008). In their study, they trained the subjects in an adaptive dual n-back task that used both spatial and auditory features for around 25 minutes a day. The more days they trained, the more their psychometric intelligence improved. Although this study (Jaeggi, et al., 2008) was criticized by other scientist (Moody, 2009), because the time to solve the intelligence task was to short, the idea of a strong relationship between working memory and intelligence is comprehensible. Thus, the question arises, how this transfer effect can occur. The authors concluded that transfer could occur if the training and transfer tasks engage similar cognitive processes. Moreover, neural association between the training and the transfer task is necessary requisite for the training to results in transfer. Although the brain networks underlying intelligence and working memory, primarily the frontal and parietal regions, provide additional evidence for a shared neural networks, they are far from being isomorphic (Conway, et al., 2003). To date, it is not clear how large the overlap of activated brain regions during training and transfer task has to be in order to result in transfer effects. Furthermore, it is not clear which processes and their neural

correlates of training and target task must be similar in order to result in transfer. Halford and colleagues suggested that fluid intelligence and working memory share a common memory capacity constraint (Halford, et al., 2007). So, one could conclude that training on working memory might have a beneficial impact in intelligence because of this shared cognitive component. The reason for a common capacity could also by caused by the common demand for attention, when temporary binding processes are taking place to form representations in reasoning tasks (Gray, et al., 2003; Halford, et al., 2007). Other theories have suggested that the ability to infer abstract relations and maintain a large set of possible goals in working memory explain individual differences in intelligence (Carpenter, et al., 1990).

4. Experiments

4.1. Experiment 1: Functional Brain Network Efficiency Predicts Intelligence

Langer, N.[1], Pedroni A.[1,2], Gianotti L.R.R.[2], Hänggi J[1], Knoch, D.[2], Jäncke L.[1]

1 Division Neuropsychology, Institute of Psychology, University of Zurich, 8050 Zurich, Switzerland

2 Division Social and Affective Neuroscience, Department of Psychology, University of Basel, Switzerland

4.1.1. Abstract

The neuronal causes of individual differences in mental abilities such as intelligence are complex and profoundly important. Understanding these abilities has the potential to facilitate their enhancement. The purpose of this study was to identify functional brain network characteristics and their relation to psychometric intelligence. In particular, we examined whether the functional network exhibits efficient small-world network attributes (high clustering and short path length) and whether these small-world network parameters are associated with intellectual performance. High-density resting state electroencephalography (EEG) was recorded in 74 healthy subjects to analyze graph-theoretical functional network characteristics at an intracortical level. Ravens advanced progressive matrices were used to assess intelligence. We found that the clustering coefficient and path length of the functional network are strongly related to intelligence. Thus, the more intelligent the subjects are the more the functional brain network resembles a small-world network. We further identified the parietal cortex as a main hub of this resting state network as

indicated by increased degree centrality that is associated with higher intelligence. Taken together this is the first study that substantiates the neural efficiency hypothesis as well as the Parieto-Frontal Integration Theory (P-FIT) of intelligence in the context of functional brain network characteristics. These theories are currently the most established intelligence theories in neuroscience. Our findings revealed robust evidence of an efficiently organized resting state functional brain network for highly productive cognitions.

4.1.2. Introduction

The human brain is organized as a highly interconnected structural network (Herculano-Houzel, 2009) that functionally links adjacent and distant brain areas. This functional coupling is present during the processing of cognitive tasks and it is even present during rest (Jann, et al., 2010; Laufs, 2008). Recent studies have shown that the functional and anatomical connections of the brain network are organized in a highly efficient small-world manner (Stam, 2004). A small-world organization of the brain network implies a high level of local neighborhood clustering (indexed by the clustering coefficient) combined with global efficiency of information transfer (indexed by the path length) (Bullmore and Sporns, 2009). Thus, the small-world networks explain how the brain minimizes wiring costs while simultaneously maximizing the efficiency of information propagation (Achard and Bullmore, 2007; Kaiser and Hilgetag, 2006; Sporns, et al., 2004). It is unclear to date whether individual differences in cognitive functions such as intelligence are associated with differences in small-world characteristics of functional brain networks. While intelligence is one of the most influential factors characterizing individuals in decision-making, job placement and education (Deary, et al., 2010), the psychophysiological underpinnings of interindividual differences in intelligence are still hardly understood.

Most studies of human intelligence have been conducted in the context of two influential theories: the neural efficiency hypothesis of intelligence (Neubauer and Fink, 2009) and the Parieto-Frontal Integration Theory of intelligence (P-FIT) (Jung and Haier, 2007). Studies supporting the neural efficiency hypothesis demonstrate that more intelligent subjects need less neural resources (primarily in frontal brain areas) to solve cognitive tasks (Neubauer and Fink, 2009). Most of

the studies also fit to the P-FIT of intelligence. This theory is mainly based on brain imaging data obtained with positron emission tomography (PET) or functional magnetic resonance imaging (fMRI), but also supported by structural findings derived from voxel-based morphometry (Jung and Haier, 2007). The P-FIT of intelligence emphasizes that there is no focused intelligence centre in the brain, but that intelligence emerges from a network comprising frontal and parietal brain areas. In this context, the parietal cortex is thought to generate symbols and abstract rules, while the prefrontal cortex tests hypotheses, elaborates solutions to given problems, and generates, selects and inhibits actions. Although the P-FIT of intelligence suggests that variations in a distributed network exhibits the best prediction for individual differences, no neuroscientific investigation has examined the P-FIT of intelligence in the context of EEG resting-state network analyses.

To date, only three studies have related small-world network features to psychometric intelligence. Two recent brain imaging studies (one using fMRI (van den Heuvel, et al., 2009) and the other DTI (Li, et al., 2009)) demonstrated associations between psychometric intelligence and a particular brain network topology organized according to a small-world network. Since the characteristics of a network are not merely defined by its morphological properties (e.g. anatomical connections) and because communication in the brain is faster than the time resolution of seconds (as measured with fMRI), it is preferable to study brain network characteristics using high-density EEG or magnetoencephalography (MEG) data. High-density EEG and MEG have the advantages of capturing neurophysiological activations in the millisecond range and, in contrast to fMRI, do not rely on metabolic signals such as the blood

oxygenation level dependent (BOLD) signal that is only indirectly related to neurophysiological activations. We therefore calculated small-world properties of dynamic brain networks on the basis of high-density EEG. EEG has only been used once to study small-world characteristics in relation to intellectual abilities (Micheloyannis, et al., 2006b). However, the findings of this study do not entirely fit with the results of the fMRI and DTI studies mentioned above. While the cause of this discrepancy is not yet clear, there are methodological issues of concern, such as the limited set of surface electrodes and unsolved problems with volume conductivity (see Method section). To circumvent these methodological issues, we re-addressed the question whether psychometric intelligence is related to a functional resting network resembling a small-world network architecture by using high-density EEG in association with a valid method to estimate the intracortical sources of surface EEG standardized low resolution brain electromagnetic tomography (sLORETA) (Pascual-Marqui, 2002).

In the present study, we focus on the so-called resting EEG and its relation to psychometric intelligence, and on the upper alpha band as it has been repeatedly associated with intelligence (Jausovec and Jausovec, 2000; Klimesch, 1999; Thatcher, et al., 2008). Given that some studies also identified relationships between psychometric intelligence and other frequency bands (e.g. theta, beta, gamma) (Jausovec and Jausovec, 2000; Klimesch, 1999; Thatcher, et al., 2007), we combined our hypotheses with a data driven approach. In order to not constrict the analysis to a particular frequency band, we firstly performed a scalp map analysis for the whole frequency spectrum. The power of the different frequency bands were computed for each subject and clusters of electrodes and correlated with the performance in the intelligence test. For the purpose of estimating the

intracortical electrical sources, all topographical EEG frequency data were transformed in a second step into the intracortical space. Thus, we obtained for all frequency bands and each voxel a particular current density value correlated with psychometric intelligence. For those frequency bands that revealed significant correlations based on both the topographical analysis and the analysis in the intracortical space, additional graph-theoretical analyses based on coherence were performed. The advantage of graph-theoretical network analyses over the classical EEG analyses is that this analysis provides additional information about functional connectivity between different brain areas and electrodes respectively. Thus graph-theoretical network analyses are ideal to investigate the neural efficiency hypothesis and the P-FIT of intelligence. Based on the evidence summarized above, we hypothesize that small-world network characteristics (clustering coefficient, path length and degree) are correlated with psychometric intelligence, especially in parietal and frontal regions.

4.1.3. Methods

Subjects

Seventy-five healthy male students (mean/standard deviation: 25.5/4.86 years, range 19-43 years) participated in the study. All were right-handed according to the Annett-Handedness-Questionnaire (Annett, 1970) and native Swiss German speakers. They were screened to ensure that they had no history of neurological or psychiatric disorders, neuropsychological problems, or medication and drug abuse. One subject did not agree to conduct the Ravens Advanced Progressive Matrices (RAPM). The local ethics committee approved the study and all participants gave written informed consent to participate in the study.

Task

RAPM is a widely used to measure psychometric intelligence (Raven, 2003) and was administered after the EEG recordings. The RAPM is a reasoning-based intelligence test, which focuses on visual-spatial abilities. In addition, working memory plays a crucial role in this task, particularly the executive control of attention to overcome distraction or interference. Gray and Thompson (Gray and Thompson, 2004) described that the performance RAPM best reflects the general factor of intelligence (g).

Procedure

Subjects were sitting comfortably in a chair in a dimly illuminated, sound-shielded Faraday recording cage. Subjects were instructed that EEG recording is done while they rested with their eyes alternately open or closed. The EEG protocol consisted of the participants resting with their eyes open for 20 s, followed by 40 s with their eyes closed; this was repeated five times. Only data from the 200 s eyes closed condition were analyzed. After the recording of the resting EEG, subjects conducted Raven Advanced Progressive Matrices (RAPM).

Electroencephalographical Recording

The high-density EEG was recorded at a sampling rate of 250 Hz with a bandpass of 0.1 to 100 Hz with a 128-channel EEG Geodesic Netamps system (Electrical Geodesics, Eugene, Oregon, USA). Recording reference was at Cz (vertex of the head). Impedances were kept below 20 kOhm. Independent component analysis was used to remove eye-movement artifacts from the EEG. In addition to the application of an automated artifact rejection procedure, data were visually inspected for noise like eye movements, eye blinks, sweating and muscular artifacts. After artifact rejection the electrodes in the outermost circumference

(chin and neck) as well as other artifact channels were excluded and interpolated to a standard 111-channel electrode array (Perrin, et al., 1987). The artifact-free EEG was recomputed against the average reference and segmented into 2 s epochs. In a second step, a discrete Fourier transformation algorithm was applied to the artifact-free 2 s epochs (45 segments per subjects). The power spectrum of 1.5-49.5 Hz (resolution: 0.488 Hz) was calculated. The spectra for each channel were averaged over all epochs for each subject. Absolute power spectra were integrated for the following eight independent frequency bands following classification proposed by Kubicki and colleagues (Kubicki, et al., 1979): delta (1.5-6 Hz), theta (6.5-8 Hz), alpha1 (8.5–10 Hz), alpha2 (10.5–12 Hz), beta1 (12.5–18Hz), beta2 (18.5–21 Hz), beta3 (21.5–30 Hz), and gamma (30-49.5). All the analyses applied in the present study are summarized in a workflow (Fig. 1).

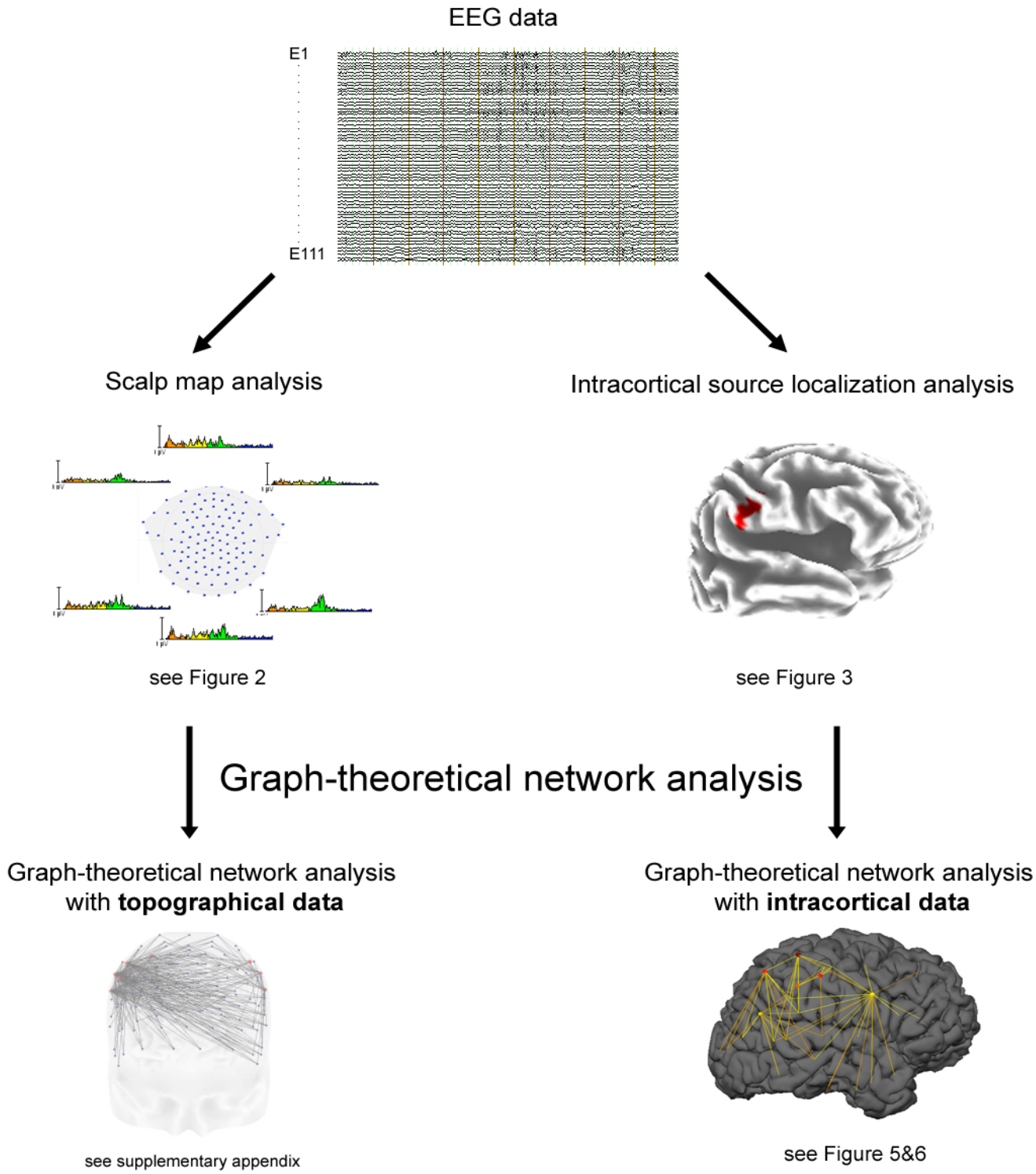

Figure 1. The workflow of all the analyses, which were implemented in this study are summarized as an overview.

Scalp map analysis

After the preprocessing steps, the data of 111 electrodes were collapsed into three anterior and three posterior electrode clusters: anterior (left, middle, right), posterior (left, middle, right). Partial regression analyses were calculated for each cluster and frequency band between EEG power and RAPM-performance, after co-varying out age effects. Statistical significance was assessed by means of a nonparametric randomization test (Fisher, 1935; Nichols and Holmes, 2002). An error probability of $p \leq 0.05$ (corrected for multiple comparisons) was used to indicate significant correlations.

Intracortical source localization analysis

For the purpose of estimating the intracortical electrical sources standardized low resolution brain electromagnetic tomography (sLORETA, (Pascual-Marqui, 2002)) was employed. sLORETA computes, from the recorded scalp electric potential differences, the three-dimensional distribution of the electrically active neuronal generators in the brain as standardized units of current density (A/cm^2) at each voxel by assuming similar activation among neighboring neuronal clusters (Pascual-Marqui, 2002). In the current implementation of sLORETA, computations were made in a realistic head model (Fuchs, et al., 2002) using the MNI152 template (Mazziotta, et al., 2001) with the three-dimensional solution space restricted to cortical gray matter as determined by the probabilistic Talairach atlas (Lancaster, et al., 2000). The standard electrode positions on the MNI152 scalp were taken from (Jurcak, et al., 2007) and (Oostenveld and Praamstra, 2001). The intracerebral volume is partitioned in 6239 voxels at 5 mm spatial resolution. Thus, sLORETA images represent the standardized electric activity at each voxel in Montreal Neurological Institute (MNI) stereotaxic space

as the exact magnitude of the estimated current density. Anatomical labels are reported as Brodmannn areas transformed into MNI space (Brett, et al., 2002). sLORETA solves the inverse problem by taking into account the well-known effects of the head as a volume conductor. Conventional LORETA and the more recent sLORETA analyses have been frequently used in previous experiments to localize brain activations on the basis of EEG or MEG data (Langer, et al., 2010; Mulert, et al., 2004; Zaehle, et al., 2009).

Voxel-wise partial correlations between current density and RAPM-performance were calculated while controlling for age effects. Statistical significance was assessed by means of a nonparametric randomization test (Fisher, 1935; Nichols and Holmes, 2002). An error probability of $p \leq 0.05$ (corrected for multiple comparisons) was used to assess significant correlations between psychometric intelligence and the intracortical sources of activation.

Graph-theoretical network analysis

Background

In order to mathematically describe small-world networks, graph-theoretical analysis techniques are generally used (Bullmore and Sporns, 2009), which are abstract representations of networks consisting of sets of vertices (nodes) linked by connections (edges). These graphs are characterized by specific measures: clustering coefficients and path lengths. In comparison with randomly organized networks, a relative high clustering coefficient and a similar path length characterize small-world networks. Small-world features of the human brain have been identified on the basis of functional and anatomical data (Reijneveld, et al., 2007; Stam, 2004; Yu, et al., 2008).

Measures of connectivity

In the context of this study connectivity parameters at the level of brain-topographic data (see SI Appendix) and for intracortical sources of brain oscillations were analyzed. In particular, the connectivity measure of linear instantaneous dependence (coherence) was used to calculate small-world parameters. This measure was used in other studies before (De Vico Fallani, et al., 2010; Pascual-Marqui, 2007b) and is deemed an adequate measure for computing resting state networks. Linear instantaneous connectivity is a function that operates in the frequency domain and generates a value between 0 and 1. Given two signals x and y, the linear instantaneous connectivity is calculated in a particular frequency f by taking the square of the cross-spectrum

$$\left|S_{xy}(f)\right|^2$$

and the dividing by the product of the two corresponding auto power spectra:

$$SC_{xy}(f)=\frac{\left|S_{xy}(f)\right|^2}{S_{xx}(f)S_{yy}(f)}$$

For an extensive discussion on different measures of causal dependencies and their computation, please refer to reference (Pascual-Marqui, 2007b) and (Geweke, 1982). Compared with coherence calculations on the surface scalp, the intracortical analysis of coherence is less contaminated by non-physiological influences due to volume conduction (for a discussion see reference (Pascual-Marqui, 2007b)). Several studies concluded that an intracortical approach represents a clear methodological improvement compared to analysis at surface electrodes (Lehmann, et al., 2006; Mulert, et al., 2004; Pascual-Marqui, 2007b; Sinai and Pratt, 2003). Finally, conducting the analysis on the intracortical level made it possible to estimate coherence between any number of brain areas (i.e.

distributed cortical networks) instead of being restricted to a given array of scalp electrodes (Babiloni, et al., 2004a).

Construction of the connectivity matrix

On the basis of the stereotactic space provided by the Montreal neurological institute (MNI) template (Pascual-Marqui, 2007a), 42 anatomical regions of interest (ROI) in each hemisphere were defined according to Brodmann areas (Mazziotta, et al., 2001). With these 84 ROIs, the entire cortex was delineated into separate regions for which current densities were computed (Brodmann, 1909).

Within the sLORETA analysis framework, coherence between 84 anatomical regions of interest (ROI) in both hemispheres was computed. We chose to use the centroid voxels of each region of interest (ROI) instead of calculation of average coherence measures of each ROI, because sLORETA estimates the solution of the inverse problem based on the assumption that the smoothest of all possible activation distributions is the most plausible one. This assumption is supported by neurophysiological data demonstrating that neighboring neuronal populations show highly correlated activity. Because of this assumption of sLORETA, signals of spatially near voxels of neighboring ROIs are highly correlated inducing larger coherence, which might be not physiological in nature. By taking just the single center voxel of each ROI, we reduced such contamination. Because of the spatially smooth inverse solution of sLORETA, information of the centroid voxel is an accurate representative for activity within the ROIs.

The coherence was computed between all 84 ROIs. Since our preceding analyses only obtained significant correlations between the upper alpha power and psychometric intelligence using the surface EEG data, we calculated intracortical coherence for the upper alpha frequency band (10.5-12 Hz).

These intracortical coherence measures between the 84 ROIs were subjected to graph-theoretical network analysis. The input for this analysis consisted of a 84x84 coherence-matrix (84 ROIs) for each subject. An individual network is represented by the weighted connectivity matrix with nodes and edges, where nodes represent ROIs and edges represent the undirected weighted connections (coherence) between ROIs.

Defining the threshold for the small-world network analysis

In a first step, the correlation threshold, which corresponds to a small-world topology, was determined on the basis of the average network across all subjects. There is currently no definitive and generally accepted strategy for applying a particular threshold. According to previous small-world network analyses (Evans, et al., 1993; Li, et al., 2009; Stam, et al., 2007a; Stam and Reijneveld, 2007), the average network was therefore thresholded repeatedly over a wide range of correlation thresholds in increments of r = 0.05 from r = 0.65 to r = 0.95. The thus obtained thresholded average correlation matrices were then subjected to the network analysis software *tnet* (Micheloyannis, et al., 2009; Opsahl, 2009) to quantify small-worldness (Opsahl and Panzarasa, 2009; Watts and Strogatz, 1998). Small-world indices were derived from the comparison of the real (measured) networks with 100 random networks comprising the same number of nodes, edges and degree distribution as the real network (Bullmore and Sporns, 2009). Based on the comparison of the real network indices with those of the random networks, key measures describing the overall architecture of the real network were computed. Key measures of a small-world network are the clustering coefficient C, the characteristic path length L, and the degree distribution D (Opsahl, et al., 2008). The clustering coefficient C is given by the

ratio of the number of closed triplets to the total value of triplets and provides information about the level of local connectedness within a network. The characteristic path length L of a network gives the average number of connections that have to be crossed to travel from each node to every other node in the network and provides information about the level of global communication efficiency of a network (Watts and Strogatz, 1998). For details about the calculation of the clustering coefficient and path length and their formula see (Opsahl and Panzarasa, 2009; van den Heuvel, et al., 2009).

Small-world organized networks are characterized by a clustering coefficient C that is higher than the C of a randomly organized network (C random), but still with a short characteristic path length L that is similar to that of an equivalent random network (L random) (Humphries, et al., 2006; Watts and Strogatz, 1998). Formally, small-world networks show a ratio γ defined as C real / C random of >> 1 and a ratio λ defined as L real / L random of ~ 1 (Humphries and Gurney, 2008; Sporns and Zwi, 2004; Watts and Strogatz, 1998). A high γ reflects a high level of local neighborhood clustering within a network, and a short travel distance λ expresses a high level of global communication efficiency within a network (Bullmore and Sporns, 2009; Humphries and Gurney, 2008; Sporns, et al., 2004).

In summary, the mean correlation matrix (averaged across all subjects) was thresholded with a set of different thresholds (range 0.55-0.95). In a second step, network parameters (clustering coefficient, path length, γ and λ) were calculated for the different thresholded mean coherence matrices. The particular threshold, which identified γ and λ of the mean correlation matrix (over all subjects) that best corresponds to a small-world topology was chosen and applied to the correlation matrices of each individual subject. Subsequently, the correlation

matrix of each subject was subjected to *tnet* software, which calculated the small-world indices (clustering coefficient and path length) as described above.

Regional node analysis

Hub regions based on weighted degree centrality (Opsahl, 2009; Watts and Strogatz, 1998) were evaluated in addition. Degree is a global centrality measure within a network and is often taken as the sum of weights and labeled node strength (Freeman, 1978; Newman, 2004). Therefore, every node exhibits its own degree centrality score. In addition, the betweenness centrality was analyzed. Betweenness centrality relies on the calculation of shortest distances in the network (Barrat, et al., 2004). Nodes that occur on many shortest paths (geodesics) between other nodes have higher betweenness centrality than those that do not. A node with high betweenness centrality is interpreted as a gatekeeper that is able to control the information flow through the node.

For statistical comparisons of the relationship between the small-world indices (number of edges, clustering coefficient, path length), regional node index (degree centrality scores) and the performance in the RAPM we used partial correlation analysis controlling for age. For these small-world indices error probability was set to $p < 0.05$, corrected for multiple comparisons, through a modified Bonferroni method proposed by (Shaffer, 1995; Wasserman and Faust, 1994) that is more powerful than the traditional Bonferroni approach but maintains experiment wise error rate. For the regional node index, error probability was set to < 0.05, uncorrected for multiple comparisons. Because of our strong a priori hypotheses, in particular the parieto-frontal network, we did not use a correction for multiple comparisons for the regional node index.

4.1.4. Results

Behavioral results

Raw scores obtained for the Ravens Progressive Matrices (RAPM) ranged between 10-31, (mean = 22.2, standard deviation = 5.53). The RAPM scores correlated negatively with age (Pearson's r = -0.40; p = 0.001).

Scalp map analysis

Psychometric intelligence was positively correlated with upper alpha oscillations in the right posterior electrode cluster (r = 0.361, p = 0.014) after removing the effect of age. For further electrode clusters, upper alpha frequency revealed also high correlations, but did not reach statistical significance (Fig. 2). The analysis of the clusters of all other frequency bands revealed no significant relationship with RAPM performance.

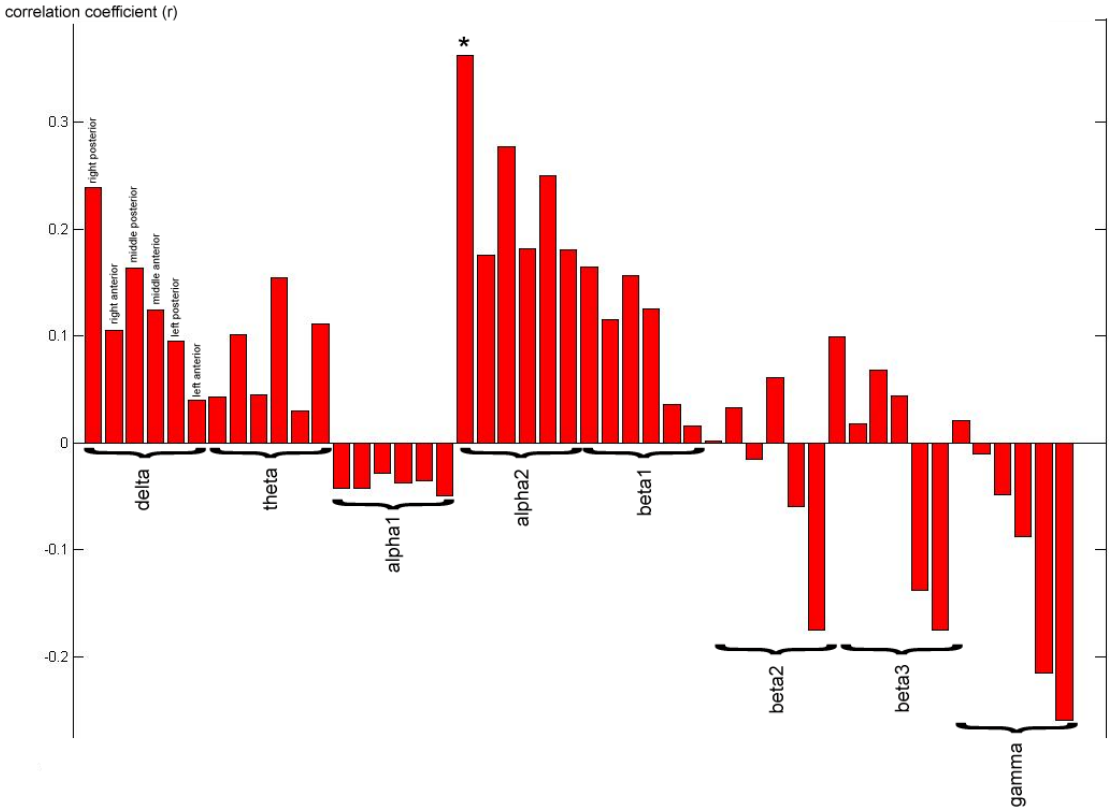

Figure 2. The partial correlation analysis between the performance in the RAPM and the six electrode clusters of all frequency bands is displayed. The correlation coefficient is plotted on the y-axis. The Fisher's permutation test revealed only significant relationship in the right posterior cluster of the upper alpha band ($p < 0.05$, corrected for multiple comparisons).

Intracortical source localization analysis

After removing the effect of age, the intracortical source localization analysis of all frequency bands revealed a significantly positive correlation only between the upper alpha activity and the RAPM performance ($r = 0.459$, $p = 0.0068$, corrected for multiple comparison). The maximum of this significant correlation was localized in the right parietal cortex (Fig.3). The partial correlations of all other frequency bands revealed no significant effects.

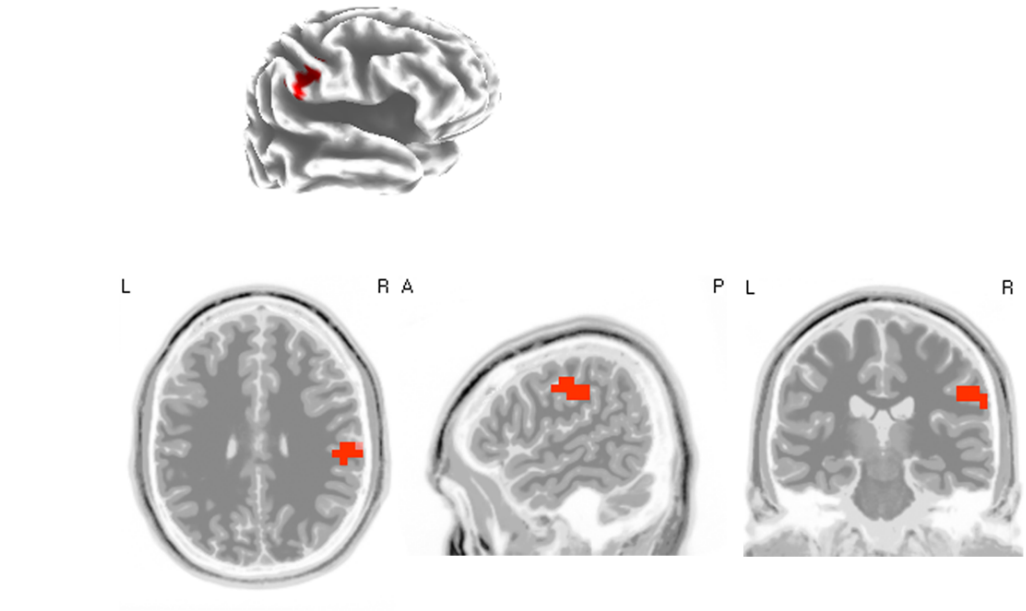

Figure 3. After removing the effect of age, the intracortical source localization analysis (with Fisher's permutation test) revealed a positive significant correlation between upper alpha activity in the right parietal cortex and psychometric intelligence ($p < 0.05$, corrected for multiple comparisons). The significant cluster is displayed in red. The MNI-coordinates of the local maximum are (X = 55, Y = -25, Z = 30).

Graph-theoretical network analysis

Across the whole range of relevant correlation thresholds, the threshold of r = 0.85 revealed the network that represents the best small-world topology, which is defined by a high γ and a $\lambda \approx 1$. This network (the average correlation matrix across all subjects) is composed of 84 nodes and 1040 edges; connection density: 0.149. Table 1 and Fig.4 display all small-world indices for the differently thresholded average matrices.

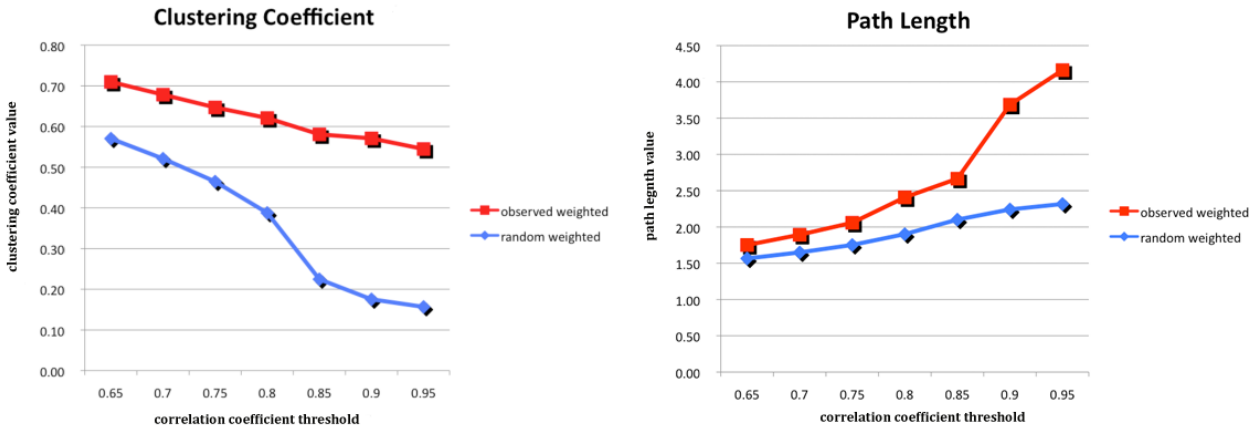

Figure 4. The different clustering coefficients and path length of the differently thresholded mean-weighted correlation matrices and the computed random correlation matrices of the intracortical graph-theoretical network analysis are plotted in the two diagrams. The x-axis shows the different correlation coefficient thresholds. On the y-axis the values for the real and the random clustering coefficient and the path length respectively are displayed.

Table 1. The *small-world* indices of the differently thresholded mean correlation-matrices of the intracortical graph-theoretical network analysis are displayed. Across the whole range of relevant correlation thresholds, the threshold of r = 0.85 (bold) elucidated the network, which represents the best *small-world* network organization.

Threshold	0.65	0.7	0.75	0.8	0.85	0.9	0.95
Edges	2,640	2,278	1,904	1,468	**1,040**	746	518
Density	0.379	0.327	0.273	0.211	**0.149**	0.107	0.074
C	0.71	0.678	0.647	0.621	**0.581**	0.571	0.545
L	1.751	1.893	1.385	1.595	**2.665**	3.686	4.161
γ weighted	1.244	1.302	1.392	1.601	**2.585**	3.255	3.475
λ weighted	1.118	1.148	1.175	1.267	**1.268**	1.644	1.796

After applying this particular threshold (r = 0.85) to each subject, the small world indices (edges, clustering coefficient, path length and degree) were computed for each subject individually and partial correlations between the small-world indices and the performance in the RAPM were calculated. The partial correlation analyses revealed positive correlations for the number of edges (r = 0.352, p = 0.004) and the clustering coefficients (r = 0.373, p = 0.002), while for the path

length a negative relationship emerged (r = -0.305, p = 0.014). All correlations are summarized in Table 2 (for all the other frequency bands see Table S7).

Table 2. Listed are the correlations coefficients of the partial correlation analysis between the *small-world* indices of the intracortical graph-theoretical network analysis and the intelligence performance. In addition, the p value whit the correlations are presented (p< 0.05, corrected for multiple comparisons).

	Edges	*C*	*L*
r	0.352	0.373	−0.305
p	0.004	0.002	0.014

Identification of hub regions: Hub regions were evaluated by weighted degree centrality and betweenness centrality (Table S8) measurements for the correlation threshold (network) that represents the best small-world organization properties (r = 0.85). The partial correlation analysis between weighted degree centrality and intelligence revealed significant positive correlations primarily in the parietal cortex, anterior cingulate gyrus and fusiform cortex. The higher the intelligence the higher was the degree centrality in these regions (Fig. 5). Significant negative correlations of the RAPM with the intracortical organization of the hub regions were found primarily in the frontal cortex and posterior cingulate gyrus. The higher the intelligence the lower was the degree centrality in these regions (Fig. 6). The exact positive and negative correlation coefficients are summarized in Table S1 and S2 (see supplementary material).

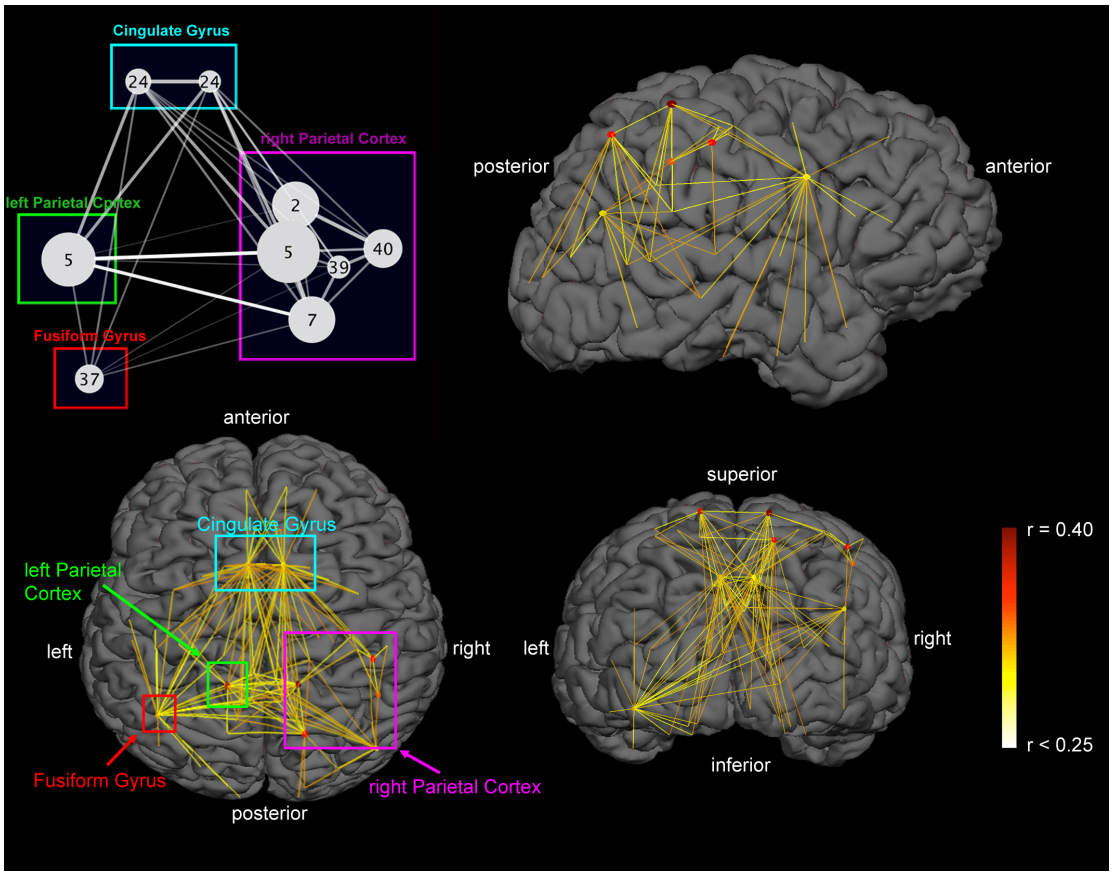

Figure 5. The weighted degree centrality measurements of the intracortical graph-theoretical network analysis, which were significant positively correlated with intelligence, are displayed depending on the magnitude of the correlation coefficient (dark red corresponds to the highest correlation). A significant degree of a node is defined by exceeding the significance threshold $p<0.05$ (uncorrected for multiple comparisions). Furthermore, the connections of hub regions in which the hubs were positively correlated with the intelligence ($p<0.05$) are presented as lines between the different nodes. The hub regions in the image are shown according to a glass brain to facilitate the view of the entire network. In addition a schematic visualization of the network is provided, which includes the significant Brodmann areas and their interaction with each other. The size of the Brodmann areas represents the magnitude of the correlation with the intelligence test performance.

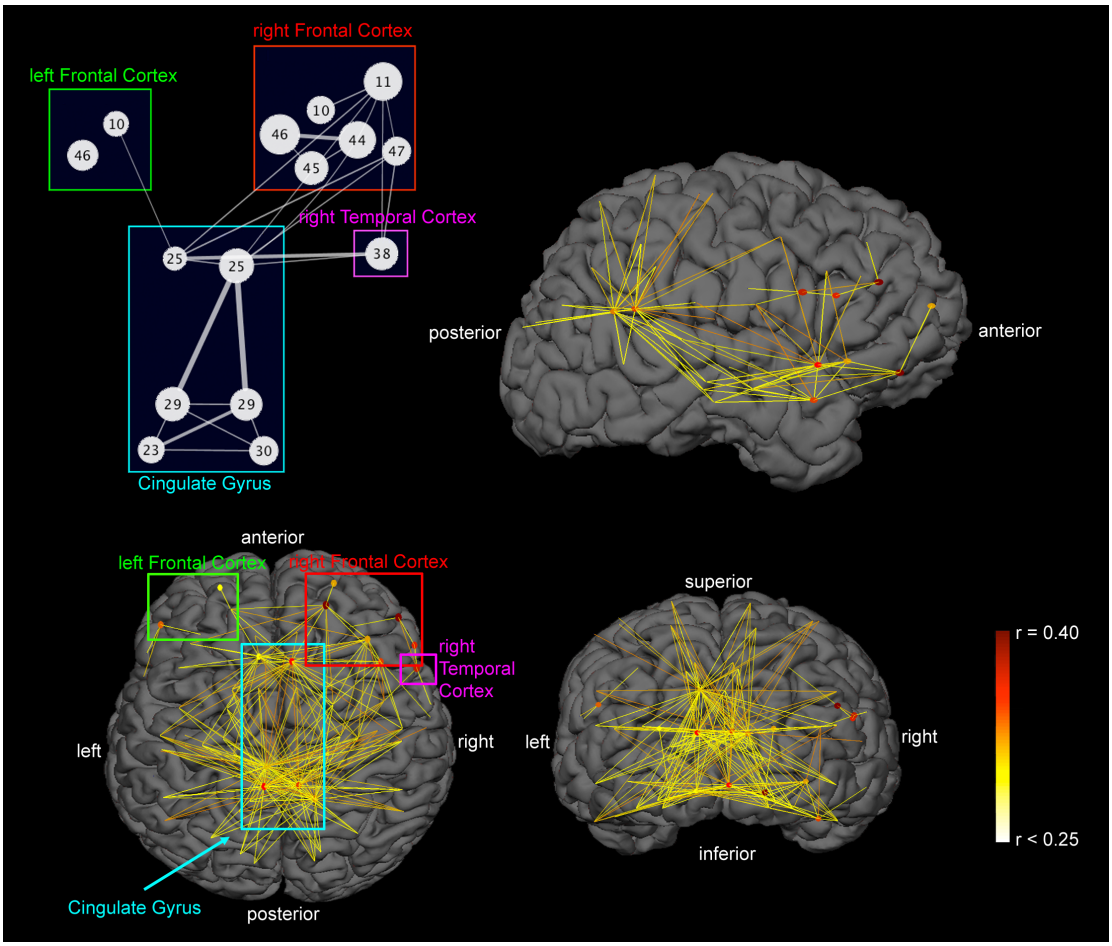

Figure 6. The weighted degree centrality measurements of the intracortical graph-theoretical network analysis, which were significant negatively correlated with intelligence, are displayed depending on the magnitude of the correlation coefficient (dark red accords to the highest correlation). A significant degree of a node is defined by exceeding the significance threshold $p<0.05$ (uncorrected for multiple comparisions). Furthermore, the connections of hub regions in which the hubs were positively correlated with the intelligence ($p<0.05$) are presented as lines between the different nodes. The hub regions in the image are shown according to a glass brain to facilitate the view of the entire network. In addition a schematic visualization of the network is provided, which includes the significant Brodmann areas and their interaction with each other. The size of the Brodmann areas represents the magnitude of the correlation with the RAPM.

4.1.5. Discussion

This study sought to delineate the relationship between functional brain network characteristics on the basis of resting state EEG and psychometric intelligence. The intra-individual stability of resting EEG measures has repeatedly been demonstrated (Vogel, 2000; Tang, Chorlian et al., 2007; Smit, Wright et al., 2006; Posthuma, Neale et al., 2001; Orekhova, Stroganova et al., 2003; Neuper, Grabner et al., 2005; Näpflin, Wildi et al., 2007; Linkenkaer-Hansen, Smit et al., 2007; Ivonin, Tsitseroshin et al., 2004; Anokhin, Müller et al., 2006; Ambrosius, Lietzenmaier et al., 2008). For example, Näpflin et al. (Holm, 1979)) showed that the shape of alpha band power spectra is fairly stable across 12-40 months. Their reliability measures revealed a sensitivity of 88% and specificity 99.5% for classifying individual subjects by their resting EEG measures. Other studies using more conventional reliability measures report strong retest reliabilities for the alpha and beta band power ranging from r_{tt}=0.8 to r_{tt} >0.9 (Näpflin, et al., 2007). Finally, on the basis of twin studies resting EEG measures have been demonstrated to be more similar in monozygotic twins than in dizygotic twins, thus resulting in high heritability scores for these measures (Tang, Chorlian et al., 2007; Smit, Wright et al., 2006; Posthuma, Neale et al., 2001; Orekhova, Stroganova et al., 2003; Linkenkaer-Hansen, Smit et al., 2007; Ivonin, Tsitseroshin et al., 2004; Anokhin, Müller et al., 2006; Ambrosius, Lietzenmaier et al., 2008). Thus, resting EEG can be taken as a stable biological marker for individual brain activity that can be related to cognitive performance. The resting state can be viewed as a kind of starting point from which subsequent cognitions are generated and monitored. Thus, a more efficient resting state (indexed by increased small-worldness) would be beneficial for subsequent cognitions (see

also reference (Kondacs and Szabó, 1999)). Our hypothesis was that more intelligent subjects rely on a functional resting state network that resembles more strongly a small-world network than less intelligent subjects. In fact we identified a significant correlation between small-worldness and psychometrically determined intelligence. Higher psychometric intelligence was associated with increased small-world organization of the upper alpha band. In the following, we will first discuss why the upper alpha band is so important for our study. Subsequently, we will then relate our findings in the network analysis to published findings in the neurophysiological and psychological literature.

A data driven approach was used for the scalp map analysis in which power values were obtained for the different frequency bands and the different electrodes were correlated with intelligence. Using this approach, we identified only one significant "electrode cluster" correlating with psychometric intelligence. This cluster was located on the right posterior scalp. This correlation was obtained for the upper alpha band. In addition, our intracortical source localization analysis revealed a significant correlation between the current densities of the upper alpha band in the right parietal cortex and psychometric intelligence, suggesting that the upper alpha band is a strong predictor of intelligence. Because the scalp map and intracortical source localization analysis revealed only significant results in the upper alpha band, we focused the graph-theoretical network analysis on the upper alpha band.

Alpha power emerges as a result of synchronous oscillations of synaptic potentials in large populations of neurons (mainly pyramidal cells) spread over the cortex (Klimesch, 1999). Although the exact mechanisms of alpha rhythm generation and its functional meaning are not yet fully understood, there is

mounting evidence that synchronized oscillatory activity in the cerebral cortex is essential for spatiotemporal information coordination and integration (Michel, et al., 2009; Singer and Gray, 1995; Varela, et al., 2001; Womelsdorf, et al., 2007). Several studies suggested that synchronized oscillatory activity in cell assemblies plays a key role in encoding, storage, and retrieval of information in the brain (Klimesch, 1999; Lisman and Idiart, 1995). Moreover, alpha power correlates positively with indices of mental activity level, academic performance in high school students, performance on memory tasks, and with the performance in intelligence tests (Birbaumer, et al., 1990; Klimesch, 1999).

The main purpose of our study was to identify a functional network associated with intelligence. Therefore, we applied a graph-theoretical network analysis using topographic EEG measures and intracortical current densities. Small-world networks are attractive models for the description of complex brain networks because these networks explain how the brain minimizes wiring costs while simultaneously maximizing the efficiency of information propagation and therefore are ideal to test neural efficiency theory and P-FIT intelligence (Achard and Bullmore, 2007; Golubeva, 1980; Kaiser and Hilgetag, 2006). Assuming that small-world networks reflect an optimal balance between local processing specialization/integration and global information propagation, the longer paths combined with lower clustering in the networks of less intelligent subjects indicate a deviation of the normal balance and render their networks more similar to a regular (less efficient) network configuration. It has been suggested that regular configurations have reduced signal propagation speed and synchronizability compared with small-world networks (Sporns, et al., 2004). A similar less efficient network architecture as found in the present study for the

less intelligent subjects (but to a lesser degree) was found in patients with Alzheimer‘s disease (de Haan, et al., 2009; Strogatz, 2001), schizophrenia (Stam, et al., 2007a) and brain tumor (Rubinov, et al., 2009). Thus, low performance in intelligence tests can be related to changes in small-world network characteristics that might reflect a less optimal topological network organization. Using diffusion tensor imaging (DTI), Li and colleagues (Bartolomei, et al., 2006) identified a similar relationship between small-world network indices (derived from fiber tractography) and psychometrical intelligence as we found in the present study.

Closer inspection of the hubs and nodes of the identified network revealed four most prominent brain areas in this network: the parietal lobe, the fusiform gyrus, the cingulate gyrus and the frontal cortex. The strongest positive correlations between degree centrality and intelligence were found bilaterally (more pronounced on the right hemisphere) in the parietal cortex (BA 5, 7, 39, 40). Thus, our *a priori* hypothesis with respect to the core role of the parietal cortex in monitoring intelligence was substantiated. The finding of the parietal cortex as a hub region in psychometric intelligence is in close correspondence with findings of other studies using fMRI or PET (Jung and Haier, 2007; Li, et al., 2009). In addition, Jung and Haier emphasized in their meta-analysis that more than 80% of the included studies report activations within BA 7 in association with the performance in intelligence tests (Gray, et al., 2003). The parietal cortex can thus be considered as a main hub region for controlling intelligence.

The fusiform gyrus (BA 37) is known as a processing centre for category specific perception (Jung and Haier, 2007), expert perception (Martin, et al., 1996) or logical rule identification (Wong, et al., 2009). In addition, changes in grey and

white matter in the parietal cortex and the fusiform gyrus were found in children with developmental dyscalculia compared to a control group (Tachibana, et al., 2009). The dominant left-sided involvement of the fusiform gyrus identified in our study needs additional explanation. First, left-sided activity in the fusiform gyrus has been identified as core activity related to intelligence in the meta-analysis by Jung and Haier (Rykhlevskaia, et al., 2009). In addition, the left-sided fusiform gyrus is known to be involved in retrieval of words (Jung and Haier, 2007) and in the imagination of perceiving objects (Tsapkini and Rapp, 2009). Thus, it is possible that solving intelligence tasks requires the application of imagination abilities. In the case of the intelligence test used in our study (RAPM), it is necessary to use mental imagery to determine whether a particular item fits into a particular pattern.

The third hub region was identified in the anterior cingulate gyrus (BA 24). This finding is in accordance with the finding of Haier and colleagues (Ishai, et al., 2000) who found the strongest functional connectivity between BA 19, 37 and the cingulate gyrus differentiating between subjects with high and low intelligence. They interpreted their results as individual differences in the ability to resolve competition among incoming visual stimuli (Haier, et al., 2003). The key role pinpointed here is response selection and response inhibition, which are psychological functions known to be related to activity in the anterior cingulate cortex. Although none of the previous studies investigated this issue from the perspective of a distributed brain network and did not relate this activity to small-world network characteristics, they nevertheless support our findings.

Negative correlations between degree centrality (local connectivity) and intelligence were found in the frontal cortex and the posterior cingulate gyrus.

The frontal cortex has been associated with decision-making, accommodation of novelty and planning complex cognitive behaviors, which could be summarized under the term executive function (Haier, et al., 2003; Miller and Cohen, 2001). Most studies investigating intelligence found intelligence-related activity in frontal brain areas (cf. reference (Andersen and Cui, 2009) for an extensive review). According to the neural efficiency theory (Jung and Haier, 2007), only specific brain areas such as the frontal regions demonstrate neural efficiency for intelligence, whereas other brain regions such as the parietal cortex show a positive association. Our results are exactly in line with these assumptions of the neural efficiency theory.

Further studies using graph-theoretical analysis at an intracortical level could be improved by referring to the individual brain anatomy, which creates less uncertainty for inverse modelling than an average brain. In addition, one of the unsolved problems in connectivity analysis based on EEG data is the volume conduction, although to a lesser extent in the intracortical space than at sensor level, which could even be improved by using only the lagged coherence. We used the coherence measure, because the other valid connectivity measure, phase synchrony as used by Singer and Gray (Neubauer and Fink, 2009), has not revealed any small world topology. Another issue in studying intelligence is the influence of age. We found a strong correlation between age and IQ and thus use age as a covariate to statistically eliminate age effects on the EEG data. However, the implicit assumption here is that age is linearly related to alpha2 activity; however, it might be that there are also non-linear associations, which we did not detect in our analyses (Fig. S2 & S3 and Table S6).

To our knowledge, this is the first study that investigated the relationship between psychometric intelligence and brain functional networks using intracortical current densities and graph-theoretical network analysis. We showed that psychometric intelligence correlates with small-word network properties of functional brain networks at the resting state. Increased performance in the intelligence test was associated (1) with a higher clustering coefficient reflecting increased local network efficiency and (2) with a shorter characteristic path length suggesting faster global information propagation. In other words, the more intelligent the subjects the more their functional network is organized according to a small-world network. Our results corroborated the P-FIT of intelligence (Singer and Gray, 1995) and emphasized the important role of a distributed network including parietal and frontal areas. Our finding is also in line with the neural efficiency hypothesis since this theory also emphasizes a fronto-parietal network that is important for intelligence (Jung and Haier, 2007).

4.1.6. References

Achard S, Bullmore E (2007): Efficiency and cost of economical brain functional networks. PLoS Comput Biol 3(2):e17.

Ambrosius U, Lietzenmaier S, Wehrle R, Wichniak A, Kalus S, Winkelmann J, Bettecken T, Holsboer F, Yassouridis A, Friess E (2008): Heritability of sleep electroencephalogram. Biol Psychiatry 64(4):344-8.

Andersen RA, Cui H (2009): Intention, action planning, and decision making in parietal-frontal circuits. Neuron 63(5):568-83.

Angelakis E, Lubar JF, Stathopoulou S (2004): Electroencephalographic peak alpha frequency correlates of cognitive traits. Neurosci Lett 371(1):60-3.

Annett M (1970): A classification of hand preference by association analysis. Br J Psychol 61(3):303-21.

Anokhin AP, Müller V, Lindenberger U, Heath AC, Myers E (2006): Genetic influences on dynamic complexity of brain oscillations. Neurosci Lett 397(1-2):93-8.

Babiloni C, Binetti G, Cassetta E, Cerboneschi D, Dal Forno G, Del Percio C, Ferreri F, Ferri R, Lanuzza B, Miniussi C, Moretti DV, Nobili F, Pascual-Marqui RD, Rodriguez G, Romani GL, Salinari S, Tecchio F, Vitali P, Zanetti O, Zappasodi F, Rossini PM (2004): Mapping distributed sources of cortical rhythms in mild Alzheimer's disease. A multicentric EEG study. Neuroimage 22(1):57-67.

Barrat A, Barthelemy M, Pastor-Satorras R, Vespignani A (2004): The architecture of complex weighted networks. Proc Natl Acad Sci U S A 101(11):3747-52.

Bartolomei F, Bosma I, Klein M, Baayen JC, Reijneveld JC, Postma TJ, Heimans JJ, van Dijk BW, de Munck JC, de Jongh A, Cover KS, Stam CJ (2006): Disturbed functional connectivity in brain tumour patients: evaluation by graph analysis of synchronization matrices. Clin Neurophysiol 117(9):2039-49.

Birbaumer N, Elbert T, Canavan AG, Rockstroh B (1990): Slow potentials of the cerebral cortex and behavior. Physiol Rev 70(1):1-41.

Brett M, Johnsrude IS, Owen AM (2002): The problem of functional localization in the human brain. Nature Reviews Neuroscience 3(3):243-249.

Brodmann K. (1909). Vergleichende Lokalisationslehre der Grosshirnrinde in ihren Prinzipien dargestellt auf Grund des Zellenbaues. Leipzig: Barth.

Bullmore E, Sporns O (2009): Complex brain networks: graph theoretical analysis of structural and functional systems. Nat Rev Neurosci 10(3):186-98.

de Haan W, Pijnenburg YA, Strijers RL, van der Made Y, van der Flier WM, Scheltens P, Stam CJ (2009): Functional neural network analysis in frontotemporal dementia and Alzheimer's disease using EEG and graph theory. BMC Neurosci 10:101.

De Vico Fallani F, Maglione A, Babiloni F, Mattia D, Astolfi L, Vecchiato G, De Rinaldis A, Salinari S, Pachou E, Micheloyannis S (2010): Cortical network analysis in patients affected by schizophrenia. Brain Topogr 23(2):214-20.

Deary IJ, Penke L, Johnson W (2010): The neuroscience of human intelligence differences. Nat Rev Neurosci 11(3):201-11.

Doppelmayr M, Klimesch W, Stadler W, Pöllhuber D, Heine C (2002): EEG alpha power and intelligence. Intelligence 30(3):289-302.

Eguíluz VM, Chialvo DR, Cecchi GA, Baliki M, Apkarian AV (2005): Scale-free brain functional networks. Phys Rev Lett 94(1):018102.

Evans AC, Collins DL, Mills SR, Brwon ED, Kelly RL, Pters TM. (1993): 3d statistical neuroanatomical models from 305 MRI volumes. In: Processings IEEE Nuclear Science Symposium and Medical Imaging Conference. San Francisco CA. p 1813-1817.

Fisher RA. (1935). The Design of Experiment. New York: Hafner.

Freeman LC (1978): Centrality in social networks: Conceptual clarification. Social Networks 1:215-239.

Fuchs M, Kastner J, Wagner M, Hawes S, Ebersole JS (2002): A standardized boundary element method volume conductor model. Clinical Neurophysiology 113(5):702-712.

Geweke J (1982): Measurement of Linear-Dependence and Feedback between Multiple Time-Series. Journal of the American Statistical Association 77(378):304-313.

Golubeva EA. (1980). Individual characteristics of human memory: A psychophysiological study. Moscow.

Gray JR, Chabris CF, Braver TS (2003): Neural mechanisms of general fluid intelligence. Nat Neurosci 6(3):316-22.

Gray JR, Thompson PM (2004): Neurobiology of intelligence: science and ethics. Nat Rev Neurosci 5(6):471-82.

Haier RJ, White NS, Alkire MT (2003): Individual differences in general intelligence correlate with brain function during nonreasoning tasks. Intelligence 31(5):429-441.

Herculano-Houzel S (2009): The human brain in numbers: a linearly scaled-up primate brain. Frontiers in human neuroscience 3:31.

Holm S (1979): A simple sequentially rejective multiple test procedure Scandinavian Journal of Statistics(6):65-70.

Humphries MD, Gurney K (2008): Network 'small-world-ness': a quantitative method for determining canonical network equivalence. PLoS One 3(4):e0002051.

Humphries MD, Gurney K, Prescott TJ (2006): The brainstem reticular formation is a small-world, not scale-free, network. Proc Biol Sci 273(1585):503-11.

Ishai A, Ungerleider LG, Haxby JV (2000): Distributed neural systems for the generation of visual images. Neuron 28(3):979-90.

Ivonin AA, Tsitseroshin MN, Pogosyan AA, Shuvaev VT (2004): Genetic determination of neurophysiological mechanisms of cortical-subcortical integration of bioelectrical brain activity. Neurosci Behav Physiol 34(4):369-78.

Jann K, Koenig T, Dierks T, Boesch C, Federspiel A (2010): Association of individual resting state EEG alpha frequency and cerebral blood flow. Neuroimage 51(1):365-72.

Jausovec N, Jausovec K (2000): Differences in resting EEG related to ability. Brain Topogr 12(3):229-40.

Jung RE, Haier RJ (2007): The Parieto-Frontal Integration Theory (P-FIT) of intelligence: converging neuroimaging evidence. Behav Brain Sci 30(2):135-54; discussion 154-87.

Jurcak V, Tsuzuki D, Dan I (2007): 10/20, 10/10, and 10/5 systems revisited: Their validity as relative head-surface-based positioning systems. Neuroimage 34(4):1600-1611.

Kaiser M, Hilgetag CC (2006): Nonoptimal component placement, but short processing paths, due to long-distance projections in neural systems. PLoS Comput Biol 2(7):e95.

Klimesch W (1999): EEG alpha and theta oscillations reflect cognitive and memory performance: a review and analysis. Brain Res Brain Res Rev 29(2-3):169-95.

Kondacs A, Szabó M (1999): Long-term intra-individual variability of the background EEG in normals. Clinical neurophysiology : official journal of the International Federation of Clinical Neurophysiology 110(10):1708-16.

Kubicki S, Herrmann WM, Fichte K, Freund G (1979): Reflections on the topics: EEG frequency bands and regulation of vigilance. Pharmakopsychiatr Neuropsychopharmakol 12(2):237-45.

Lancaster JL, Woldorff MG, Parsons LM, Liotti M, Freitas ES, Rainey L, Kochunov PV, Nickerson D, Mikiten SA, Fox PT (2000): Automated Talairach Atlas labels for functional brain mapping. Human Brain Mapping 10(3):120-131.

Langer N, Beeli G, Jancke L (2010): When the sun prickles your nose: an EEG study identifying neural bases of photic sneezing. PLoS One 5(2):e9208.

Laufs H (2008): Endogenous brain oscillations and related networks detected by surface EEG-combined fMRI. Hum Brain Mapp 29(7):762-9.

Lehmann D, Faber PL, Gianotti LR, Kochi K, Pascual-Marqui RD (2006): Coherence and phase locking in the scalp EEG and between LORETA model sources, and microstates as putative mechanisms of brain temporo-spatial functional organization. J Physiol Paris 99(1):29-36.

Li Y, Liu Y, Li J, Qin W, Li K, Yu C, Jiang T (2009): Brain anatomical network and intelligence. PLoS Comput Biol 5(5):e1000395.

Linkenkaer-Hansen K, Smit DJ, Barkil A, van Beijsterveldt TE, Brussaard AB, Boomsma DI, van Ooyen A, de Geus EJ (2007): Genetic contributions to long-range temporal correlations in ongoing oscillations. J Neurosci 27(50):13882-9.

Lisman JE, Idiart MA (1995): Storage of 7 +/- 2 short-term memories in oscillatory subcycles. Science 267(5203):1512-5.

Martin A, Wiggs CL, Ungerleider LG, Haxby JV (1996): Neural correlates of category-specific knowledge. Nature 379(6566):649-52.

Mazziotta J, Toga A, Evans A, Fox P, Lancaster J, Zilles K, Woods R, Paus T, Simpson G, Pike B, Holmes C, Collins L, Thompson P, MacDonald D, Iacoboni M, Schormann T, Amunts K, Palomero-Gallagher N, Geyer S, Parsons L, Narr K, Kabani N, Le Goualher G, Boomsma D, Cannon T, Kawashima R, Mazoyer

B (2001): A probabilistic atlas and reference system for the human brain: International Consortium for Brain Mapping (ICBM). Philosophical Transactions of the Royal Society B-Biological Sciences 356(1412):1293-1322.

Michel CM, Koenig T, Brandeis D, Gianotti LR, Wackermann J. (2009). Electrical Neuroimaging. Cambridge: Cambridge University Press.

Micheloyannis S, Pachou E, Stam CJ, Vourkas M, Erimaki S, Tsirka V (2006): Using graph theoretical analysis of multi channel EEG to evaluate the neural efficiency hypothesis. Neurosci Lett 402(3):273-7.

Micheloyannis S, Vourkas M, Tsirka V, Karakonstantaki E, Kanatsouli K, Stam CJ (2009): The influence of ageing on complex brain networks: a graph theoretical analysis. Hum Brain Mapp 30(1):200-8.

Miller EK, Cohen JD (2001): An integrative theory of prefrontal cortex function. Annu Rev Neurosci 24:167-202.

Mulert C, Jager L, Schmitt R, Bussfeld P, Pogarell O, Moller HJ, Juckel G, Hegerl U (2004): Integration of fMRI and simultaneous EEG: towards a comprehensive understanding of localization and time-course of brain activity in target detection. Neuroimage 22(1):83-94.

Näpflin M, Wildi M, Sarnthein J (2007): Test-retest reliability of resting EEG spectra validates a statistical signature of persons. Clinical neurophysiology : official journal of the International Federation of Clinical Neurophysiology 118(11):2519-24.

Neubauer AC, Fink A (2009): Intelligence and neural efficiency. Neurosci Biobehav Rev 33(7):1004-23.

Neuper C, Grabner RH, Fink A, Neubauer AC (2005): Long-term stability and consistency of EEG event-related (de-)synchronization across different cognitive tasks. Clin Neurophysiol 116(7):1681-94.

Newman ME (2004): Analysis of weighted networks. Phys Rev E Stat Nonlin Soft Matter Phys 70(5 Pt 2):056131.

Nichols TE, Holmes AP (2002): Nonparametric permutation tests for functional neuroimaging: A primer with examples. Human Brain Mapping 15(1):1-25.

Oostenveld R, Praamstra P (2001): The five percent electrode system for high-resolution EEG and ERP measurements. Clinical Neurophysiology 112(4):713-719.

Opsahl T. (2009): Structure and evolution of weighted networks. London: University of London (Queen Mary College).

Opsahl T, Colizza V, Panzarasa P, Ramasco JJ (2008): Prominence and Control: The Weighted Rich-Club Effect. Physical Review Letters 101(16):-.

Opsahl T, Panzarasa P (2009): Clustering in weighted networks. Social Networks 31(2):155-163.

Orekhova EV, Stroganova TA, Posikera IN, Malykh SB (2003): Heritability and "environmentability" of electroencephalogram in infants: the twin study. Psychophysiology 40(5):727-41.

Pascual-Marqui RD (2002): Standardized low-resolution brain electromagnetic tomography (sLORETA): technical details. Methods Find Exp Clin Pharmacol 24 Suppl D:5-12.

Pascual-Marqui RD. (2007a): Discrete, 3D distributed, linear imaging methods of electrical neuronal activity. Part 1: exact, zerror error localization. .

Pascual-Marqui RD. (2007b): Instantaneous and lagged measurements of linear and nonlinear dependence between groups of multivariate times series: frequency decomposition. arXiv:0711.1455[stat.ME].

Perrin F, Pernier J, Bertrand O, Giard MH, Echallier JF (1987): Mapping of scalp potentials by surface spline interpolation. Electroencephalogr Clin Neurophysiol 66(1):75-81.

Posthuma D, Neale MC, Boomsma DI, de Geus EJ (2001): Are smarter brains running faster? Heritability of alpha peak frequency, IQ, and their interrelation. Behav Genet 31(6):567-79.

Raven J, Raven, J.C., Court, J.H. (2003). Manual for Raven's Progressive Matrices and Vocabulary Scales. Section1: General Overview. San Antonia: Harcourt Assessment.

Reijneveld JC, Ponten SC, Berendse HW, Stam CJ (2007): The application of graph theoretical analysis to complex networks in the brain. Clinical neurophysiology : official journal of the International Federation of Clinical Neurophysiology 118(11):2317-31.

Rubinov M, Knock SA, Stam CJ, Micheloyannis S, Harris AW, Williams LM, Breakspear M (2009): Small-world properties of nonlinear brain activity in schizophrenia. Hum Brain Mapp 30(2):403-16.

Rykhlevskaia E, Uddin LQ, Kondos L, Menon V (2009): Neuroanatomical correlates of developmental dyscalculia: combined evidence from morphometry and tractography. Front Hum Neurosci 3:51.

Shaffer JP (1995): Mutiple hypothesis testing. Annual Review of Psychology(46):561-584.

Sinai A, Pratt H (2003): High-resolution time course of hemispheric dominance revealed by low-resolution electromagnetic tomography. Clin Neurophysiol 114(7):1181-8.

Singer W, Gray CM (1995): Visual feature integration and the temporal correlation hypothesis. Annu Rev Neurosci 18:555-86.

Smit CM, Wright MJ, Hansell NK, Geffen GM, Martin NG (2006): Genetic variation of individual alpha frequency (IAF) and alpha power in a large adolescent twin sample. Int J Psychophysiol 61(2):235-43.

Sporns O, Chialvo DR, Kaiser M, Hilgetag CC (2004): Organization, development and function of complex brain networks. Trends Cogn Sci 8(9):418-25.

Sporns O, Kötter R (2004): Motifs in brain networks. PLoS Biol 2(11):e369.

Sporns O, Zwi JD (2004): The small world of the cerebral cortex. Neuroinformatics 2(2):145-62.

Stam CJ (2004): Functional connectivity patterns of human magnetoencephalographic recordings: a 'small-world' network? Neurosci Lett 355(1-2):25-8.

Stam CJ, Jones BF, Nolte G, Breakspear M, Scheltens P (2007): Small-world networks and functional connectivity in Alzheimer's disease. Cereb Cortex 17(1):92-9.

Stam CJ, Reijneveld JC (2007): Graph theoretical analysis of complex networks in the brain. Nonlinear Biomed Phys 1(1):3.

Strogatz SH (2001): Exploring complex networks. Nature 410(6825):268-76.

Tachibana K, Suzuki K, Mori E, Miura N, Kawashima R, Horie K, Sato S, Tanji J, Mushiake H (2009): Neural activity in the human brain signals logical rule identification. J Neurophysiol 102(3):1526-37.

Tang Y, Chorlian DB, Rangaswamy M, Porjesz B, Bauer L, Kuperman S, O'Connor S, Rohrbaugh J, Schuckit M, Stimus A, Begleiter H (2007): Genetic influences on bipolar EEG power spectra. Int J Psychophysiol 65(1):2-9.

Thatcher RW, North D, Biver C (2007): Intelligence and EEG current density using low-resolution electromagnetic tomography (LORETA). Hum Brain Mapp 28(2):118-33.

Thatcher RW, North DM, Biver CJ (2008): Intelligence and EEG phase reset: a two compartmental model of phase shift and lock. Neuroimage 42(4):1639-53.

Tsapkini K, Rapp B (2009): The orthography-specific functions of the left fusiform gyrus: Evidence of modality and category specificity. Cortex.

van den Heuvel MP, Stam CJ, Kahn RS, Hulshoff Pol HE (2009): Efficiency of Functional Brain Networks and Intellectual Performance. J. Neurosci. 29(23):7619-7624.

Varela F, Lachaux JP, Rodriguez E, Martinerie J (2001): The brainweb: phase synchronization and large-scale integration. Nat Rev Neurosci 2(4):229-39.

Vogel F. (2000). Genetics and the electroencephalogram. Berlin: Springer.

Wasserman S, Faust K. (1994). Social Network Analysis. Cambridge, MA: Cambridge University Press.

Watts DJ, Strogatz SH (1998): Collective dynamics of 'small-world' networks. Nature 393(6684):440-2.

Womelsdorf T, Schoffelen JM, Oostenveld R, Singer W, Desimone R, Engel AK, Fries P (2007): Modulation of neuronal interactions through neuronal synchronization. Science 316(5831):1609-12.

Wong ACN, Palmeri TJ, Rogers BP, Gore JC, Gauthier I (2009): Beyond Shape: How You Learn about Objects Affects How They Are Represented in Visual Cortex. PLoS One 4(12):e8405.

Yu S, Huang D, Singer W, Nikolic D (2008): A small world of neuronal synchrony. Cereb Cortex 18(12):2891-901.

Zaehle T, Frund I, Schadow J, Tharig S, Schoenfeld MA, Herrmann CS (2009): Inter- and intra-individual covariations of hemodynamic and oscillatory gamma responses in the human cortex. Front Hum Neurosci 3:8.

4.1.7. Supplementary Data

Table S1 related to figure 4. All hub regions of the intracortical graph-theoretical network analysis and their Brodmann area label are listed. The significant positive correlation coefficients between their degree centrality measurements and the performance in the RAPM are in bold numbers highlighted.

Brodmann Area left hemisphere	Spearmann correlation r	Brodmann Area right hemisphere	Spearmann correlation r
1	-0.180	1	0.087
2	0.135	2	**0.336**
3	0.210	3	0.210
4	0.217	4	0.194
5	**0.361**	5	**0.391**
6	0.000	6	0.051
7	0.225	7	**0.335**
8	-0.121	8	0.117
9	-0.120	9	-0.136
10	-0.258	10	-0.284
11	-0.135	11	-0.389
13	0.172	13	0.159
17	0.176	17	-0.028
18	0.005	18	-0.025
19	-0.157	19	0.038
20	0.010	20	0.074
21	-0.054	21	0.030
22	0.038	22	0.212
23	-0.271	23	-0.197
24	**0.261**	24	**0.249**
25	-0.243	25	-0.353
27	-0.056	27	-0.144
28	-0.196	28	-0.204
29	-0.348	29	-0.327
30	-0.197	30	-0.295
31	-0.189	31	0.010
32	-0.193	32	-0.226
33	-0.067	33	-0.060
34	-0.176	34	-0.203
35	-0.136	35	-0.083
36	0.023	36	-0.036
37	**0.271**	37	0.020
38	-0.178	38	-0.332
39	0.212	39	**0.252**
40	0.101	40	**0.307**
41	0.141	41	-0.007
42	-0.056	42	0.209
43	-0.118	43	0.035
44	-0.041	44	-0.378
45	-0.047	45	-0.341
46	-0.313	46	-0.406
47	-0.129	47	-0.292

Table S2 related to figure 5. All hub regions of the intracortical graph-theoretical network analysis and their Brodmann area label are listed. The significant negative correlation coefficients between their degree centrality measurements and the performance in the RAPM are in bold numbers highlighted.

Brodmann Area left hemisphere	Spearmann correlation r	Brodmann Area right hemisphere	Spearmann correlation r
1	-0.180	1	0.087
2	0.135	2	0.336
3	0.210	3	0.210
4	0.217	4	0.194
5	0.361	5	0.39
6	0.000	6	0.051
7	0.225	7	0.335
8	-0.121	8	0.117
9	-0.120	9	-0.136
10	**-0.258**	10	**-0.284**
11	-0.135	11	**-0.389**
13	0.172	13	0.159
17	0.176	17	-0.028
18	0.005	18	-0.025
19	-0.157	19	0.038
20	0.010	20	0.074
21	-0.054	21	0.030
22	0.038	22	0.212
23	**-0.271**	23	-0.197
24	0.261	24	0.249
25	**-0.243**	25	**-0.353**
27	-0.056	27	-0.144
28	-0.196	28	-0.204
29	**-0.348**	29	**-0.327**
30	-0.197	30	**-0.295**
31	-0.189	31	0.010
32	-0.193	32	-0.226
33	-0.067	33	-0.060
34	-0.176	34	-0.203
35	-0.136	35	-0.083
36	0.023	36	-0.036
37	0.271	37	0.020
38	-0.178	38	**-0.332**
39	0.212	39	0.252
40	0.101	40	0.307
41	0.141	41	-0.007
42	-0.056	42	0.209
43	-0.118	43	0.035
44	-0.041	44	**-0.378**
45	-0.047	45	**-0.341**
46	**-0.313**	46	**-0.406**
47	-0.129	47	**-0.292**

Table S6. Listed are the correlations coefficients of the age-uncorrected correlation analysis between the *small-world* indices (C = Clustering Coefficient; L = path length) of the intracortical graph-theoretical network analysis and the intelligence performance. In addition, the p value whit the correlations are presented ($p < 0.05$, corrected for multiple comparisons).

	Edges	**C**	**L**
r	0.403	0.430	-0.379
p	0.0009	0.0004	0.0019

Table S7. Listed are the correlation coefficients of the partial correlation analysis between the *small-world* indices of the intracortical graph-theoretical network analysis and the intelligence performance for all further frequency bands (not upper alpha). The p-values associated with the correlation coefficients are also presented. There were no significant correlations.

		Edges	Density	C	L
delta	r	0.15	0.15	0.001	-0.14
	p	0.23	0.23	0.99	0.28
theta	r	0.11	0.11	0.14	-0.10
	p	0.40	0.40	0.28	0.41
alpha1	r	0.18	0.18	0.12	-0.19
	p	0.15	0.15	0.33	0.12
beta1	r	0.18	0.18	0.12	-0.19
	p	0.15	0.15	0.33	0.12
beta2	r	0.16	0.16	0.20	-0.04
	p	0.20	0.20	0.10	0.76
beta3	r	0.14	0.14	0.15	-0.11
	p	0.25	0.25	0.22	0.38
gamma	r	0.08	0.08	0.10	-0.09
	p	0.53	0.53	0.42	0.47

Table S8. Listed are the results of the betweenness centrality analysis. Betweenness centrality relies on the calculation of shortest distances in the network. Nodes that occur on many shortest paths (geodesics) between other nodes have higher betweenness centrality than those that do not. A node with high betweenness centrality is interpreted as a gatekeeper that is able to control the information flow through the node. For the alpha2 frequency bands, all nodes of the intracortical graph-theoretical network analysis, which revealed significantly positive or negative correlation between betweenness centraliy and intelligence, are listed with their Brodmann area label and the correlation coefficients ($p<0.05$, uncorrected for multiple comparisons).

	hemisphere	**BA**	**r**
betweenness positive correlations	left	9	0.25
	left	24	0.25
	right	24	0.24
	right	37	0.24
betweenness negative correlations	left	20	-0.27
	left	21	-0.30
	left	30	-0.28
	left	31	-0.31
	right	2	-0.23
	right	30	-0.25
	right	31	-0.26

Graph-theoretical network analysis with topographical data

Methods

In an additional step, topographical data was used to conduct the graph-theoretical network analysis based on complex frequency data the coherence between all channels (cross-correlation). For our analysis, measures of linear dependence (coherence) were used. Based on complex frequency data the coherence between all channels (cross-correlation) was calculated for each subject individually. The coherence provides an indication of the dependence of the data between the individual electrodes (111 electrodes). The coherence was calculated using the following formula:

(1) $Coh(c1, c2)(f) = | Cov(c1, c2)(f) |^2 / (| Cov(c1, c1)(f) | | Cov(c2, c2)(f) |)$,

in conjunction with

(2) $Cov(c1, c2)(f) = \Sigma (c1, i (f) – avg(c1 (f))) (c2, i (f) – avg(c2 (f)))^*$.

Coherence (Coh); Covariance (Cov); Frequency (f) and Electrodes (c)

This method results in an 111x111 connectivity matrix for each subject with correlation coefficients ranging between 0 and 1, which represent the edges of our networks (graphs).

For the following graph-theoretical analysis we used the identical procedure as applied to the intracortical graph-theoretical network analysis (as described in the main text).

Results

The network with the best *small-world* organization characteristics of the average correlation matrix is comprised of 111 nodes and 1349 edges; connection

density: 0.2209. The analysis of binary and weighted networks revealed qualitatively similar results; hence, we focus on the results derived from the undirected weighted network analysis. Across the whole range of relevant correlation thresholds, the threshold of r = 0.35 elucidated the network that represents the best small world network organization, which is defined by a high γ and a $\lambda \approx 1$. Table S3 display all *small-world* indices for the differently thresholded average matrix.

Table S3. Listed are the *small-world* indices of the differently thresholded mean correlation matrix of the topographical analysis. Across the whole range of relevant correlation thresholds, the threshold of r = 0.35 (bold) elucidated the network, which represents the best *small-world* network organization.

Threshold (correlation coefficient)	**0.2**	**0.25**	**0.3**	**0.35**	**0.4**	**0.45**	**0.5**
Edges	2630	2108	1691	**1349**	1038	791	580
Density	0.431	0.345	0.277	**0.221**	0.17	0.13	0.095
Clustering Coefficient Cω	0.762	0.737	0.711	**0.685**	0.643	0.609	0.585
Path Length C_L	1.724	1.912	2.107	**2.319**	2.617	2.983	3.511
Gamma γ	1.473	1.684	1.964	**2.4**	3.271	5.123	10.473
Lamda λ	1.427	1.424	1.427	**1.442**	1.487	1.554	1.642

The threshold of r = 0.35 was then applied to each subject's correlation matrix and the network indices (edges, density, clustering coefficient, path length) for each subject were computed. The partial correlation analyses between these *small-world* indices and the performance in the RAPM revealed significant results. Whereas the edges (r = 0.303, p = 0.009) and clustering coefficient (r = 0.294, p = 0.012) demonstrated a positive correlation with the RAPM, the path length (r = -.289, p = 0.013) exhibited a negative relationship with the RAPM. All correlation analyses are summarized in Table S4.

Table S4. Presented are the correlations coefficients of the partial correlation analysis between the small-world indices of the topographical analysis and the intelligence performance. In

addition the p value if the correlations are listed. Cω = clustering coefficient; C_L = path length

	Edges	Cω	C_L
r	0.303	0.294	-0.289
p	0.009	0.012	0.013

Identification of hub regions: Hub regions were evaluated by weighted degree centrality measurements at the correlation threshold that represents the best small-world organization properties (r = 0.35). The weighted degree centrality scores are plotted as networks in Figure S1. The weighted degree centrality measurements of these hub regions are summarized in Table S5.

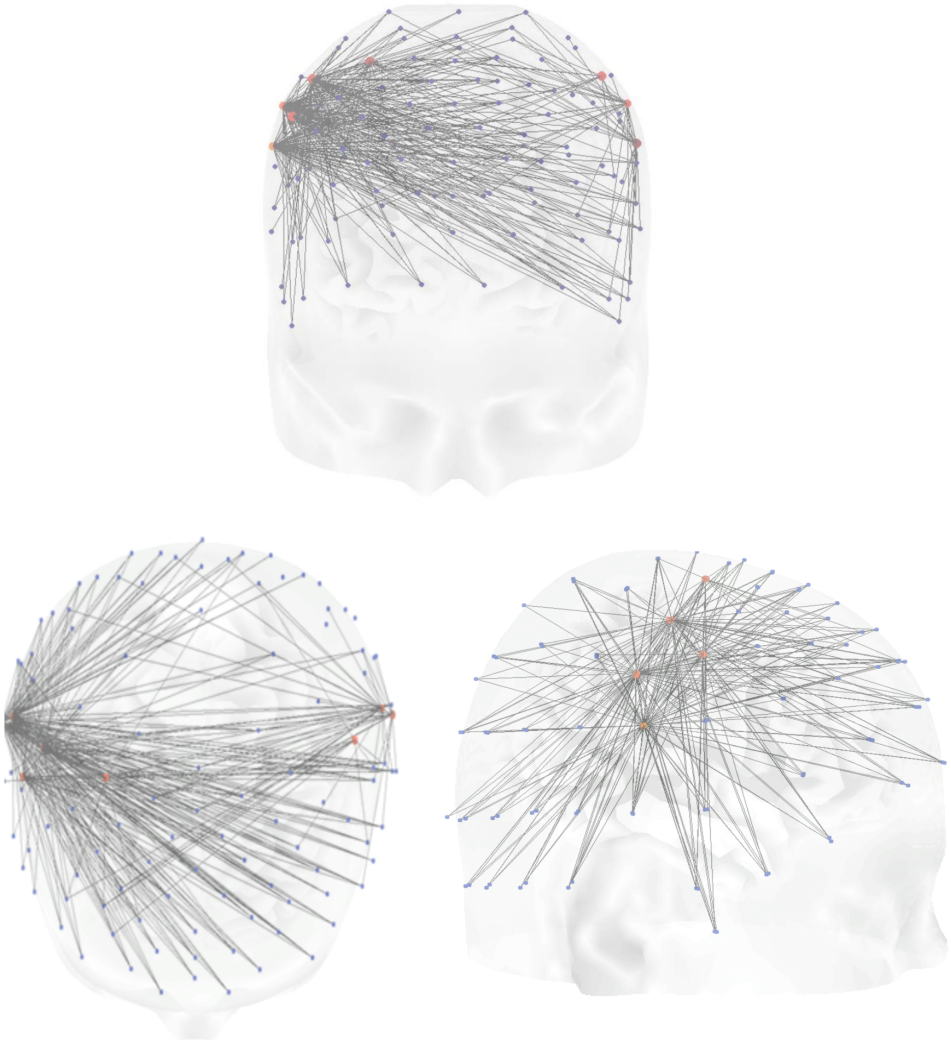

Figure S1. The weighted degree centrality measurements of the topographical analysis, which were significantly and positively correlated with psychometric intelligence, are displayed as red dots. Furthermore, the connections of the significant degrees, which exhibit a significant correlation with the RAPM, are presented as grey lines between the nodes.

Significant positive correlations of the RAPM with the topological organization of the hub regions were found primarily in electrodes over the right parietal cortex. Higher intelligence score goes with higher degree centrality in the electrodes over the right parietal cortex.

Table S5. All hub regions of the topographical analysis and the X, Y, Z coordinates in the MNI-space of the electrodes are listed. The significant positive correlation coefficients between their degree centrality measurements and the performance in the RAPM are in bold numbers highlighted.

MNI-coordinates			Spearman	MNI-coordinates			Spearman
X	Y	Z	correlation r	X	Y	Z	correlation r
69	40	-26	-0.252	-31	-69	87	-0.034
58	56	17	-0.266	-1	-89	76	-0.092
36	59	49	-0.128	-55	-90	-46	-0.126
25	53	64	0.065	-51	-101	-17	0.042
13	42	77	0.215	-44	-105	20	-0.137
1	30	85	0.030	-25	-101	53	-0.191
-10	14	91	0.013	-35	-104	-47	-0.044
49	70	-2	-0.258	-30	-114	-18	-0.094
29	75	31	-0.149	-19	-115	20	-0.109
18	67	52	-0.048	-1	-109	44	-0.181
1	58	66	0.189	-12	-112	-47	-0.037
-11	41	77	0.202	-1	-121	-17	0.071
-19	25	83	0.027	16	-115	20	0.077
16	86	7	-0.309	24	-101	54	-0.103
2	79	35	-0.094	31	-68	88	0.042
2	70	51	0.005	25	-33	97	0.203
-15	67	52	0.011	19	-3	95	0.057
-22	52	64	0.032	10	-113	-48	-0.001
-31	37	70	0.037	28	-115	-19	0.106
-13	86	7	-0.192	43	-104	20	0.053
-26	75	31	-0.180	53	-81	59	-0.003
-34	58	49	-0.055	50	-45	84	0.125
-38	45	59	-0.036	39	-13	88	**0.288**
-48	70	-3	-0.364	34	-104	-48	0.102
-57	55	17	-0.285	50	-101	-18	0.106
-54	41	44	-0.144	62	-88	21	0.027
-50	30	59	-0.141	70	-57	54	0.127
-42	20	73	0.000	65	-26	70	**0.268**
-33	8	84	-0.023	55	-89	-48	0.130
-18	-4	95	0.181	67	-84	-15	0.050
-69	37	-28	-0.240	75	-64	23	0.154
-73	26	1	-0.162	79	-40	46	**0.257**
-71	17	35	-0.163	70	-69	-48	0.182
-63	7	58	-0.063	76	-66	-16	0.190
-53	-1	74	0.025	83	-37	23	**0.239**
-39	-15	88	0.154	74	-13	55	**0.269**
-77	10	-43	-0.040	53	2	73	0.158
-83	-15	-14	0.153	34	9	84	-0.017
-82	-15	25	0.083	11	15	91	-0.034
-74	-17	54	0.139	83	-42	-16	0.143
-66	-30	70	**0.269**	82	-11	26	0.164
-74	-11	-68	0.012	64	10	58	0.081
-78	-19	-49	0.094	43	22	73	-0.059
-81	-46	-15	0.167	21	26	83	-0.003
-82	-41	23	**0.306**	79	-15	-49	0.065
-77	-44	45	**0.259**	84	-11	-14	-0.075
-75	-68	-15	0.184	72	21	35	-0.314
-74	-67	22	0.055	51	32	59	-0.212
-70	-60	54	0.108	33	38	70	0.058
-50	-47	83	0.134	75	-7	-68	-0.008
-25	-34	97	0.159	78	14	-42	-0.175
0	-17	100	0.107	74	29	2	-0.316
-69	-71	-46	0.047	56	43	44	-0.328
-66	-85	-14	-0.002	40	46	59	-0.107
-62	-89	21	-0.036	1	3	96	0.013
-54	**-82**	**58**	**-0.084**				

4.2. Experiment 2: The Effects of Working Memory Training on Functional Brain Network Efficiency

Langer, N.[1,a] von Bastian, C. C.[2] Wirz, H.[1], Oberauer K.[2], Jäncke, L.[1,3]

[1] Division Neuropsychology, Department of Psychology, University of Zurich, 8050 Zurich, Switzerland

[2] Division Cognitive Psychology, Department of Psychology, University of Zurich, 8050 Zurich, Switzerland

[3] The International Normal Aging and Plasticity Imaging Center

4.2.1. Abstract

The human brain is a highly interconnected network. Recent studies have shown that the functional and anatomical features of this network are organized in an efficient small-world manner that confer high efficiency of information processing at relatively low connection cost. However, it has been unclear how the architecture of functional brain networks is related to performance in working memory (WM) tasks and if these networks can be modified by WM training. Therefore, we conducted a double-blind training study enrolling 66 young adults. Half of the subjects practiced three WM tasks and were compared to an active control group practicing three tasks with low WM demand. High-density resting-state EEG was recorded before and after training to analyze graph-theoretical functional network characteristics at an intra-cortical level. WM performance was uniquely correlated with power in the theta frequency and theta power was increased by WM training. Moreover, the better a person's WM performance, the more their network exhibited small-world topology. WM training shifted network characteristics in the direction of high-performers, showing increased small-worldness within a distributed fronto-parietal network.

Taken together, this is the first longitudinal study which provides evidence for the plasticity of the functional brain network underlying working memory.

4.2.2. Introduction

Our perceptions, thoughts and experiences are the product of dynamic interactions occurring between functionally specialized regions of the brain. Better understanding of such phenomena will only be possible once we understand how these interactions are organized and coordinated. Recent studies have shown that the functional and anatomical features of this network are organized in an efficient small-world manner (Bassett and Bullmore, 2009; Bullmore and Sporns, 2009; Neubauer and Fink, 2009). Typical features of small-world networks are high *clustering coefficients* and low characteristic *path lengths* (Bullmore and Bassett, 2011). A high *clustering coefficient* is characterized by a high level of local neighborhood clustering, which is responsible for efficient local information processing. A low *path length* characterizes a high level of global communication efficiency (Achard and Bullmore, 2007; Bullmore and Bassett, 2011; Watts and Strogatz, 1998).

In this study, we are interested in the functional network organization underlying working memory (WM) performance. WM is defined as the ability to maintain and manipulate information for higher order cognition (Baddeley, 2003; Baddeley, 2002; Sporns and Zwi, 2004). It has been shown to be crucial for daily life skills, such as reading comprehension (Jonides, et al., 2008), planning and problem-solving (deJonge and deJong, 1996), and to learn new skills (Shah and Miyake, 1999). The involvement of fronto-parietal regions in WM tasks was shown with different neuroimaging methods such as the intracranial electroencephalography (Meltzer, et al., 2008; Pickering, 2006), functional magnetic imaging (Raghavachari, et al., 2006) and transcranial magnetic stimulation (Owen, et al., 2005).

Whether individual differences in WM ability are related to a specific small-world network organization has not been studied so far. Further, it is unclear to date, whether WM related small-world networks can be changed and optimized by WM training. In general, there is no study investigating the possible adaptive capacity of small-world networks.

Here we calculated small-world properties of functional brain networks on the basis of high-density EEG coherence measures on an intracortical level. Previous EEG studies showed increased theta band coherence in frontal and parietal regions during a difficult WM task (Oliveri, et al., 2001). Patients with a WM deficit, such as those suffering from Alzheimer's disease or schizophrenia, exhibit reduced fronto-parietal EEG coherence mainly in theta (Babiloni, et al., 2004b; Ford, et al., 2002; Hogan, et al., 2003; Sauseng, et al., 2005; Uhlhaas and Singer, 2006). Therefore, we expected small-world characteristics in the functional network within the theta band to reflect individual differences and training effects on WM. Our first hypothesis is that the functional small-world topology of theta-band coherence inter-individually varies as a function of WM performance. Second, we anticipate a change in the theta band based small-world topology as a consequence of an intensive WM training, especially in parietal and frontal regions. Because some studies also identified relationships between WM and other frequencies (Hsieh, et al., 2011; Klimesch, 1999; Palva, et al., 2010a; Winterer, et al., 2003), we did not limit our analysis to the theta band, but rather performed a scalp map analysis for the whole frequency spectrum.

4.2.3. Methods

Subjects

Sixty-six young adults participated in the study. Thirty-four (mean age: 23±3.90, 22 females) trained on three WM tasks, representing the three functional categories of the WM model of Oberauer (Polania, et al., 2011). An active control group of 32 subjects (mean age: 23±3.86, 21 females) practiced tasks with low WM demand. Participants were assigned to the two groups at random. The two groups were matched according to age, gender, experience using a computer, and cognitive activity in daily life. All were consistently right-handed according to the Annett-Handedness-Questionnaire (Oberauer, et al., 2003), and highly proficient Swiss German or German Speakers. Subjects reported no history of psychiatric or neurological disease, neuropsychological problems or medication and drug abuse. All gave written informed consent to participate in the study. This study was conducted according to the principles expressed in the Declaration of Helsinki and was approved by the Institutional Review Board of "Kantonale Ethikkommission" (EK: E-80/2008). For various reasons, such as drop out, technical problems during EEG recording or not enough valid EEG data, six participants were discarded form further analysis, leading to a total of 60 remaining data sets (30 per group).

Training

Participants trained extensively for four weeks, about 30 minutes each session (20 sessions in total). Training was self-administered at home via the software Tatool (von Bastian, Locher, and Ruflin, submitted manuscript), a Java based open-source training and testing tool. Training data were automatically uploaded to a webserver running Tatool Online after each training session. Tatool Online

allows monitoring training progress and participants' commitment constantly. For example, session duration and percentage correct were automatically analyzed online to detect any obvious irregularities.

The training tasks were based on the facet model of WM capacity (Oberauer et al., 2000; Oberauer et al., 2003), which assumes three functional categories of WM capacity: Storage and processing, executive processes, and relational integration. Storage and processing is defined as the simultaneous maintenance and manipulation of information. Executive processes involve the selective activation of relevant representations and the suppression of irrelevant distracting ones. Relational integration is defined as the coordination of information elements into structures (Annett, 1970; Oberauer, et al., 2000). The WM group trained one task per functional category of the WM model. We chose the training tasks based on a previous study examining effects of training the three functional categories separately (von Bastian and Oberauer, submitted manuscript). To train storage and processing, we used a numerical version of a complex span task (cf. (Oberauer, et al., 2003), in which participants had to memorize and recall lists of two-digit numbers. In between two successive memoranda, participants had to complete a distracting task, in which they had to decide whether a single digit shown was odd or even. Executive processes were trained using the task-switching paradigm (cf. (Daneman and Carpenter, 1980). In this task, participants had to categorize bivalent figural stimuli (simple geometric shapes) according to two different rules that changed every second trial. The stimuli and the corresponding set of rules were replaced every fifth session to enhance variability of the task. Relational integration was trained by a self-constructed task ("tower of fame"), in which participants had to imagine a building with

apartments on several floors. Sentences were presented sequentially, giving information about which famous person lives in which apartment (e.g., "Tom Cruise lives on the second floor in apartment A"). This statement then disappeared and was followed by a second statement (e.g., "Britney Spears lives 2 floors above in the apartment vis-à-vis"). At the end, participants had to recall which famous person lives where. For an illustration of the trained WM tasks see the supplemental figure S1.

To evaluate effects of a training intervention, it is crucial to compare the trained group to an active control group. This differentiates training effects not only from repetition effects, but also from intervention effects (e.g., effects of regular computer use), and expectancy effects (Monsell, 2003). For the latter purpose it is important that the alternative training is perceived by participants as a potentially effective cognitive training. To control for placebo effects, training conditions for the control group were identical to those of the intervention group. Therefore, participants in the control group trained the same amount of time. The active control group practiced tasks with low WM demand, which were a knowledge quiz and two visual search tasks (circle-task, digit-task). The quiz was composed of a question on general knowledge with four response options, one of them being correct. In the "circle-task", all circles had two gaps, except for one circle that had only one gap. The task was to find this deviant circle and to indicate the direction of the gap by pressing the respective arrow key on the keyboard. In some trials, all circles had two gaps, in this case participants had to press "A". In the "digit-task", numbers between one and nine were presented on the screen. Each number should be presented as often in a row as the digit indicated (e.g. 55555, 333). The subjects had to check whether this rule was

broken (i.e., a number was presented too many or too few times), and press the number key indicating the number that broke the rule. For example, if there was a block of six “5”s in a row, participants had to press the “5” on the keyboard.

For all training tasks, difficulty was adapted stepwise to individual performance by using the adaptive level algorithm provided by Tatool (von Bastian, Locher, and Ruflin, submitted manuscript). The algorithm set an individual benchmark between 80 % and 90 % based on the performance of the participant after 40 % of the number of trials in each session. If the participant’s performance in the following 40 % of the trials (counted across training sessions) was greater than the individual benchmark, task difficulty was increased and a new individual benchmark was set after the next 40 % of trials. However, if performance was lower than the benchmark for three times in a row, task difficulty was decreased. For example, in the complex span task, the number of memoranda was raised with increasing performance.

Tasks for Pretest and Posttest

Before and after the training intervention, participants were invited to the Department of Psychology. All subjects completed a cognitive test battery covering different aspects of WM and reasoning. Half of the participants in each intervention group completed a broad cognitive test battery before the EEG resting recordings, and half of the participants completed it afterwards. There were no effects of order on behavioral and electrophysiological data and order was not analyzed further. Overall, the test battery comprised test versions of the three WM training tasks, three structurally similar WM tasks with different material (verbal complex span task, verbal task switching, and kinship integration), two matrix reasoning tasks, and a control task to which we did not

expect any transfer (quiz on general knowledge). The complete behavioral results of test battery will be reported elsewhere (von Bastian, Langer, Jäncke, and Oberauer, submitted manuscript). In this study, we focus on the WM training tasks and the structurally similar transfer tasks. The test versions of the complex span task comprised 15 trials with varying list lengths (i.e., number of elements to memorize) between three and seven memoranda. In the verbal version of the complex span task, memoranda were words and the distracting processing task was to decide whether a letter presented was a consonant or a vowel. The tests to measure task switching comprised 80 trials of bivalent stimuli. As during training, task switches occurred in alternating runs of two. In the figural version of the task, participants had to either categorize the stimuli as blue or green objects, or as being round or angular. In the verbal version, stimuli were words shown on the screen. Participants had either to categorize the font color of the words (green or blue) or to decide whether the word was a river or a city (e.g., London or Thames). The test version of the "tower of fame" task comprised 18 trials with the number of sentences (i.e., information elements to be integrated) ranging from two to four. The other task used to measure relational integration was the kinship integration task (cf. von Bastian and Oberauer, submitted manuscript). As in the "tower of fame" task, single relational statements are presented sequentially. In the kinship task, these were verbal descriptions of the relationship between two people (e.g., "Anne is Barbara's sister", "Barbara is Charlie's mother"). Participants were then asked to indicate the implied (but not explicitly described) relationship between two of the people mentioned in several consecutive sentences (e.g., "Anne is Charlie's?" with the correct answer being

"aunt"). Participants had to complete 16 trials with the number of sentences varying between two and three.

To obtain a single WM capacity measure we first calculated a factor analysis. This factor analysis yielded a solution with two factors with an eigenvalue >1. Whereas storage and processing tasks and the relational integration tasks all loaded similarly strong on *Factor1* (eigenvalue = 2.86; explained variance = 71.59%), the executive processes tasks loaded on the *Factor2* (eigenvalue = .48; explained variance = 11.7%). The factor loadings were the following: *Factor1:* storage and processing (numerical: r = .799; verbal: r = .735), relational integration (tower of fame: r = .761; kinship task: r = .758) and executive processes (figural: r = .048; verbal: r = .176); *Factor2:* storage and processing (numerical: r = - 0.017; verbal: r = .251), relational integration (tower of fame: r = .229; kinship task: r = .391) and executive processes (figural: r = .693; verbal: r = .376). This confirmed findings from previous studies showing that the two functional categories *storage and processing* and *relational integration* are more strongly related to each other than to *executive processes* (Oken, et al., 2008). Moreover, the WM training group did not show any performance improvements in the executive processes tasks. Therefore, our WM capacity measure was a composite score calculated by averaging the performance only in the tasks measuring storage and processing (numerical and verbal complex span) and relational integration (tower of fame and kinship task). For this WM composite score, we calculated a repeated measure 2x2 ANOVA with the between-subject factor *Group* (WM group, control group) and within-subject factor *Time* (pre-training, post-training). For ANOVAs which exceeded the statistical threshold of

$p < .05$, subsequently Bonferroni-Holm adjusted post-hoc t-tests were applied ($p < .05$).

Electroencephalographical Recording

The EEG measurements took place in a sound-shielded Faraday cage. Subjects were sitting comfortably in a chair and were instructed that EEG recording will be done while they rested with their eyes alternately open or closed. The EEG protocol consisted of the participants resting with eyes open for 20 s, followed by 40 s with their eyes closed; this was repeated five times. Only data from the 200s eyes-closed condition were analyzed, because data quality is higher in that condition. High-density EEG was recorded at a sampling rate of 500 Hz with a bandpass of .1 to 100 Hz with a 256-channel EEG Geodesic Netamps system (Electrical Geodesics, Eugene, Oregon). Recording reference was at Cz (vertex of head). Impedances were kept below 30 kOhm. Independent component analysis was used to remove eye movement artifacts from the EEG. In addition to the application of an automated artifact rejection procedure, data were all visually inspected for noise like eye movements, eye blinks, sweating, and muscular artifacts. After artifact rejection, the electrodes in the outermost circumference (chin and neck) as well as other artifact channels were excluded and interpolated to a standard 204 electrode array (Oberauer, et al., 2003). The artifact-free EEG was recomputed against the average reference and segmented into 2 s epochs. In a second step a discrete Fourier transformation algorithm was applied to the artifact free 2 s epochs (68 segments per subjects). The power spectrum of 1.5-49.5 Hz (resolution .5 Hz) was calculated. The spectra for each channel were averaged over all epochs for each subject.

Scalp Map Analysis

Analysis of the neural correlates of working memory capacity

For the investigation of the neural correlates of WM, by analyzing only the pre-training data, we included all 60 subjects in a regression analysis. We conducted the analysis according to our previous study (Britz, et al., 2009). To this end, data of the 204 electrodes were collapsed into three anterior and three posterior electrode clusters: anterior (left, middle, right), posterior (left, middle, right). Each cluster consisted of 28 electrodes. Several electrodes could not be classified certainly to a cluster and therefore they were excluded from the electrode cluster analysis. Moreover, the absolute power spectra were integrated in the following independent frequency bands following classification proposed by (Langer, et al., 2011): delta (1.5-6 Hz), theta (6.5-8 Hz), alpha1 (8.5-10 Hz), alpha2 (10.5-12 Hz), beta1 (12.5-18 Hz), beta2 (18.5-21 Hz), beta3 (21.5-30 Hz), and gamma (30-49.5 Hz). We ran the regression analysis between the pre-training WM capacity measure and the EEG power spectra of each cluster and frequency band. Statistical significance was assessed by means of a non-parametric randomization test (Kubicki, et al., 1979). An error probability of $p < .05$ (corrected for multiple comparisons across all frequencies and electrode clusters) was used to indicate significant correlations.

Analysis of the neural effects of the working memory training

For the investigation of the effects of the WM training, the proportional change between pre- and post-training (post-training/ pre-training *100) was computed for each subject, electrode, and frequency bin. The proportional change, also called percent signal-change, is a frequently used measure (Dietz, et al., 2009;

Nichols and Holmes, 2002; Takahashi, et al., 2005) and was calculated because of large interindividual variability in EEG power. We were primarily interested in the training-induced change within each individual. The proportional change score eliminates the interindividual differences, such that the analysis focuses only on the intraindividual change induced by the WM training. The proportional change of each electrode cluster (described above) was first compared between the pre- and post-training sessions for each group separately, and then compared between the two groups. Differences (within and between groups) were evaluated through t-tests, and statistical significance was calculated by a nonparametric randomization test (Babiloni, et al., 2011), correcting for multiple comparisons across all frequencies and electrode clusters. The statistical threshold was set to $p < .05$ (corrected for multiple comparisons).

Graph-Theoretical Network Analysis

Graph-theoretical network analysis is used to quantify small-world networks. Graph theory provides a method for describing a complex system, such as the brain, as a set of nodes interconnected by a set of edges (Nichols and Holmes, 2002). Small-world networks are defined as the combination of a high *clustering coefficient* and a short characteristic *path length* (Bullmore and Bassett, 2011). A high *clustering coefficient* reflects a high level of local connectedness within a network, whereas a short characteristic *path length* represents high global efficiency of information transfer between nodes of a network (Watts and Strogatz, 1998). Graph-theoretical network analyses have shown that small-world topology can be found in any scale, modality or volume of neuroscientific data (Bassett and Bullmore, 2006; van den Heuvel, et al., 2009).

Several papers concluded that an intra-cortical approach to the analysis of EEG data represents a clear methodological improvement over the graph-theoretical network analysis at the surface level (Babiloni, et al., 2004a; Lehmann, et al., 2006; Mulert, et al., 2004; Sporns, 2010). Therefore, we conducted our graph-theoretical network analysis on the basis of intra-cerebral brain oscillations. We are aware that the precision of the EEG-source localization is limited although the source reconstruction that we used in the present study (Sinai and Pratt, 2003) has been experimentally validated in various studies and under diverse conditions (Khateb, et al., 2001; Langer, et al., 2010; Pascual-Marqui, 2002), and it has been cross-validated with fMRI (Pizzagalli, et al., 2000; Seeck, et al., 1998). For the estimation of the intra-cerebral electrical sources that generated the scalp-recorded activity, we employed standardised low resolution brain electromagnetic tomography (sLORETA, (Worrell, et al., 2000)) (freely available at http://www.uzh.ch/keyinst/loreta.htm). sLORETA calculates, based on the recorded scalp electric potential differences, the three-dimensional distribution of the electrically active neuronal generators in the brain as standardised units of current density (A/cm^2) at each voxel by assuming similar activation among neighbouring neuronal clusters (Pascual-Marqui, 2002). In the current implementation of sLORETA, computations were made in a realistic head model (Pascual-Marqui, 2002), using the MNI152 template (Fuchs, et al., 2002), with the three-dimensional solution space restricted to cortical gray matter, as determined by the probabilistic Talairach atlas (Mazziotta, et al., 2001). The standard electrode positions on the MNI152 scalp were taken from (Lancaster, et al., 2000) and Oostenveld and Pramstra (Jurcak, et al., 2007). The intracerebral volume is partitioned in 6239 voxels at 5 mm spatial resolution. Thus, sLORETA

images represent the standardised electric activity at each voxel in neuroanatomic Montreal Neurological Institute (MNI) space as the exact magnitude of the estimated current density. sLORETA estimates the inverse problem by taking into account the well-known effects of the head as a volume conductor. The two-second epochs of the preprocessed EEG-data of each subject were imported into the sLORETA software. To subdivide the entire brain into separate regions, the current density was measured in 42 anatomical ROI's in each hemisphere, which were defined according to Brodmann areas (Oostenveld and Praamstra, 2001). SLORETA estimates the solution of the inverse problem based on the assumption that the smoothest of all possible activation distributions is the most plausible one. This assumption is supported by neurophysiological data demonstrating that neighboring neuronal populations show highly correlated activity. Because of this assumption of sLORETA, we took just the single center voxel of each ROI to reduce possible contamination of non-physiological connectivity between the ROI's, as we did in our previous study (Brodmann, 1909).

Within the sLORETA analysis framework, coherence between the 84 anatomical regions of interest (ROI) in both hemispheres was computed. Coherence was calculated as linear instantaneous connectivity. This measure was used in other studies before (Jancke and Langer, 2011; Langer, et al., 2011) and is deemed an adequate measure for computing resting state networks. Mathematical details can be found in (De Vico Fallani, et al., 2010), here we give a brief description. The linear instantaneous connectivity is a general measure that operates in the frequency domain. This measure ranges between 0 in the case of independent times series, and 1 in the case of maximally synchronous signals. Given two

signals x and y, the linear instantaneous connectivity is calculated for a particular frequency f by taking the square of the cross-spectrum

$|S_{xy}(f)|^2$

and by dividing the product of the two corresponding auto power spectra:

$$\mathrm{SC}_{xy}(f) = \frac{|S_{xy}(f)|^2}{S_{xx}(f)S_{yy}(f)}$$

In contrast to the classical coherence measure, the coherence measure used in the present study is an amplitude independent measure, because of the division of the product of the corresponding power spectra, which eliminates the involvement of the amplitude. This is an important issue, since training-induced changes in power could result in more "artifactual" local or long-range connections by using the classical coherence measure. Therefore it is important to use an amplitude free coherence measure, which is not biased by power changes. Intracerebral coherence measures of 84 ROIs were subjected to graph theoretical network analysis. An individual network is represented by the weighted connectivity matrix with nodes and edges, where nodes represent ROIs and edges represent the undirected weighted connections (correlations) between the signals of ROIs.

Because there is currently no generally accepted strategy for applying a particular threshold on correlations matrices, we thresholded repeatedly over a wide range of correlation thresholds in increments of r = .05 from r = .65 to r = .95. The so obtained thresholded connectivity matrices were then subjected to the network analysis software *tnet* (Opsahl and Panzarasa, 2009; Pascual-Marqui,

2007b) to quantify small-worldness indices (Opsahl, 2009; Watts and Strogatz, 1998). The typical key characteristic of small-world networks were computed, including the *clustering coefficient,* the characteristic *path length* and the *degree centrality* measures (analyzed in the regional node analysis section) (Bullmore and Sporns, 2009). The *clustering coefficient* is given by the ratio between the number of connections between the direct neighbors of a node and the total number of possible connections between these neighbors (Watts and Strogatz, 1998). The characteristic *path length* of a network gives the average number of connections that have to be crossed to travel from each node to every other node in the network (Watts and Strogatz, 1998).

Regional node analysis

In order to identify and discriminate important hub regions within the small-world network, weighted *degree centrality* measures were calculated for each individual node and plotted as *degree distribution* (Opsahl and Panzarasa, 2009; Watts and Strogatz, 1998). *Degree* (which is a particular *centrality* measure) is defined as the number of connections of a node (i.e. the sum of weights of the edges connected to a particular node). Therefore, each node is characterized by its own *degree* value. To visualize the *degree* values graphically, BrainNet Viewer was used, which is a MATLAB toolbox (http://www.nitrc.org/projects/bnv/).

In the same manner to the scalp map analysis, a regression analysis and statistical comparisons between groups and conditions were conducted. To investigate the neuronal correlates of WM, only the pre-training data were analyzed. Each participant's pre-training WM performance was correlated with that participant's small-world indices (clustering coefficient, path length) and their weighted

degree centrality at each ROI. In order to investigate the effects of the WM training, a 2x2 repeated measure ANOVA with the between-subject factor *Group* (WM training group, control group) and the within-subjects factor *Time* (pre-training, post-training) was computed for each small-world index. For the significant main effects, we employed post-hoc t-test with a significance level of $p < .05$ (Bonferroni corrected for multiple comparisons) (Freeman, 1978; Holm, 1979).

For the regional node analysis (degree centrality measure), we investigated the effects of the WM training analogically to the training effects in the scalp map analysis by computing the proportional change of the *degree centrality* between pre- and post-training (post-training/ pre-training *100). The proportional change score eliminates the interindividual differences in *degree centrality*, such that the analysis focuses only on the intraindividual change induced by the WM training. First, we compared proportional change of degree centrality within each group separately by one-sample t-tests. Then we investigated through a two-sample t-test, whether the pre-post change in degree centrality differed between groups. For the regional node index, error probability was set to $p < .05$, uncorrected for multiple comparisons. Because of our strong a priori hypothesis predicting training-related changes in the fronto-parietal network, we did not use a correction for multiple comparisons for the regional node index analysis.

4.2.4. Results

Behavioral results

A WM capacity score was computed for each subject and time point by averaging z-transformed scores from the tasks measuring storage and processing (numerical and verbal complex span) and relational integration (tower of fame, kinship test); for a description of these constructs see (Shaffer, 1995). Behavioral data showed that WM training led to significant improvements in the trained as well as some non-trained tasks (see von Bastian, Langer, Jäncke, and Oberauer, submitted manuscript). This pattern was also reflected in the composite score used for this study, where we used a repeated 2x2 ANOVA with the between-subjects factor *Group* (WM training group, control group) and the within-subjects factor *Time* (pre-training, post-training). For the WM composite score, we found a significant main effect of *Time* ($F = 94.00$, $p = 1.38E^{-13}$) and an interaction effect (*Time x Group*) ($F = 7.97$, $p = .007$). The subsequent post-hoc t-tests revealed significant superior performance in the post-training session for the WM training group compared to the control group ($T = 2.77$, $p = .008$, corrected for multiple comparisons). Furthermore, there was a significant increase from the pre- to the post-training session in WM composite score for the WM training group ($T = -8.36$, $p = 4.34E^{-9}$ corrected for multiple comparisons) and the control group ($T = -4.80$, $p = 3.77E^{-5}$, corrected for multiple comparisons). The complete behavioral results of the test battery will be reported elsewhere (von Bastian, Langer, Jäncke, and Oberauer, submitted manuscript).

Scalp map analysis

Investigating the neural correlates of WM performance based on the pre-training data and across the all frequency bands, the electrode cluster analysis revealed an exclusive positive correlation with theta power in the right anterior electrode cluster ($r = .33$, $p = .037$, corrected for multiple comparisons) (Figure 1A). The other electrode clusters in the theta band also revealed strong but not significant correlations, after corrections for multiple testing. The scalp map distribution of the correlation between WM performance and the theta power are shown in Figure 1B.

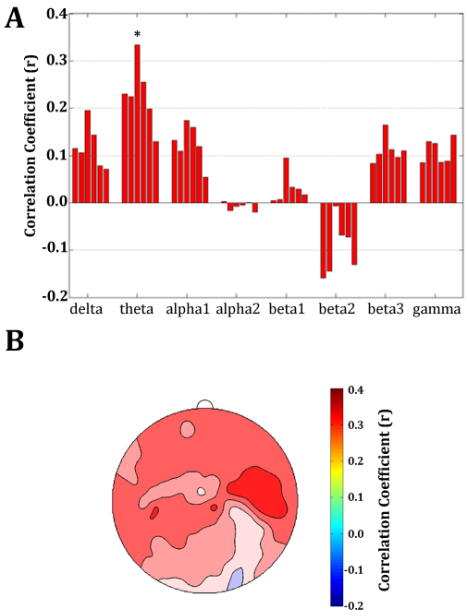

Figure 1. Scalp Map Analysis of pre-training measurements.

The correlation between WM performance and the EEG power on the electrode level for all frequencies in the pre-training measurements is displayed. A) The correlation between WM performance and the six electrode clusters is displayed for eight frequency bands. Each bar group represents one frequency band. The six bars in each frequency band represent the six electrode clusters (ordered: anterior left, anterior middle, anterior right, posterior left, posterior middle, posterior right). The Fischer's permutation test revealed a significant relationship only in the right anterior cluster of the theta band ($p < .05$, corrected for multiple comparisons). B) The distribution of the correlation coefficients over the scalp is displayed for the theta frequency.

The investigation of the WM training effects on the electrode cluster analysis revealed significant changes from pre- to post-training session only in the WM training group, namely in the theta power in left anterior (t = 3.92, p = .008) and middle anterior (t = 4.00, p = .004) electrode clusters (corrected for multiple comparisons) (Figure 2). The other electrode clusters in the theta frequency also showed alterations, but these changes did not survive the multiple comparisons adjustment. No electrode cluster significantly changed in the control group (Figure 2). The comparison regarding differences between the two groups in the proportional change in EEG power spectra revealed strong effects in the theta frequency, but they also did not survive the correction for multiple comparisons (Figure 2).

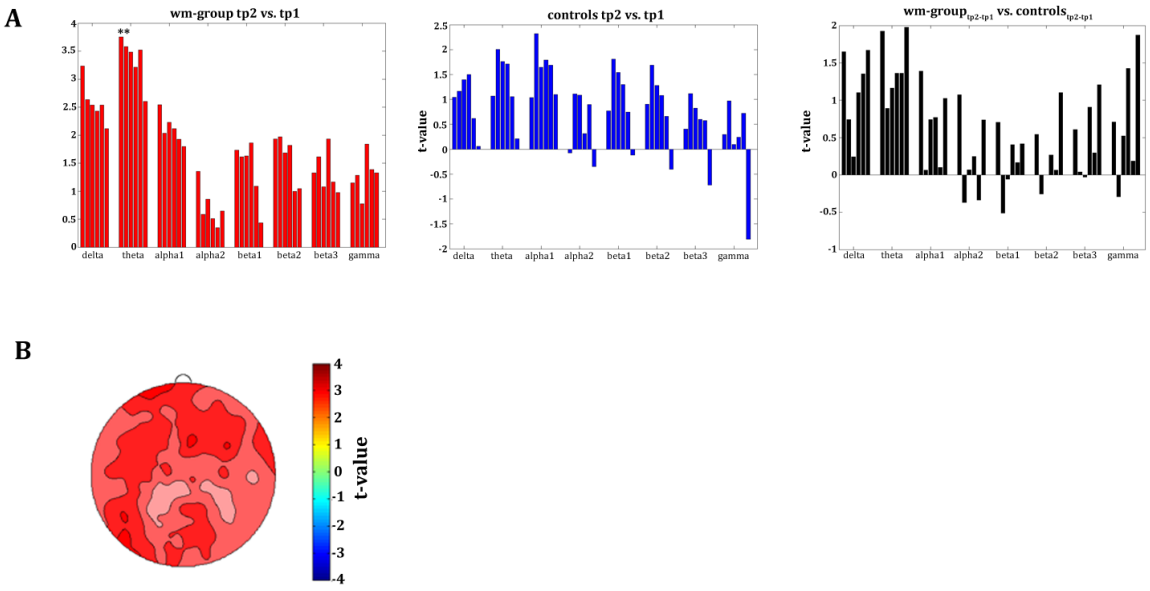

Figure 2. Scalp Map Analysis of the working memory training effects.

Displayed are the alterations (% signal change) and the group comparisons of the alterations in the EEG power from the pre-training to the post-training session on the electrode level. A) Differences in power between pre- and post-test for eight frequency bands and six electrode clusters are represented by the t-values for the pre-post comparison. Red bars in the upper panel represent pre-post differences for the WM training group, and blue bars in the middle panel represent pre-post differences in the control group. The black bars in the bottom graph show the comparison of the pre- and post-training changes between the two groups. There were only two

clusters, namely the anterior left and midline electrode cluster in the theta band in the WM training group, which survived the correction for multiple comparisons ($p < .05$). The six bars in each frequency band represent the six electrode clusters (ordered: anterior left, anterior middle, anterior right, posterior left, posterior middle, posterior right. B) The distribution of the t-value over the scalp is displayed for the theta frequency for comparison pre-training vs. post-training in the WM training group.

Graph-Theoretical Network Analysis

Because of our hypothesis regarding the relationship between WM and theta oscillations as well as the results of the scalp map analysis, which revealed significant effects only in the theta band, we performed the graph-theoretical network analysis only for the theta frequency band. The graph-theoretical network analysis on the intracortical level revealed nearly identical results for all thresholds, hence, we only report the results for the threshold of $r = .85$. This threshold is based on our previous studies showing that the network with a threshold at $r = .85$ represents the most adequate small-world topology (Jancke and Langer, 2011; Oberauer, et al., 2007). The results of the other thresholds revealed are summarized in the supplemental Table S1 and S2. The average network (correlation matrix across all subjects) in the theta frequency is composed of 84 nodes and 1718 edges. For the investigation of the neural basis of WM, again analyzing only the pre-training data, the small-world indices (*clustering coefficient, path length*) were computed for each subject individually, and correlations between the small-world indices and the WM performance of the pre-training data were calculated. We found a positive correlation for the *clustering coefficient* ($r = .32$. $p = .03$), whereas a negative relationship emerged for the *path length* ($r = -0.30$, $p = .04$, corrected for multiple comparisons) (Figure 3).

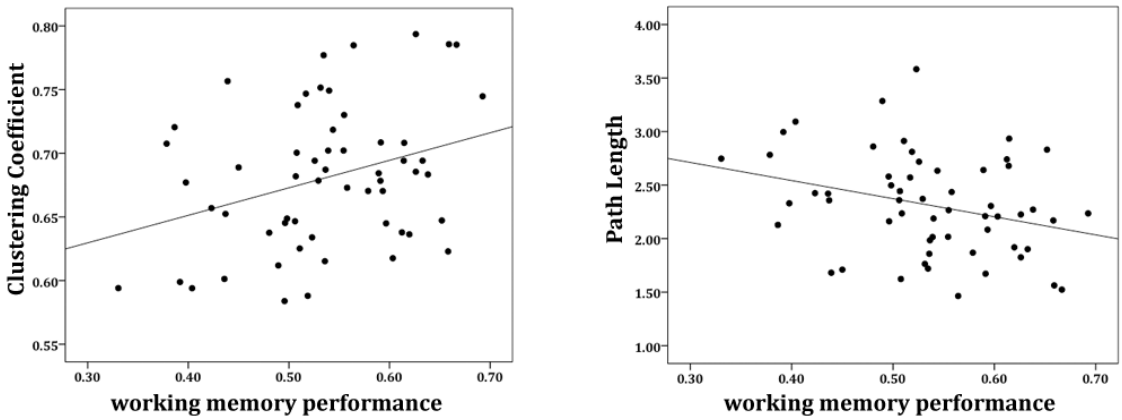

Figure 3. Correlation of small world parameters with working memory performance.
Scatter plots for the correlation between the small-world indices of the graph-theoretical network analysis (*clustering coefficient* and *path length*) in the theta frequency band and WM performance at pretest

For the investigation of WM training effects on small-world parameters, we first subjected each small-world index separately to a 2x2 ANOVA with the between-subject factor *Group* (WM training group, control group) and within-subject factor *Time* (pre-training, post-training). For the *clustering coefficient* we found a significant main effect for the factor *Time* ($F = 6.30$, $p = .01$) and a significant *Time x Group* interaction ($F = 5.44$, $p = .02$). The post-hoc t-test revealed a significant increase from the pre- to the post-training session in the WM training group ($t = -3.40$, $p = .002$, corrected for multiple comparisons). In addition, we found a significant difference between the WM training group and the control group in the post-training session. In the post-training session, the WM training group had a larger *clustering coefficient* than the control subjects ($t = 2.37$, $p = .02$, corrected for multiple comparisons) (Figure 4). The ANOVA of the path length showed a significant *Group x Time* interaction ($F = 5.44$, $p = .02$). The post-hoc t-test demonstrated a decrease of the *path length* in the WM training group from the pre- to the post-training session ($t = 2.12$, $p = .04$, corrected for multiple

comparisons). Moreover, in the post-training session, the WM training group showed a significantly decreased characteristic *path length* compared to the control group (t = -2.52, p = .002, corrected for multiple comparisons) (Figure 4).

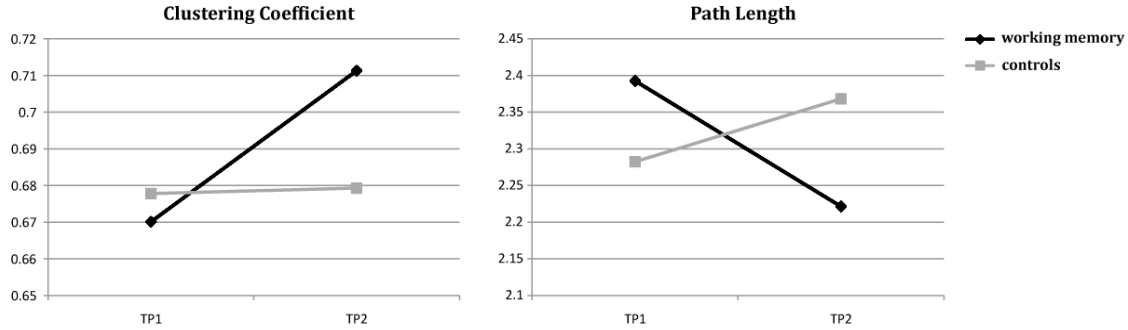

Figure 4. Graph-theoretical network analysis of the working memory training effects.
Displayed are the mean values of the *clustering coefficient* and *path length* for the WM training group (black) and control group (gray) in the pre- and post-training session. Significant post-hoc t-tests ($p < .05$, corrected for multiple comparisons) are indicated by asterisks.

Identification of hub regions

Degree centrality was evaluated to identify the nodes in the networks that are responsible for the WM performance and WM training effects. The first analysis, where we investigated the relationship between WM performance and *degree centrality* in the pre-training session, revealed significant positive correlations primarily in the parietal cortex (bilateral), right superior temporal gyrus, the right insular cortex and the right secondary sensory area (visual and auditory). The higher a person's WM performance, the higher was their *degree centrality* in these regions. On the other hand, we found significant negative correlations primarily bilaterally in the frontal cortex, the cingulate cortex, as well as the medial temporal lobe and hippocampal regions (see Figure 5).

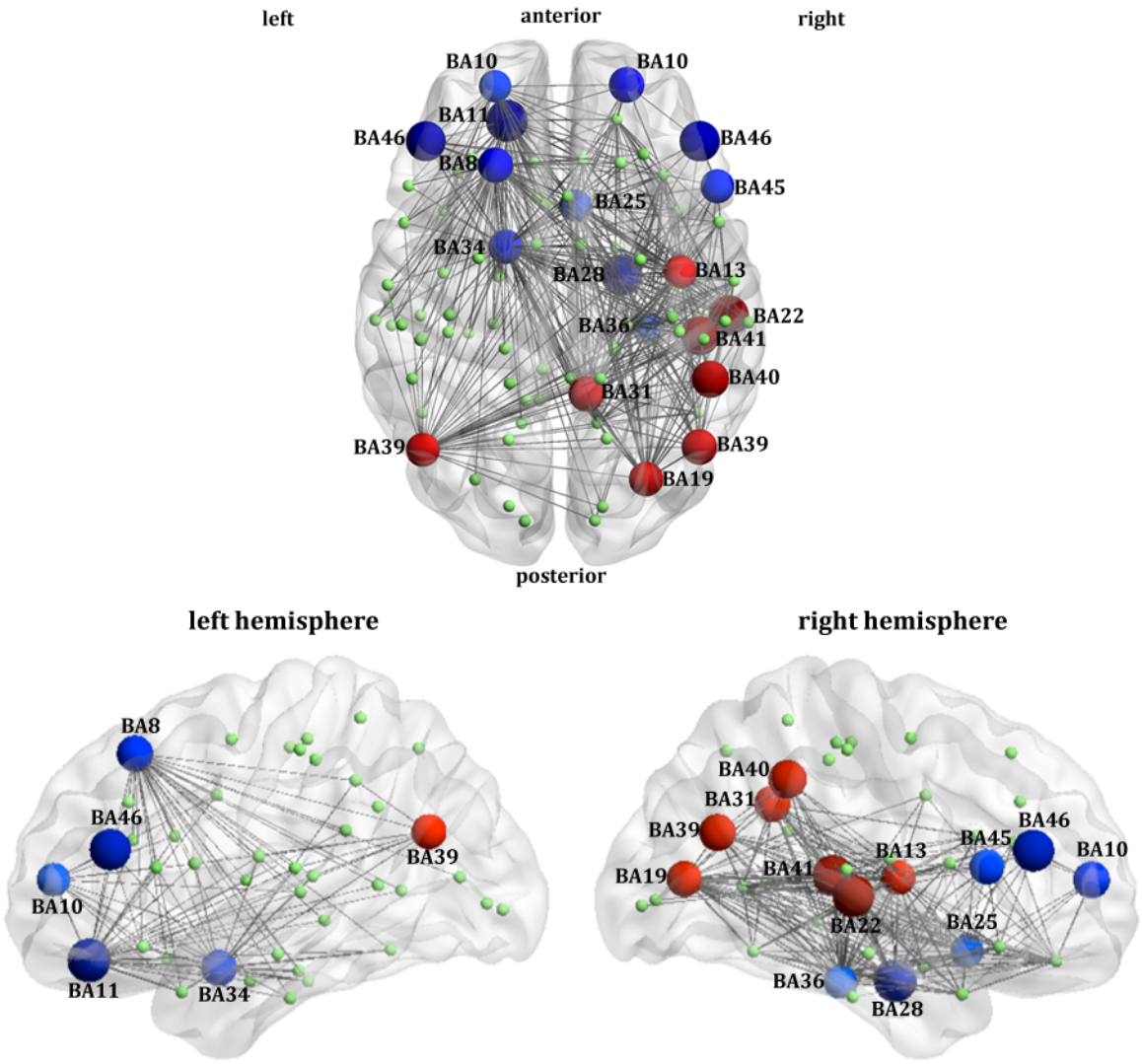

Figure 5. Correlation of degree centrality with working memory performance.

The weighted *degree centrality* measurements of the intracortical graph-theoretical network analysis are illustrated. Brain regions, which *degree* was positively correlated with WM performance are marked in red, and brain regions with negative correlations are blue. The sizes and the darkness of the sphere reflect the sizes of the correlations. A significant correlation between *degree* of a node and WM performance is defined as a correlation exceeding the threshold of $p < .05$ (uncorrected for multiple comparisons). Furthermore, the connections of hub regions in which the hubs were significantly correlated with WM performance are presented as lines between different nodes. The hub regions in the figure are shown according to a glass brain to facilitate the view of the entire network.

The analysis of the WM training effects revealed similar hub regions. In comparison to the control group, the WM training group showed after training enhanced *degree centrality* measures in the parietal regions, the right superior

temporal gyrus and the left inferior frontal gyrus. In contrast, we found a decreased *degree centrality* in the prefrontal areas, the right enthorinal and premotor cortex in the WM training group compared to the control group (Figure 6). The exact statistical values of the *degree centrality* analyses are summarized in the supplemental Table S3 and S4.

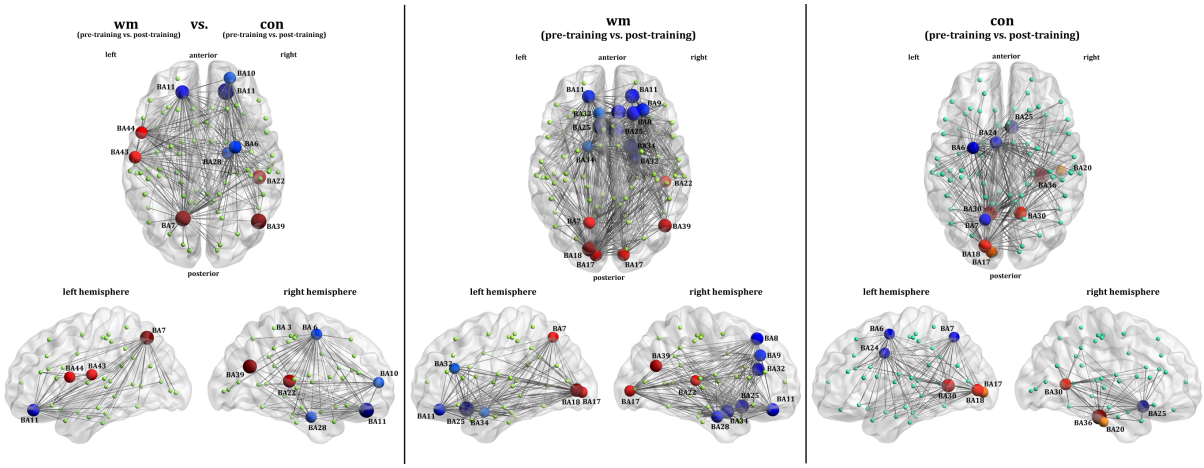

Figure 6. Changes in degree centrality induced by working memory training.
The WM training effects on the *degree centrality* is illustrated. On the left side, the proportional change of *degree centrality* measurements, which were significantly larger (red) or smaller (blue) in the WM training group compared to the control group, are displayed depending on the magnitude of the difference (the darker and bigger the higher the effect). The proportional changes from the pre- to post-training in the *degree centrality* are presented for the WM training group (middle figure) and the control group separately (right figure). A significant *degree* of a node is defined by exceeding the significant threshold of $p < .05$ (uncorrected for multiple comparisons). Furthermore, the connections of hub regions in which the hubs were significantly different between the WM training group and the control group or between the pre- to post-training within each group are presented as lines between different nodes.

4.2.5. Discussion

This study aimed to extend our knowledge about the plasticity of functional brain networks. We were particularly interested in examining whether intensive WM training could shift the brain networks, based on resting state EEG, more towards small-world topology. The resting state can be viewed as a kind of starting point from which subsequent cognitions are generated and monitored (Langer, et al., 2011). Thus, our hypothesis was that intensive WM training would modify this starting point, represented by increased small-worldness of the functional brain networks, and would be beneficial for subsequent WM performance. In fact, we first determined through an exploratory scalp-map analysis that the power in the theta band was correlated with WM performance, and that power in the theta band was increased by intensive WM training. Therefore we focused our connectivity analysis on theta. We found that a more efficient functional network in the theta band, as indexed by a higher degree of small-worldness, was correlated with higher WM performance before training. We further demonstrated that WM training increased small-world topology in the same functional brain networks. In the following, we discuss the importance of the theta band and relate our findings of the network analysis to recent findings of the neuropsychological literature of WM.

Theta and working memory

Across analyses of a broad spectrum of frequencies and six electrode clusters, we found that only the EEG power in the anterior electrodes around the theta frequency was correlated with WM performance and was increased by WM training.

In humans, theta waves are usually in the 4-8 Hz frequency range and have been associated with spatial navigation (de Araujo, et al., 2002; Langer, et al., 2011) and WM processing (Kahana, et al., 1999; Klimesch, 1999; Klimesch, et al., 1997b; Onton, et al., 2005; Raghavachari, et al., 2006). In a study of Raghavachari and collegues, cortical theta activity was increased during encoding and retention of information in a Sternberg-like WM task (Sauseng, et al., 2005). Moreover, an enhancement of frontal theta activity has been related to increasing working memory load (Raghavachari, et al., 2001). Sauseng and colleagues suggested that interregional theta synchronization might play an important role for the co-activation of neural structures, which are involved in different sub-processes of complex WM functions (Jensen and Tesche, 2002). This hypothesis gains support from Sarnthein and colleagues, who suggested that the prefrontal supervisionary system accesses the tempo-parietal modality specific subsystems by interregional theta coherence (Sauseng, et al., 2010). The theta oscillations are considered to result from an interaction within neuronal networks mainly in the pyramidal cells of the hippocampus. Several feedback loops connecting the hippocampal formation with different cortical regions, the prefrontal cortex in particular (Klimesch, 1999; Miller, 1991; Sarnthein, et al., 1998). In addition, several studies have shown a cross-frequency coupling between theta and higher frequency oscillations (i.e. gamma) (Canolty, et al., 2006; Steriade, et al., 1990). This might reflect the organization of multiple items into sequential WM representations (Lisman and Idiart, 1995).

The functional network of working memory

We identified a network of coherent theta activity that was associated with higher WM performance before training, and changed during WM training. This network, comprises seven main brain regions: the bilateral dorsolateral frontal region (BA 9, 46), the bilateral rostral prefrontal cortex or frontal pole (BA 10, 11), the bilateral (but with a right hemispheric dominance) parietal cortex (BA 39/40), the left premotor cortex (BA 6, 8), the right insular cortex (BA 13), the bilateral areas of the limbic system, such as the entorhinal cortex (BA 28, 34), the posterior cingulated cortex (BA 29, 30, 31), and the secondary sensory areas (BA 22 and BA19).

This network was characterized by a dissociation between frontal and parietal areas, in line with other WM and intelligence studies (Olesen, et al., 2004; Sauseng, et al., 2010). In particular, most of the correlations between WM performance and *degree centrality* in prefrontal areas and the entorhinal cortex were negative, and the training effects on *degree centrality* in these areas were also negative. In contrast, we found positive correlations, and increases after training, for degree centrality in parietal regions, the insular cortex and the superior temporal gyrus. This fronto-parietal dissociation is in good agreement with neural-efficiency theory, which postulates that better performing subjects need less neural resources primarily in the frontal brain regions to solve a cognitive task (Langer, et al., 2011). An alternative explanation for the fronto-parietal dissociation is proposed by the dual-process theory of (Neubauer and Fink, 2009), which postulates a practice-related redistribution of functional activations, such as controlled task performance gradually transitioning into automated task performance, which is associated with a decrease in general control centers (frontal brain regions) but an increase in task specific regions

(parietal cortex). In the following, we will briefly discuss these regions within the WM network.

The prefrontal cortex was found to play a role in the maintenance of goal-related information, the integration of information to build new relations, and task context biases, as it is required in the present WM tasks (Chein and Schneider, 2005). In the present study, WM training might have increased the efficiency of neural processing in the prefrontal cortex, resulting in decreased neurophysiological coherence. In addition to changes in the prefrontal cortex, WM studies frequently report concomitant activations in parietal regions (Jonides, et al., 1993; Owen, et al., 1996; Owen, et al., 2005). Smith and Jonides suggested that the posterior parietal cortex is activated whenever short-term storage of verbal memory is required (Awh, et al., 1996). Moreover, the parietal cortex is involved in retaining temporal information and in reactivating relevant information (Smith and Jonides, 1998), which is also essential to solve the WM task of the present study. The premotor cortex has again been frequently described in many studies of WM (Owen, et al., 1996; Ravizza, et al., 2004). On this basis, it has been suggested that activity in this region is related to the maintenance of visuospatial attention during WM (Jonides, et al., 1993). However, the premotor cortex as well as the secondary sensory regions and the insular cortex could also be attributed to the common output demands of the reading and repetition demands of the task (Owen, et al., 2005). Although the insular cortex was positively correlated with WM in other WM studies (Petersen, et al., 1998), the specific involvement in memory formation remains unclear. Moreover, the fronto-parietal network identified in the present study is typically found by other research groups studying WM (Engvig, et al., 2010; Hampson, et al., 2006; Jolles,

et al., 2011). For example, Hampson and colleagues demonstrated in their fMRI connectivity analysis during WM performance a very similar connectivity pattern as revealed in our study (Takeuchi, et al., 2011). In addition, a study of Sammer and colleagues using EEG and fMRI simultaneously identified an EEG theta network comprising equal brain regions during a mental arithmetic task as in the present study (Hampson, et al., 2006).

Further studies using graph-theoretical analysis on the basis of intracerebral activity could be improved by referring to the individual brain anatomy, which creates improved estimations for inverse modeling compared to an average brain by taking head size and cortical folding in to account. In addition one of the unsolved problems in connectivity analysis based on EEG data is the volume conduction, although to a lesser extent in the intracortical space than at sensor level, especially by using only the single centroid voxel of each ROI as it was done in the present study. Nevertheless, the analysis could even be improved by using lagged coherence, which however has not revealed any small-world topology in our preceding pilot study. In addition, a recent study of Palva et al. (Sammer, et al., 2007) demonstrated that primarily alpha- and beta-frequency bands networks exhibit a memory-load dependent small-world structure during a visual working memory maintenance. Therefore future studies investigating working-memory training effects should also investigate training induced neurophysiological changes during working-memory task performance and should discriminate between encoding, retention and recall period.

To our knowledge, this is the first longitudinal study that investigated the capacity of functional brain networks to adapt to changing demands by using graph-theoretical network analyses. To conclude, there were four main findings

in the present study. (1) Theta oscillations in the resting EEG are correlated with WM performance and could be increased by intensive WM training. (2) The better the WM performance, the more the functional networks in the theta band exhibit small world topology. (3) Better WM performance was correlated with higher *degree centrality* of parietal cortical areas, and lower degree centrality of frontal areas. (4) WM training changed the network in the direction of network characteristics of high performers, with a shift of *degree centrality* from frontal to parietal areas, and a general increase of small-worldness.

Acknowledgments and funding

We thank Marc Züst, Katharina Vogt, Eszter Montvai, Veronica Heusser, Melanie Künzli and Sabrina Guye for research assistance during the conduct of the experiments. This research was supported by grants of University of Zurich to LJ and to CvB from the Forschungskredit of the University of Zurich and the Suzanne and Hans Biäsch Foundation for Applied Psychology.

4.2.6. References

Achard S and Bullmore E. Efficiency and cost of economical brain functional networks. *PLoS Comput Biol,* 3: e17, 2007.

Annett M. A classification of hand preference by association analysis. *Br J Psychol,* 61: 303-21, 1970.

Awh E, Jonides J, Smith EE, Schumacher EH, Koeppe RA, and Katz S. Dissociation of storage and rehearsal in verbal working memory: Evidence from positron emission tomography. *Psychological Science,* 7: 25-31, 1996.

Babiloni C, Binetti G, Cassetta E, Cerboneschi D, Dal Forno G, Del Percio C, Ferreri F, Ferri R, Lanuzza B, Miniussi C, Moretti DV, Nobili F, Pascual-Marqui RD, Rodriguez G, Romani GL, Salinari S, Tecchio F, Vitali P, Zanetti O, Zappasodi F, and Rossini PM. Mapping distributed sources of cortical rhythms in mild alzheimer's disease. A multicentric eeg study. *Neuroimage,* 22: 57-67, 2004.

Babiloni C, Ferri R, Moretti DV, Strambi A, Binetti G, Dal Forno G, Ferreri F, Lanuzza B, Bonato C, Nobili F, Rodriguez G, Salinari S, Passero S, Rocchi R, Stam CJ, and Rossini PM. Abnormal fronto-parietal coupling of brain rhythms in mild alzheimer's disease: A multicentric eeg study. *Eur J Neurosci,* 19: 2583-90, 2004.

Babiloni F, De Vico Fallani F, and Cincotti F. Multimodal integration of eeg, meg, and functional mri in the study of human brain activity. In Cerutti S. and Marchesi C. (Eds.), *Advanced methods of biomedical signal processing*. Hoboken: John Wiley & Sons, Inc., 2011.

Baddeley A. Working memory: Looking back and looking forward. *Nature Reviews Neuroscience,* 4: 829-839, 2003.

Baddeley AD. Is working memory still working? *European Psychologist,* 7: 85-97, 2002.

Bassett DS and Bullmore E. Small-world brain networks. *Neuroscientist,* 12: 512-23, 2006.

Bassett DS and Bullmore ET. Human brain networks in health and disease. *Curr Opin Neurol,* 22: 340-7, 2009.

Britz J, Landis T, and Michel CM. Right parietal brain activity precedes perceptual alternation of bistable stimuli. *Cereb Cortex,* 19: 55-65, 2009.

Brodmann K. *Vergleichende lokalisationslehre der grosshirnrinde in ihren prinzipien dargestellt auf grund des zellenbaues*. Leipzig: Barth, 1909.

Bullmore E and Sporns O. Complex brain networks: Graph theoretical analysis of structural and functional systems. *Nat Rev Neurosci,* 10: 186-98, 2009.

Bullmore ET and Bassett DS. Brain graphs: Graphical models of the human brain connectome. *Annu Rev Clin Psychol,* 7: 113-40, 2011.

Canolty RT, Edwards E, Dalal SS, Soltani M, Nagarajan SS, Kirsch HE, Berger MS, Barbaro NM, and Knight RT. High gamma power is phase-locked to theta oscillations in human neocortex. *Science,* 313: 1626-8, 2006.

Chein JM and Schneider W. Neuroimaging studies of practice-related change: Fmri and meta-analytic evidence of a domain-general control network for learning. *Brain Res Cogn Brain Res,* 25: 607-23, 2005.

Daneman M and Carpenter PA. Individual differences in working memory and reading. *Journal of Verbal Learning & Verbal Behavior,* 19: 450-466, 1980.

de Araujo DB, Baffa O, and Wakai RT. Theta oscillations and human navigation: A magnetoencephalography study. *J Cogn Neurosci,* 14: 70-8, 2002.

De Vico Fallani F, Maglione A, Babiloni F, Mattia D, Astolfi L, Vecchiato G, De Rinaldis A, Salinari S, Pachou E, and Micheloyannis S. Cortical network analysis in patients affected by schizophrenia. *Brain Topogr,* 23: 214-20, 2010.

deJonge P and deJong PF. Working memory, intelligence and reading ability in children. *Personality and Individual Differences,* 21: 1007-1020, 1996.

Dietz V, Grillner S, Trepp A, Hubli M, and Bolliger M. Changes in spinal reflex and locomotor activity after a complete spinal cord injury: A common mechanism? *Brain,* 132: 2196-205, 2009.

Engvig A, Fjell AM, Westlye LT, Moberget T, Sundseth O, Larsen VA, and Walhovd KB. Effects of memory training on cortical thickness in the elderly. *Neuroimage,* 52: 1667-76, 2010.

Ford JM, Mathalon DH, Whitfield S, Faustman WO, and Roth WT. Reduced communication between frontal and temporal lobes during talking in schizophrenia. *Biol Psychiatry,* 51: 485-92, 2002.

Freeman LC. Centrality in social networks: Conceptual clarification. *Social Networks,* 1: 215-239, 1978.

Fuchs M, Kastner J, Wagner M, Hawes S, and Ebersole JS. A standardized boundary element method volume conductor model. *Clinical Neurophysiology,* 113: 702-712, 2002.

Hampson M, Driesen NR, Skudlarski P, Gore JC, and Constable RT. Brain connectivity related to working memory performance. *J Neurosci,* 26: 13338-43, 2006.

Hogan MJ, Swanwick GR, Kaiser J, Rowan M, and Lawlor B. Memory-related eeg power and coherence reductions in mild alzheimer's disease. *Int J Psychophysiol,* 49: 147-63, 2003.

Holm S. A simple sequentially rejective multiple test procedure *Scandinavian Journal of Statistics*: 65-70, 1979.

Hsieh LT, Ekstrom AD, and Ranganath C. Neural oscillations associated with item and temporal order maintenance in working memory. *J Neurosci,* 31: 10803-10, 2011.

Jancke L and Langer N. A strong parietal hub in the small-world network of coloured-hearing synaesthetes during resting state eeg. *J Neuropsychol,* 5: 178-202, 2011.

Jensen O and Tesche CD. Frontal theta activity in humans increases with memory load in a working memory task. *Eur J Neurosci,* 15: 1395-9, 2002.

Jolles DD, van Buchem MA, Crone EA, and Rombouts SA. Functional brain connectivity at rest changes after working memory training. *Hum Brain Mapp*, 2011.

Jonides J, Lewis RL, Nee DE, Lustig C, Berman MG, and Moore KS. The mind and brain of short-term memory. *Annual Review of Psychology,* 59: 193-224, 2008.

Jonides J, Smith EE, Koeppe RA, Awh E, Minoshima S, and Mintun MA. Spatial working memory in humans as revealed by pet. *Nature,* 363: 623-5, 1993.

Jurcak V, Tsuzuki D, and Dan I. 10/20, 10/10, and 10/5 systems revisited: Their validity as relative head-surface-based positioning systems. *Neuroimage,* 34: 1600-1611, 2007.

Kahana MJ, Sekuler R, Caplan JB, Kirschen M, and Madsen JR. Human theta oscillations exhibit task dependence during virtual maze navigation. *Nature,* 399: 781-4, 1999.

Khateb A, Michel CM, Pegna AJ, Thut G, Landis T, and Annoni JM. The time course of semantic category processing in the cerebral hemispheres: An electrophysiological study. *Brain Res Cogn Brain Res,* 10: 251-64, 2001.

Klimesch W. Eeg alpha and theta oscillations reflect cognitive and memory performance: A review and analysis. *Brain Res Brain Res Rev,* 29: 169-95, 1999.

Klimesch W, Doppelmayr M, Schimke H, and Ripper B. Theta synchronization and alpha desynchronization in a memory task. *Psychophysiology,* 34: 169-76, 1997.

Kubicki S, Herrmann WM, Fichte K, and Freund G. Reflections on the topics: Eeg frequency bands and regulation of vigilance. *Pharmakopsychiatr Neuropsychopharmakol,* 12: 237-45, 1979.

Lancaster JL, Woldorff MG, Parsons LM, Liotti M, Freitas ES, Rainey L, Kochunov PV, Nickerson D, Mikiten SA, and Fox PT. Automated talairach atlas labels for functional brain mapping. *Human Brain Mapping,* 10: 120-131, 2000.

Langer N, Beeli G, and Jancke L. When the sun prickles your nose: An eeg study identifying neural bases of photic sneezing. *PLoS One,* 5: e9208, 2010.

Langer N, Pedroni A, Gianotti LR, Hanggi J, Knoch D, and Jancke L. Functional brain network efficiency predicts intelligence. *Hum Brain Mapp*, 2011.

Lehmann D, Faber PL, Gianotti LR, Kochi K, and Pascual-Marqui RD. Coherence and phase locking in the scalp eeg and between loreta model sources, and microstates as putative mechanisms of brain temporo-spatial functional organization. *J Physiol Paris,* 99: 29-36, 2006.

Lisman JE and Idiart MA. Storage of 7 +/- 2 short-term memories in oscillatory subcycles. *Science,* 267: 1512-5, 1995.

Mazziotta J, Toga A, Evans A, Fox P, Lancaster J, Zilles K, Woods R, Paus T, Simpson G, Pike B, Holmes C, Collins L, Thompson P, MacDonald D, Iacoboni M, Schormann T, Amunts K, Palomero-Gallagher N, Geyer S, Parsons L, Narr K, Kabani N, Le Goualher G, Boomsma D, Cannon T, Kawashima R, and Mazoyer B. A probabilistic atlas and reference system for the human brain: International consortium for brain mapping (icbm). *Philosophical Transactions of the Royal Society B-Biological Sciences,* 356: 1293-1322, 2001.

Meltzer JA, Zaveri HP, Goncharova, II, Distasio MM, Papademetris X, Spencer SS, Spencer DD, and Constable RT. Effects of working memory load on oscillatory power in human intracranial eeg. *Cereb Cortex,* 18: 1843-55, 2008.

Miller R. *Cortico-hipocampal interplay and the representation of contexts in the brain*. Berlin: Springer, 1991.

Monsell S. Task switching. *Trends in Cognitive Sciences,* 7: 134-140, 2003.

Mulert C, Jager L, Schmitt R, Bussfeld P, Pogarell O, Moller HJ, Juckel G, and Hegerl U. Integration of fmri and simultaneous eeg: Towards a comprehensive understanding of localization and time-course of brain activity in target detection. *Neuroimage,* 22: 83-94, 2004.

Neubauer AC and Fink A. Intelligence and neural efficiency. *Neurosci Biobehav Rev,* 33: 1004-23, 2009.

Nichols TE and Holmes AP. Nonparametric permutation tests for functional neuroimaging: A primer with examples. *Human Brain Mapping,* 15: 1-25, 2002.

Oberauer K, Süss H-M, Wilhelm O, and Sander N. Individual differences in working memory capacity and reasoning ability. In Conway C., Jarrold M.J., Kane J., Miyake A., and Towse N. (Eds.), *Variation in working memory*. New York: Oxford University Press, 2007.

Oberauer K, Suss HM, Schulze R, Wilhelm O, and Wittmann WW. Working memory capacity - facets of a cognitive ability construct. *Personality and Individual Differences,* 29: 1017-1045, 2000.

Oberauer K, Suss HM, Wilhelm O, and Wittman WW. The multiple faces of working memory: Storage, processing, supervision, and coordination. *Intelligence,* 31: 167-193, 2003.

Oken BS, Flegal K, Zajdel D, Kishiyama S, Haas M, and Peters D. Expectancy effect: Impact of pill administration on cognitive performance in healthy seniors. *Journal of Clinical and Experimental Neuropsychology,* 30: 7-17, 2008.

Olesen PJ, Westerberg H, and Klingberg T. Increased prefrontal and parietal activity after training of working memory. *Nat Neurosci,* 7: 75-9, 2004.

Oliveri M, Turriziani P, Carlesimo GA, Koch G, Tomaiuolo F, Panella M, and Caltagirone C. Parieto-frontal interactions in visual-object and visual-spatial working memory: Evidence from transcranial magnetic stimulation. *Cereb Cortex,* 11: 606-18, 2001.

Onton J, Delorme A, and Makeig S. Frontal midline eeg dynamics during working memory. *Neuroimage,* 27: 341-56, 2005.

Oostenveld R and Praamstra P. The five percent electrode system for high-resolution eeg and erp measurements. *Clinical Neurophysiology,* 112: 713-719, 2001.

Opsahl T. *Structure and evolution of weighted networks*. *Secondary Titl*. London: University of London (Queen Mary College), 2009.

Opsahl T and Panzarasa P. Clustering in weighted networks. *Social Networks,* 31: 155-163, 2009.

Owen AM, Evans AC, and Petrides M. Evidence for a two-stage model of spatial working memory processing within the lateral frontal cortex: A positron emission tomography study. *Cereb Cortex,* 6: 31-8, 1996.

Owen AM, McMillan KM, Laird AR, and Bullmore E. N-back working memory paradigm: A meta-analysis of normative functional neuroimaging studies. *Hum Brain Mapp,* 25: 46-59, 2005.

Palva JM, Monto S, Kulashekhar S, and Palva S. Neuronal synchrony reveals working memory networks and predicts individual memory capacity. *Proc Natl Acad Sci U S A,* 107: 7580-5, 2010a.

Palva S, Monto S, and Palva JM. Graph properties of synchronized cortical networks during visual working memory maintenance. *Neuroimage,* 49: 3257-68, 2010b.

Pascual-Marqui RD. Standardized low-resolution brain electromagnetic tomography (sloreta): Technical details. *Methods Find Exp Clin Pharmacol,* 24 Suppl D: 5-12, 2002.

Pascual-Marqui RD. *Instantaneous and lagged measurements of linear and nonlinear dependence between groups of multivariate times series: Frequency decomposition. Arxiv:0711.1455[stat.Me]*. *Secondary Titl*., 2007.

Petersen SE, van Mier H, Fiez JA, and Raichle ME. The effects of practice on the functional anatomy of task performance. *Proc Natl Acad Sci U S A,* 95: 853-60, 1998.

Pickering SJ. *Working memory and education*. Oxford: Elsevier, 2006.

Pizzagalli D, Lehmann D, Koenig T, Regard M, and Pascual-Marqui RD. Face-elicited erps and affective attitude: Brain electric microstate and tomography analyses. *Clin Neurophysiol,* 111: 521-31, 2000.

Polania R, Paulus W, and Nitsche MA. Noninvasively decoding the contents of visual working memory in the human prefrontal cortex within high-gamma oscillatory patterns. *J Cogn Neurosci,* 24: 304-14, 2011.

Raghavachari S, Kahana MJ, Rizzuto DS, Caplan JB, Kirschen MP, Bourgeois B, Madsen JR, and Lisman JE. Gating of human theta oscillations by a working memory task. *J Neurosci,* 21: 3175-83, 2001.

Raghavachari S, Lisman JE, Tully M, Madsen JR, Bromfield EB, and Kahana MJ. Theta oscillations in human cortex during a working-memory task: Evidence for local generators. *J Neurophysiol,* 95: 1630-8, 2006.

Ravizza SM, Delgado MR, Chein JM, Becker JT, and Fiez JA. Functional dissociations within the inferior parietal cortex in verbal working memory. *Neuroimage,* 22: 562-73, 2004.

Sammer G, Blecker C, Gebhardt H, Bischoff M, Stark R, Morgen K, and Vaitl D. Relationship between regional hemodynamic activity and simultaneously recorded eeg-theta associated with mental arithmetic-induced workload. *Hum Brain Mapp,* 28: 793-803, 2007.

Sarnthein J, Petsche H, Rappelsberger P, Shaw GL, and von Stein A. Synchronization between prefrontal and posterior association cortex during human working memory. *Proc Natl Acad Sci U S A,* 95: 7092-6, 1998.

Sauseng P, Griesmayr B, Freunberger R, and Klimesch W. Control mechanisms in working memory: A possible function of eeg theta oscillations. *Neurosci Biobehav Rev,* 34: 1015-22, 2010.

Sauseng P, Klimesch W, Schabus M, and Doppelmayr M. Fronto-parietal eeg coherence in theta and upper alpha reflect central executive functions of working memory. *Int J Psychophysiol,* 57: 97-103, 2005.

Seeck M, Lazeyras F, Michel CM, Blanke O, Gericke CA, Ives J, Delavelle J, Golay X, Haenggeli CA, de Tribolet N, and Landis T. Non-invasive epileptic focus localization using eeg-triggered functional mri and electromagnetic tomography. *Electroencephalogr Clin Neurophysiol,* 106: 508-12, 1998.

Shaffer JP. Mutiple hypothesis testing. *Annual Review of Psychology*: 561-584, 1995.

Shah P and Miyake A. Models of working memory: An introduction. In *Models of working memory: Mechanism of active maintenance and executive control.* New York: Cambridge University Press, 1999.

Sinai A and Pratt H. High-resolution time course of hemispheric dominance revealed by low-resolution electromagnetic tomography. *Clin Neurophysiol,* 114: 1181-8, 2003.

Smith EE and Jonides J. Neuroimaging analyses of human working memory. *Proc Natl Acad Sci U S A,* 95: 12061-8, 1998.

Sporns O. *Networks of the brain*. Cambridge, MA: MIT Press, 2010.

Sporns O and Zwi JD. The small world of the cerebral cortex. *Neuroinformatics,* 2: 145-62, 2004.

Steriade M, Jones E, and Llinas RR. *Thalamic oscillations and signaling*. New York: Wiley, 1990.

Takahashi T, Murata T, Hamada T, Omori M, Kosaka H, Kikuchi M, Yoshida H, and Wada Y. Changes in eeg and autonomic nervous activity during meditation

and their association with personality traits. *Int J Psychophysiol,* 55: 199-207, 2005.

Takeuchi H, Taki Y, Hashizume H, Sassa Y, Nagase T, Nouchi R, and Kawashima R. Effects of training of processing speed on neural systems. *J Neurosci,* 31: 12139-48, 2011.

Uhlhaas PJ and Singer W. Neural synchrony in brain disorders: Relevance for cognitive dysfunctions and pathophysiology. *Neuron,* 52: 155-68, 2006.

van den Heuvel MP, Stam CJ, Kahn RS, and Hulshoff Pol HE. Efficiency of functional brain networks and intellectual performance. *J. Neurosci.,* 29: 7619-7624, 2009.

Watts DJ and Strogatz SH. Collective dynamics of 'small-world' networks. *Nature,* 393: 440-2, 1998.

Winterer G, Coppola R, Egan MF, Goldberg TE, and Weinberger DR. Functional and effective frontotemporal connectivity and genetic risk for schizophrenia. *Biol Psychiatry,* 54: 1181-92, 2003.

Worrell GA, Lagerlund TD, Sharbrough FW, Brinkmann BH, Busacker NE, Cicora KM, and O'Brien TJ. Localization of the epileptic focus by low-resolution electromagnetic tomography in patients with a lesion demonstrated by mri. *Brain Topogr,* 12: 273-82, 2000.

4.2.7. Supplementary Information

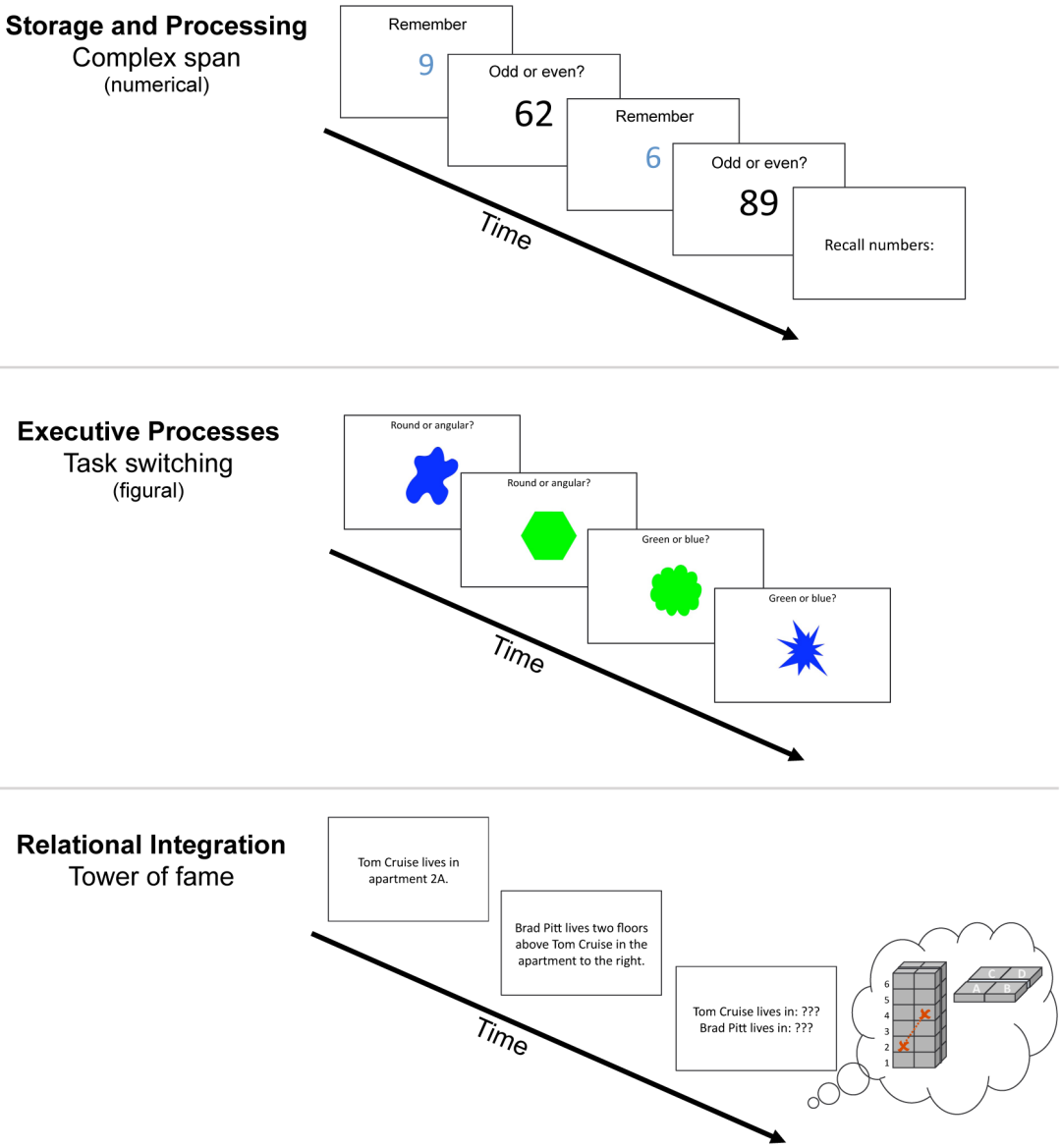

Figure S1: The course of the three working memory training task are illustrated. This figure refers to the experimental procedures section in the main text, in particular the training paragraph.

Table S1. Listed are the correlation coefficients and p-values of the correlation analysis between the small-world indices and the working memory performance of the pre-training data for all other thresholds of the theta frequency band.

		Clustering Coefficient	Path Length
threshhold	r	0.3154	-0.3211
0.95	p	0.0336	0.0298
threshhold	r	0.3369	-0.3266
0.90	p	0.0208	0.0264
threshhold	r	0.324	-0.3021
0.85	p	0.028	0.0448
threshhold	r	0.3139	-0.2841
0.80	p	0.0348	0.0644
threshhold	r	0.3089	-0.307
0.75	p	0.0388	0.0404
threshhold	r	0.3186	-0.3123
0.70	p	0.0314	0.036
threshhold	r	0.321	-0.321
0.65	p	0.0294	0.0294

Table S2. Listed are the results of the 2x2 ANOVA with one between group factor (working memory group, control group) and one within group factor (pre-training, post-training) of the small-world indices clustering coefficient and path length for all other thresholds in the theta frequency band.

	Clustering Coefficient ANOVA	 post-hoc t-tests	Path Length ANOVA	 post-hoc t-tests
threshhold 0.95	interaction (group x time): F = 5.40; p = 0.02	wm(pre- vs. post-training): t = -2.36, p = 0.03 tp2(wm vs. con): t = 2.38, p = 0.02	interaction (group x time): F = 2.86, p = 0.08	wm(pre- vs. post-training): t = 1.71, p = 0.09
threshhold 0.90	interaction (group x time): F = 6.32; p = 0.02	wm(pre- vs. post-training): t = -2.83, p = 0.01 tp2(wm vs. con): t = 2.56, p = 0.01	interaction (group x time): F = 4.13, p = 0.04	wm(pre- vs. post-training): t = 2.15, p = 0.03 tp2(wm vs. con) : t = -2.06, p = 0.04
threshhold 0.85	interaction (group x time): F = 5.44; p = 0.02 main effect time: F = 6.30; p = 0.02	wm(pre- vs. post-training): t = -3.40, p = 0.002 tp2(wm vs. con): t = 2.37, p = 0.02	interaction (group x time): F = 5.44, p = 0.02	wm(pre- vs. post-training): t =2.12, p = 0.04 tp2(wm vs. con) : t = -2.525, p = 0.002
threshhold 0.80	interaction (group x time): F = 5.10; p = 0.02	wm(pre- vs. post-training): t = -2.13, p = 0.04 tp2(wm vs. con): t = 2.30, p = 0.03		
threshhold 0.75	interaction (group x time): F = 4.33; p = 0.04	wm(pre- vs. post-training): t = -1.94, p = 0.06 tp2(wm vs. con): t = 2.14, p = 0.03		
threshhold 0.70	interaction (group x time): F = 3.878; p = 0.05	wm(pre- vs. post-training): t = -1.89, p = 0.07 tp2(wm vs. con): t = 2.04, p = 0.04	interaction (group x time): F = 2.86, p = 0.09	
threshhold 0.65	interaction (group x time): F = 3.30; p = 0.07	wm(pre- vs. post-training): t = -1.75, p = 0.09 tp2(wm vs. con): t = 1.88, p = 0.07	interaction (group x time): F = 3.53, p = 0.067	

Table S3. All hub regions of the intracortical graph-theoretical network analysis and their Brodmann area label are listed. The significant correlation coefficients between their degree centrality measurements and the working memory performance of the pre-training data are in bold numbers highlighted. This table refers to Figure 5.

Brodmann Area left hemisphere	Spearmann correlation r	Brodmann Area right hemisphere	Spearmann correlation r
BA 1	0.018	BA 1	<0.001
BA 2	0.188	BA 2	-0.002
BA 3	-0.040	BA 3	0.213
BA 4	0.001	BA 4	0.228
BA 5	-0.037	BA 5	0.067
BA 6	-0.083	BA 6	0.138
BA 7	0.121	BA 7	0.143
BA 8	**-0.304**	BA 8	-0.083
BA 9	-0.207	BA 9	-0.151
BA 10	**-0.265**	BA 10	**-0.308**
BA 11	**-0.393**	BA 11	-0.246
BA 13	0.112	BA 13	**0.282**
BA 17	0.116	BA 17	0.244
BA 18	0.164	BA 18	0.103
BA 19	0.078	BA 19	**0.294**
BA 20	-0.125	BA 20	-0.107
BA 21	0.212	BA 21	-0.032
BA 22	0.123	BA 22	**0.372**
BA 23	0.022	BA 23	0.085
BA 24	0.195	BA 24	0.198
BA 25	-0.167	BA 25	**-0.268**
BA 27	-0.203	BA 27	-0.188
BA 28	-0.207	BA 28	**-0.385**
BA 29	-0.228	BA 29	-0.227
BA 30	-0.239	BA 30	-0.252
BA 31	0.075	BA 31	**0.305**
BA 32	-0.110	BA 32	-0.038
BA 33	-0.078	BA 33	-0.009
BA 34	**-0.296**	BA 34	-0.244
BA 35	-0.163	BA 35	-0.249
BA 36	-0.020	BA 36	**-0.265**
BA 37	0.188	BA 37	0.214
BA 38	-0.196	BA 38	-0.106
BA 39	**0.285**	BA 39	**0.308**
BA 40	0.122	BA 40	**0.328**
BA 41	-0.066	BA 41	**0.355**
BA 42	0.071	BA 42	0.114
BA 43	-0.044	BA 43	-0.060
BA 44	0.064	BA 44	-0.052
BA 45	-0.164	BA 45	**-0.288**
BA 46	**-0.364**	BA 46	**-0.370**
BA 47	-0.198	BA 47	-0.114

Table S4: The exact statistical values of the degree centrality analysis for the working memory training effects comparing the pre- and post-training session and the two groups are listed. The significant contrasts are in bold numbers highlighted. This table refers to the Figure 6.

Brodmann Area	wm vs. controls t-value (p-value)	wm (pre-training vs. post-training) t-value (p-value)	controls (pre-training - post-training) t-value (p-value)
left BA 6	-1.41 (0.167)	-0.98 (0.337)	**-2.57 (0.016)**
left BA 7	**2.50 (0.016)**	**2.07 (0.048)**	**-2.15 (0.040)**
left BA 11	**-2.15 (0.037)**	**-2.41 (0.023)**	-1.00 (0.327)
left BA 17	0.04 (0.968)	**2.16 (0.040)**	**2.08 (0.046)**
left BA 18	0.47 (0.637)	**2.84 (0.008)**	**2.38 (0.024)**
left BA 24	-0.78 (0.439)	-1.50 (0.145)	**-2.28 (0.030)**
left BA 25	-1.80 (0.078)	**-3.30 (0.003)**	-1.31 (0.202)
left BA 30	-1.24 (0.220)	1.67 (0.107)	**2.69 (0.012)**
left BA 32	0.53 (0.600)	**-2.11 (0.044)**	-1.31 (0.201)
left BA 34	-0.37 (0.712)	**-2.11 (0.044)**	-1.22 (0.230)
left BA 43	**2.05 (0.046)**	1.72 (0.096)	-1.50 (0.145)
left BA 44	**2.02 (0.048)**	1.84 (0.077)	-0.99 (0.331)
right BA 6	**-2.23 (0.031)**	-0.87 (0.392)	1.71 (0.098)
right BA 8	-1.61 (0.115)	**-2.68 (0.012)**	-0.70 (0.490)
right BA 9	-0.78 (0.442)	**-2.42 (0.022)**	-1.05 (0.302)
right BA 10	**-2.07 (0.045)**	-1.13 (0.270)	1.02 (0.314)
right BA 11	**-2.77 (0.008)**	**-2.72 (0.011)**	0.74 (0.465)
right BA 17	0.68 (0.501)	**2.18 (0.038)**	1.30 (0.204)
right BA 20	-1.66 (0.105)	0.12 (0.906)	**2.06 (0.049)**
right BA 22	**2.26 (0.029)**	**2.44 (0.021)**	-0.04 (0.965)
right BA 25	-0.18 (0.856)	**-2.97 (0.006)**	**-2.47 (0.019)**
right BA 28	**-2.02 (0.049)**	**-2.51 (0.018)**	-0.34 (0.735)
right BA 30	-1.42 (0.163)	1.74 (0.094)	**2.29 (0.029)**
right BA 32	-1.82 (0.075)	**-2.75 (0.010)**	-1.08 (0.289)
right BA 34	-1.80 (0.078)	**-3.04 (0.005)**	-1.41 (0.170)
right BA 36	-1.87 (0.068)	1.56 (0.130)	**3.20 (0.003)**
right BA 39	**2.51 (0.016)**	**2.45 (0.021)**	-0.70 (0.490)

4.3. Experiment 3: The Problem of Thresholding in Small-World Network Analysis

Langer, N.[1], Pedroni, A.[2], Jäncke, L.[1]

1 Division Neuropsychology, Institute of Psychology, University of Zurich, 8050 Zurich, Switzerland

2 Division Social and Affective Neuroscience, Department of Psychology, University of Basel, Switzerland

4.3.1. Abstract

Graph theory deterministically models networks as sets of vertices, which are linked by connections. Such mathematical representation of networks, called graphs can be characterized by specific parameters (e.g. clustering coefficient, path length). In the field of neuroscience many forms of structural and functional brain networks are well modelled by small-world networks. Motivated by a small-world connectivity analysis of resting EEG-data we explored implications of a commonly used analysis approach. This common course of analysis is to compare small-world parameters between two groups using classical inferential statistics; however, it becomes problematic when using connectivity measures of inter-subject correlations (i.e. structural MRI and DTI (when only using FA-values)). In these cases, connectivity refers to voxel- or ROI-wise intercorrelations (e.g. grey matter density, fractal anisotropy). Since for each voxel there is only one data point, a measure of connectivity can only be computed for a group. To empirically determine an adequate small-world network threshold and to generate the necessary distribution of measures for classical inferential statistics, samples are generated by thresholding the

networks on the group level over a range of thresholds. We believe that there are mainly two problems with this approach. First, the number of thresholded networks is arbitrary. Second, the obtained thresholded networks are not independent samples. Here, we demonstrate potential consequences of the number of thresholds and non-independency of samples in two examples (with artificial data and with EEG data). Consequently alternative approaches are presented, which overcome these methodological issues.

4.3.2. Introduction

The human brain is organized as a highly interconnected structural network that functionally connects adjacent and distant brain areas (Palva, et al., 2010b). Such a network can be mathematically represented as a graph with vertices and nodes. The topology of such a graph is characterized by local and global parameters, namely, the cliquishness of connections between nodes in a topological neighbourhood of the graph (clustering coefficient), or the global efficiency of information transfer within the network (path length) (Bullmore and Bassett, 2011; Sporns, 2010). Networks of so-called "small-world" topology constitute an ideal balance of efficient information transmissions between distant nodes (small path length), while retaining powerful local information processing (high clustering coefficient) (Bullmore and Sporns, 2009; Watts and Strogatz, 1998). Brain networks at the scale of single neurons up to macroscopic functional networks incorporate the topology of such "small-worldness" (Bullmore and Bassett, 2011; Rubinov and Sporns, 2010). Interestingly, a growing number of studies indicates that small-world characteristics based on anatomical and functional brain measures are strongly related to intelligence (Langer, et al., 2010; Li, et al., 2009; Sporns, 2010), age (Meunier, et al., 2009; van den Heuvel, et al., 2009), sex (Micheloyannis, et al., 2009), genetics (Gong, et al., 2009), synaesthesia (Smit, et al., 2008), and/or neurological diseases (He, et al., 2008; Jancke and Langer, 2011; Micheloyannis, et al., 2006a; Rubinov, et al., 2009). Thereby, indicating that this network topology is a key factor in describing brain functions.

Although this research strategy provides promising insights, the commonly used analysis approach is associated with some particular statistical problems. In this paper we will discuss these problems and will present two alternative approaches that overcome these methodological issues.

Usually, small-world network analyses aim to test whether parameters of network efficiency (i.e. path length and average cluster coefficient) are related to specific populations. For example, the researcher aims to examine whether two or more groups differ in terms of particular network measures. In order to accomplish this comparison, the network measures are calculated for each group separately and then compared between these groups using parametric tests, such as, t-tests or ANOVAs. A common approach is to calculate various measures of dependency (i.e. correlation) between brain attributes obtained from regions of interest (i.e. cortical thickness, brain activity, etc.) that are extracted from anatomical or neurophysiological data (i.e. EEG, fMRI, MRI, or DTI). If measures of connectivity are obtained for each group separately - as with structural magnetic resonance imaging (sMRI) and diffusion tensor imaging (DTI) data (except for fibre tracking data) - (Hanggi, et al., 2011; Stam, 2010) only one network per group and per threshold can be calculated.

A commonly used strategy to conduct statistical comparisons is to use different and arbitrarily chosen thresholds from which the different network measures are calculated (Bullmore and Bassett, 2011; He, et al., 2008; Rubinov and Sporns, 2010). As a consequence of this strategy one obtains as many network measures per group as used thresholds. These different thresholded networks are pseudo-replications of group level networks, which serve as measures for classical

inferential statistics. In the context of this paper we will use the expression "multiple-thresholds-approach" to describe this analysis procedure.

Although frequently used, this "multiple-thresholds-approach" is associated with several more or less serious problems. First, depending on the number of chosen thresholds the sample size will vary considerably and this strongly influences the power of statistical testing. Second, the sets of thresholded mean correlation matrices are not independent (as classical statistics would require), because the information in a sparser correlation matrix is also comprised in a denser correlation matrix. This is particularly problematic for parametric statistical tests, since they inevitably require independence of the data. Thirdly, not only the number of used thresholds causes serious problems, but also the particular thresholds used to estimate the network parameters are problematic. For example, one could restrict the thresholds to a range from 0.2 to 0.6 or to a range from 0.3 to 0.8. Using these different ranges will generate different results.

Although the above-mentioned approach is not entirely wrong, since one may wish to compare the profiles of network parameters across the different thresholds, this approach can nevertheless lead to ambiguous results. In this paper, we will demonstrate with two examples how this approach can lead to ambiguous results. In the last part we will propose an alternative approach, which uses randomisation statistics and is not associated with the above-mentioned statistical problems.

4.3.3. Methods

Multiple-thresholds-approach

Example 1 - real data

For the first illustration of the problem associated with this approach we used EEG data from a previous study (Sporns, 2010). Seventy-four healthy male students (mean / standard deviation: 25,5/4.86 years) participated in the study. After recording seven minutes of spontaneous EEG at rest, subjects conducted the Raven Advanced Progressive Matrices (RAPM) (Langer, et al., 2011), which is a widely used measure of psychometric intelligence. In contrast to the previous study (Raven, 2003), we performed a median-split based on the performance in the RAPM. This resulted in a high IQ group (n = 25) and a low IQ group (n = 34). The median raw score was 23 correctly solved items. Subjects who scored at the median level of the RAPM were excluded. Spontaneous EEG at rest was used to analyze connectivity parameters of intracortical sources of brain oscillations in the upper alpha band (10,5-12 Hz). The coherence between 84 anatomical regions of interest in both hemispheres was computed (for the details of the analyses see (Langer, et al., 2011)). This resulted in an 84 x 84 correlation matrix (84 ROIs) for each subject. The connectivity matrices of all subjects from the low IQ group to the high IQ group were averaged separately, resulting in a mean connectivity matrix for the low IQ and high IQ groups. The connectivity matrices were then thresholded at different coherence values. This multiple-threshold approach resulted in as many networks per group as the number of thresholds applied to the connectivity matrix. Network parameters (clustering coefficient, characteristic path length and number of edges) were then calculated for each connectivity matrix by using the tnet software (Langer, et al., 2011). In order to

draw statistical inferences regarding group differences in network parameters, such as, the clustering coefficient and the characteristic path length, we used a classical parametric statistical test (t-test for independent samples). As mentioned above, this multiple-threshold-approach is problematic because both the sample size and the statistical power depend on the number of thresholds used. In addition, the key assumption of independency between samples in t-tests is violated when using differently thresholded correlation matrices.

We demonstrated this by using three different numbers of thresholds while keeping the ranges constant (range: 0.65-0.99). The sparsest network (threshold r = 0.99) was omitted, because the networks became no longer consistent. In the first trial we thresholded the connectivity matrix 10 times (increments: 0.034) resulting in 10 networks per group, in the second trial we thresholded the connectivity matrix 15 times (increments: 0.0227), and in the third trial we thresholded the connectivity matrix 35 times (increments 0.01). In a second step, the small-world parameters were calculated for each threshold per group. The different thresholded networks served as the different measurements units within each group.

Thus, in the first trial we obtained 10 measurements for each small-world parameter, in the second trial we obtained 15 measurements for each small-world parameter, and in the third trial we obtained 35 measurements for each small-world parameter. Afterwards, we separately compared these small-world parameters between the low IQ and the high IQ groups for each trial by using a t-test for independent samples ($p < 0.05$). Since we have to consider the fact that p-values depend on sample size, we also calculated effect sizes according to Cohen

(Opsahl, 2009). All statistical analyses in the present study were performed with MATLAB (Cohen)

Results

For the first trial (thresholding the matrix 10 times), there were no significant differences between the low and the high IQ groups regarding small-world parameters (clustering coefficient: $t_{(8)} = 1.87$, $p = 0.078$, Cohen's $d = 0.42$; path length: $t_{(8)} = -1.30$, $p = 0.21$, Cohen's $d = 0.31$; number of edges: $t_{(8)} = 1.85$, $p = 0.08$, Cohen's $d = 0.42$). For the second trial (thresholding the matrix 15 times), we found significantly more edges ($t_{(13)} = 2.40$, $p = 0.02$, Cohen's $d = 0.38$), a higher cluster coefficient ($t_{(13)} = 3.07$, $p = 0.004$, Cohen's $d = 0.46$), and no differences regarding characteristic path length ($t_{(13)} = -1.51$, $p = 0.14$, Cohen's $d = 0.25$) for the high IQ group compared to the low IQ group. For the third trial (thresholding the matrix 35 times), t-tests revealed highly significant differences between the high and the low IQ groups. There was a significantly increased number of edges ($t_{(33)} = 3.52$, $p = 7.76*10^{-4}$, Cohen's $d = 0.39$), and a higher clustering coefficient ($t_{(33)} = 4.44$, $p = 3.33*10^{-5}$, Cohen's $d = 0.47$) in the high IQ group. In contrast, we found a significantly decreased characteristic path length ($t_{(33)} = -2.24$, $p = 0.02$, Cohen's $d = 0.26$). An overview of this data is presented in Figure 1.

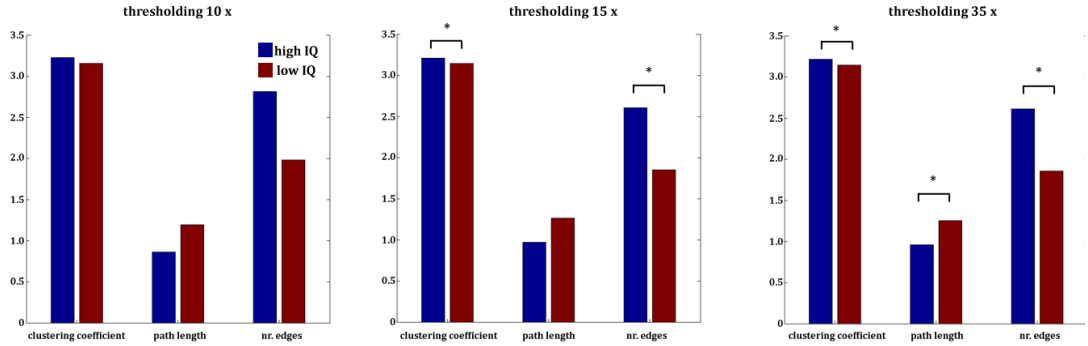

Figure 1: Mean values for the small-world parameters clustering coefficient, path length, and number of edges. We thresholded the correlation matrix 10, 15, and 35 times; this resulted in different statistical results. For the version with 10 increments, t-tests revealed no statistical differences. For the version with 15 increments, the clustering coefficient and number of edges was significantly increased in the high IQ group compared to the low IQ group. In the version with 35 different thresholds, the comparison between the high and low IQ groups revealed significant effects for all small-world parameters. The high IQ group showed a significantly enhanced small-world topology. For an optimized display, the numbers of edges were scaled (number of edges divided by 1000).

Example 2 – simulated data

In our second example, we use a simulation to illustrate how the commonly used multiple-threshold-approach may lead to false positive results. An illustration of the method is displayed in Figure 2. We set up our simulation to mimic the multiple-threshold-approach with data obtained by structural MRI or FA-DTI data. We simulated a study with 60 subjects, who comprised two experimental groups of equal size (30 subjects per group). This is a commonly used sample size for studies conducted in this field (Bullmore and Bassett, 2011; He, et al., 2007; http://www.mathworks.ch/products/matlab/). As in the first example, we used 84 brain regions (e.g. 84 Brodmann Areas). A randomly created value of a z-distribution was allocated for each of the 84 brain regions. This was done separately for each subject. Since we only have one value per node and sample, there is no possibility of calculating a correlation matrix for a single subject.

Therefore, in order to calculate the strength of the association between nodes, we needed to calculate correlations between the nodes (84 brain regions) of each group. This results in two association matrices with 84 rows and columns. Each entry of the row and column represents the correlation coefficient (connectivity strength) between the two simulated brain regions. Since there is now only one network per group, the groups cannot be statistically compared at this stage. We followed the common multiple-threshold-approach to "deal" with this problem by thresholding the two networks over a set of thresholds (range: 0.01-0.91; increments: 0.001, total: 900); this resulted in 900 networks per group. For each thresholded network we then obtained the small-world parameters, namely, the number of edges, the clustering coefficient, and the characteristic path length by using the tnet software (Salvador, et al., 2005). To compare the small-world network parameters, t-tests for independent samples ($p<0.05$) were used, which is common practice. We calculated three examples (three different threshold ranges) with the simulation data because we aimed to replicate the analysis and to demonstrate that in addition to the number of thresholds, the threshold limits (upper and lower threshold of the threshold range) might influence the results. In the first step, we extracted three different threshold ranges between 0.01 and 0.91. A low threshold range (0.01-0.06), a middle threshold range (0.50-0.54), and a high threshold range (0.86-0.91) were chosen. This resulted in 50 differently thresholded connectivity matrices per group within the threshold range. Analog to the example of the real data, we compared the networks of the two simulated groups over different numbers of thresholds. The different thresholded connectivity matrices served as the different measurement units within each group. In the first trial, we took 10 differently thresholded

connectivity matrices (increments: 0.005) for the group comparison using independent t-tests. In the second trial, we calculated with 25 connectivity matrices (increments: 0.002) per group. In the third trial, we calculated with 50 connectivity matrices (increments: 0.001) per group. This was done for the three threshold ranges (0.01-0.06; 0.50-0.54; 0.86-0.91). Because the networks were randomly generated, we hypothesized that there would be no differences between the networks of the two groups in any small-world parameter.

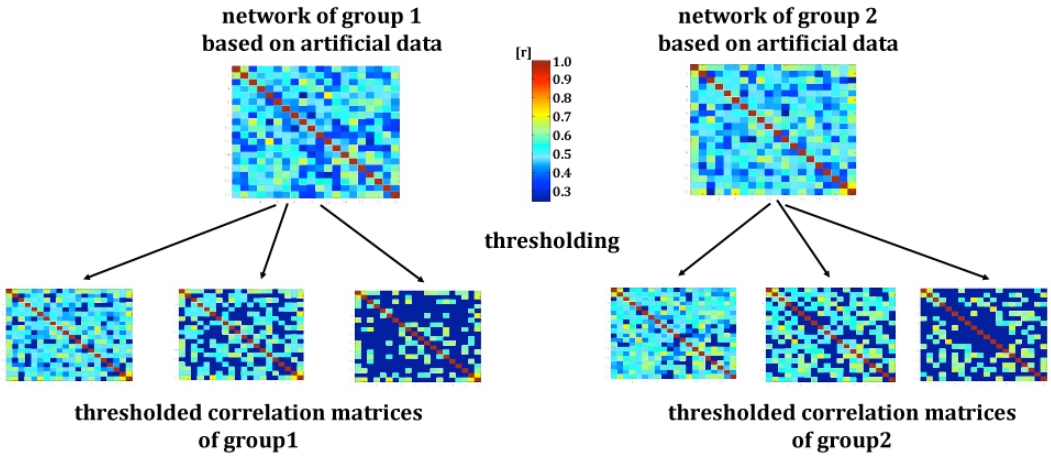

Figure 2: Networks of two groups based on artificial data. The networks were thresholded over a set of thresholds.

Results

Comparing the random networks of the two simulated groups for the first trial (10 thresholded connectivity matrices) within the threshold range of 0.86-0.91 revealed no significant difference in any of the small-world parameters. In the second trial (25 thresholded connectivity matrices), we found significantly more edges ($t_{(23)}$ = 2.18, p, = 0.03, Cohen's d = 0.29) and a lower characteristic path length ($t_{(23)}$ = -2.09, p, = 0.04, Cohen's d = 0.28) for the first group. For the third

trial (50 thresholded connectivity matrices), the t-tests revealed highly significant differences between the two simulated groups. There was also a significant increase in the number of edges ($t_{(48)}$ = 3.19, p, = 0.002, Cohen's d = 0.30) and in the clustering coefficient ($t_{(48)}$ = 2.20, p, = 0.03, Cohen's d = 0.21). In contrast, we found a significant decrease in the characteristic path length ($t_{(48)}$ = -3.05. p = 0.003, Cohen's d = 0.29).

Within the middle threshold range (0.50-0.54), there were no significant differences between the random networks of the two simulated groups in the first trial (10 thresholded connectivity matrices). However, for the second trial (25 thresholded connectivity matrices) there were only significant differences in the clustering coefficient ($t_{(23)}$ = -2.19, p, = 0.03, Cohen's d = 0.29) between the two simulated groups. The analysis of the number of edges displayed a trend to decreased number of edges in group one ($t_{(23)}$ = -1.83, p, = 0.07, Cohen's d = 0.23). In the third trial (50 thresholded connectivity matrices), the random network of the first group showed a decreased number of edges ($t_{(48)}$ = -2.61, p = 0.03, Cohen's d = 0.25) and a decreased clustering coefficient ($t_{(48)}$ = -2.97, p = 0.02, Cohen's d = 0.28) compared to the random network of the second group. The path length of the first group was significantly higher ($t_{(48)}$ = 2.24, p = 0.03, Cohen's d = 0.22).

For the lower threshold range (0.001-0.06), the first and second trials revealed no significant differences, but the third trial showed (50 thresholded connectivity matrices) a lower number of edges ($t_{(48)}$ = -2.41, p = 0.02, Cohen's d = 0.23) and a lower clustering coefficient ($t_{(48)}$ = -2.21, p = 0.03, Cohen's d = 0.22) for the first group's random network. All the results are presented in Figure 3.

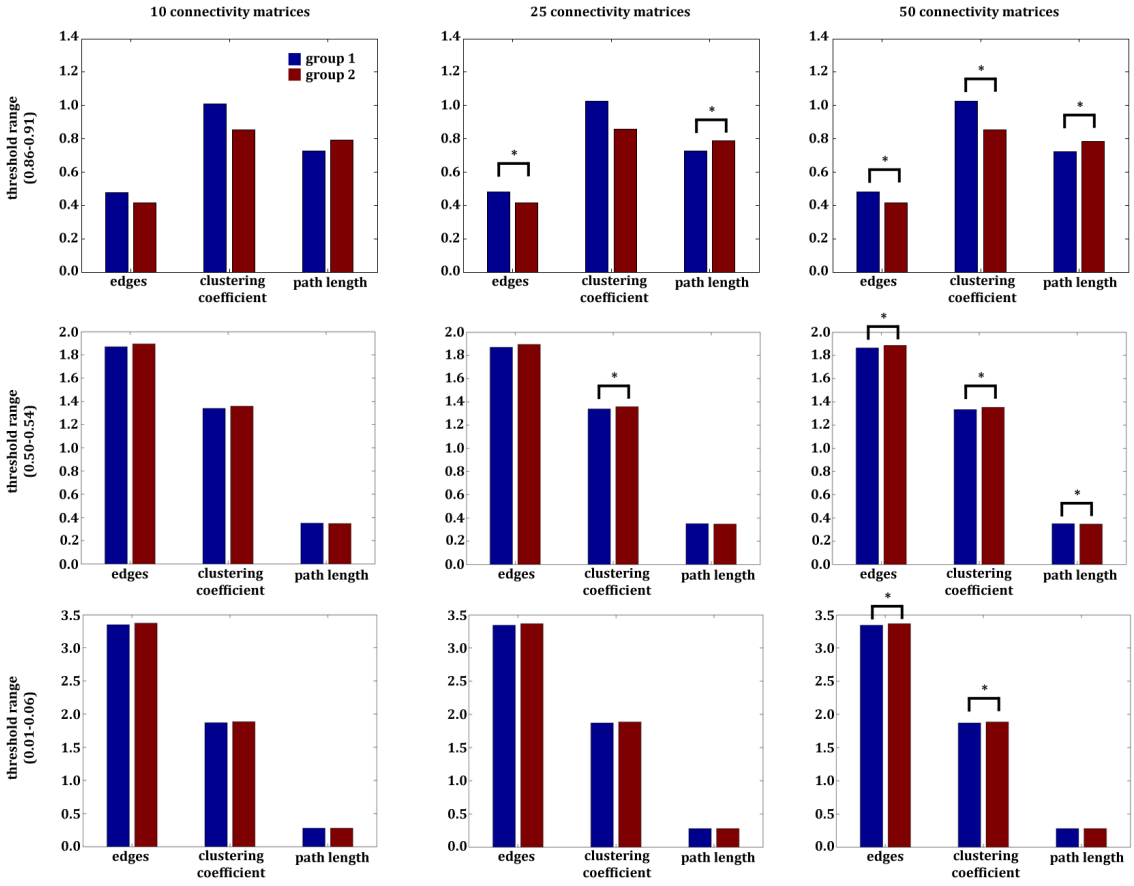

Figure 3: Displayed are the results of the second example, which used artificial data. The comparison of the two networks, based on artificial data, revealed several significant differences. Depending on the number of thresholds (defining the different measurement units within each group) and the threshold range used for the comparison, completely distinct results could be obtained. For an optimized display, the numbers of edges were scaled (number of edges divided by 1000).

Group-level-permutation-statistics-approach

Example 1 - real data

The same data set was used as in the first example, which made use of *multiple-thresholds-approach* (see above). In line with the first example using the *multiple-thresholds-approach,* we created a mean connectivity matrix (averaged across all subjects), which was then thresholded with a set of different thresholds (range r = 0.55-0.95, increments: 0.05). In the second step, small-world network parameters (clustering coefficient, path length) were calculated for the different thresholded mean coherence matrices. Here we present the results for the particular chosen threshold that best corresponds to a small-world topology (r = 0.85). This threshold was applied to the mean connectivity matrices of the low and high IQ groups. This is only one of several possible approaches to choosing a threshold. In the upcoming discussion section we delineate the other possibilities. For more information regarding the results of the other thresholds please consider the *supplementary data*.

As in the first example of the *multiple-thresholds-approach*, the subjects were allocated to a high or to a low IQ group based on a median-split, as previously described. The small-world network parameters were then calculated for the equally thresholded (threshold r = 0.85) connectivity matrices of the low and the high IQ groups. The small-world network parameters of the high IQ group were then subtracted from the parameters of the low IQ group. In order to statistically test these differences, we used permutation statistics. Permutation tests are a sub-group of non-parametric statistics. The basic principle has originally been described by Fisher (Opsahl, 2009) and has been extended by others (Edgington, 1995; Fisher, 1935; Manly, 1997; Pitman, 1937). The principle assumption is that

within a test group all subjects are equivalent and that every subject is the same before sampling started (Pitman, 1938). From this point, one can compute a statistic and then observe the amount to which this statistic is distinctive by comparing the test statistics under rearrangements of the treatment assignments (Nichols and Holmes, 2002). In contrast to classical parametric tests, which rely on theoretical probability distributions, permutation tests can be applied when the assumptions of parametric tests are untenable (Fisher, 1935). In situations where it is not feasible to compute the statistics for all the rearrangements, as is required in the Fisher's exact test, a subsample can be used (Edgington, 1995; Nichols and Holmes, 2002). Such a test is sometimes known as an approximate permutation test, because the permutation distribution is approximated by a subsample, also known as Monte-Carlo permutation tests or random permutation tests (Manly, 1997). In the present study, we used the Edgington approach. To this end, we allocated the subjects randomly to one of two groups and created 1000 randomly assigned pairs of groups. For each random group pair, we calculated the mean correlation matrix and then the small-world parameters of the networks. In the second step of analysis, the differences in small-world network parameters between the pairs were obtained. To statistically prove the real differences between the high and the low IQ groups, we tested the real differences within the distribution of the randomly generated differences and a global level of significance was set at $p<0.05$. When setting the error probability to $p < 0.05$, the real difference must exceed the extreme of 5% of the difference distribution, in order to reach statistical significance.

Results

The permutation analysis revealed that the high IQ group demonstrate significantly more edges than the low IQ group ($p < 0.001$). Moreover, we found an increased clustering coefficient ($p < 0.001$) and a decreased characteristic path length ($p = 0.004$) for the high IQ group compared to the low IQ group. Thus, the high IQ group exhibits significantly more small-world topology. All results are summarized in Figure 4.

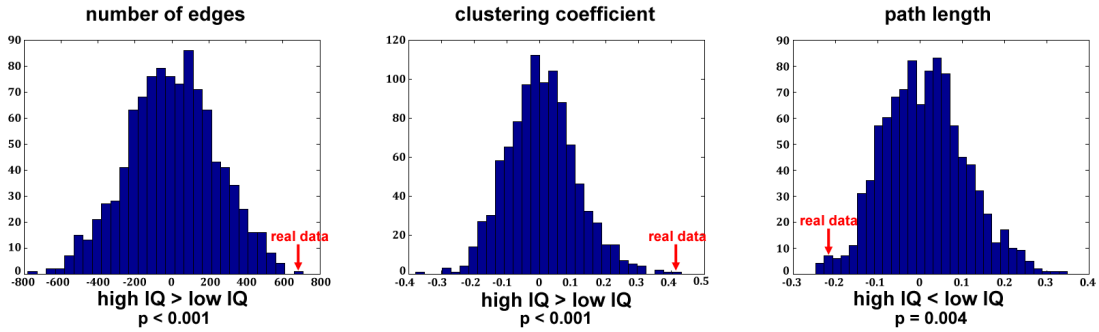

Figure 4: Displayed are the distributions of the randomly generated group pair differences. The red arrow indicates where the differences of the real data (= empirical difference between high and low IQ groups) are located within the distribution. The results show that the high IQ group revealed increased small-world network parameters.

Example 2 - simulated data

In the present example, we used the same data set as in the second example of the *multiple-thresholds-approach* with artificial random networks (connectivity matrices). Again we assume to have two different groups with 30 subjects per group, but there is only one value per node and subject (i.e. cortical thickness or FA value in this specific region). We again have 84 simulated brain regions per subject, where we again allocated random values to each simulated brain region for each single subject. These data were used to construct the correlation matrix between all pairs of nodes, resulting in an 84 x 84 association matrix (network)

for each group. They served as representation for the networks of two different groups.

However, instead of using the *multiple-thresholds-approach,* we now use no particular threshold, calculate the network parameters on the basis of the unthresholded data set, and subject these parameters to randomization tests, in order to conduct between-group comparisons. Since we did not threshold the connectivity matrices in this particular analysis, all connectivity matrices have an equal number of edges. Therefore, the between-group comparison of the number of edges is obsolete. Using unthresholded networks is only reasonable in the case of weighted networks (if every node is connected to every other node). Other alternative and valid approaches are discussed in the discussion section. However, the same procedure could also be applied to thresholded connectivity matrices. In the second step of analysis, we only computed the difference between the small-world parameters of the two groups. To statistically bolster this difference, we performed between-groups randomization tests by calculating different small-world parameters on the basis of 1000 randomized assignments of the subjects to the groups. We then computed a correlation matrix and small-world parameters for each randomization. This resulted in 1000 random group pairs. As for the originally assigned group, we again calculated the difference between the small-world parameters for each of the 1000 random group pairs, which resulted in 1000 difference values. These randomly achieved difference values now form the test-distribution and the difference of our originally assigned group of interest can now be tested using this distribution. A global level of significance was set at $p = 0.05$. Since all groups were randomly generated, we

assumed that there would be no significant differences regarding small-world topology.

Results

The permutation analysis revealed no significant differences regarding the clustering coefficient (p = 0.46, p > 0.05) or the characteristic path length (p = 0.88, p > 0.05).

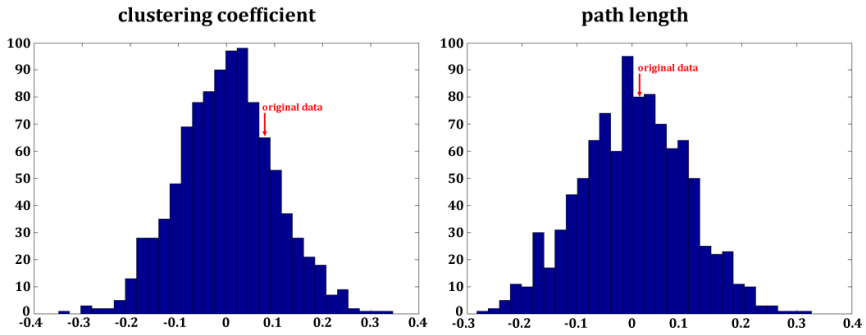

Figure 5: Displayed are the distributions of the randomly generated group pair differences. The red arrow indicates where the differences of the original data are located within the distribution. The results show, that there are no significant differences regarding the clustering coefficient or the characteristic path length.

Single-subject-connectivity-matrices-approach

Example 1 –real data

The same data set was used as in Example 1 of the *multiple-thresholds-approach* and the *group-level-permutation-statistics-approach* (See above). In contrast to the two previous methods, we now used the correlation matrix of each subject instead of averaging the connectivity matrices over the entire group. The correlation matrices were thresholded by applying a set of different thresholds (r = 0.65-0.95, increments: 0.05). The particular threshold, which identified the best small-world topology was chosen (r = 0.85) and applied to the correlation

matrices of each individual subject. For the results of the other thresholds, please refer to the *supplementary data*. Obtaining single subject correlation matrices is only available for times series data (e.g. fMRI, EEG, MEG) or DTI with fibre tractography. Subsequently the correlation matrix of each subject was subjected to tnet software (Nichols and Holmes, 2002; Opsahl, 2009; Opsahl, et al., 2008), which calculated the small-world indices for each individual subject (for further details see (Opsahl and Panzarasa, 2009)). For statistical comparisons of the small-world networks, we compared the subjects of the low IQ group with those of the high IQ group (based on median-split in the RAPM performance) by calculating a t-test for independent samples. The global level of significance was set at $p<0.05$. Another possibility would be to calculate a regression analysis between the performance in the intelligence task and the small-world parameters, as was done in our previous study (Langer, et al., 2011).

Results

The t-test for independent samples comparing the high IQ group vs. the low IQ group revealed a significantly increased number of edges ($t_{(57)} = 2.83$, $p = 0.006$), a significantly increased clustering coefficient ($t_{(57)} = 3.54$, $p = 0.001$), and a significantly decreased characteristic path length ($t_{(57)} = -2.70$, $p = 0.009$) (See (Langer, et al., 2011), for the results of the regression analysis).

Example 2 –simulated data

In this example we used a similar data set as in the second example of the *multiple-thresholds-approach* and the *group-level-permutation-statistics-approach* with artificial random networks. Again, we assume to have two different groups with 30 subjects per group, but in this example we assume that each subject has

an individual network, as is the case for MEG, EEG, resting fMRI, and DTI data when using tractography. We artificially created 60 networks with 84 nodes per network; representing for each subject a particular network. Subsequently the unthresholded weighted correlation matrix of each subject was subjected to tnet software, which calculated the small-world indices (clustering coefficient and characteristic path length) for each individual subject. The two groups were then compared with a t-test for independent samples (threshold was set $p<0.05$).

Results

The t-test for independent samples comparing the two groups did not reveal significant effects for the clustering coefficient ($t_{(58)} = 0.24$, $p = 0.81$) or for the characteristic path length ($t_{(58)} = 0.56$, $p = 0.58$).

4.3.4. Discussion

Graph-theoretical approaches are an elegant way to describe functional or structural brain networks on the basis of large anatomical and neurophysiological data sets. Although attractive, these techniques are associated with some statistical problems, which have been described in this paper. A major problem is on which basis inferential statistics are performed when statistically testing the measures obtained from graph-theoretical analyses. A typical approach is to compare the graph-theoretical measures between two different groups. Several papers have adopted the *multiple-thresholds-approach* by using different thresholds for which different graphs are computed separately for each group. The obtained graph-theoretical measures for each group are then subjected to between-groups statistical test. Typically this approach is used in the

context of graph-theoretical network analyses conducted with cortical thickness and FA data. Since for each voxel or region there is only one data point available, connectivity measures can only be computed for an entire group. Thus, there is no distribution of measures available to calculate statistical tests. To generate the necessary distribution of measures for classical inferential statistics, some studies generated an artificial distribution by thresholding the networks on group level over a range of thresholds and thus collected several connectivity measures. These different measures were then subjected to between-groups statistical tests. One problem with this approach is that these measures are not independent from each other since information of denser networks (thresholded using low thresholds) is also included in sparser networks (thresholded using high thresholds). These networks and thus the derived measures are strongly inter-correlated and should not be treated as coming from different subjects. This is a serious problem, especially for parametric inferential statistical analyses, which requires independence between the measurements. A further problem is that the power of the statistical tests strongly depends on the number of measurements and in this case on the number of thresholds used.

We demonstrated these problems on the basis of a real EEG data set and simulated data. As expected the p-values strongly depend on the number of thresholds. Thus, a researcher could easily manipulate the obtained p-value by arbitrarily manipulating the number of thresholds until he/she obtained the p-value she/he would like to achieve. In order to circumvent this problem effect size measures are more suitable because they are independent from sample size. In fact, we demonstrated similar effect size measurements that were independent of the number of thresholds. Therefore, effect sizes are an important

measurement, which should be added to the p-values if one still uses the *multiple-thresholds-approach*. If one is really interested in comparing the profiles of the network parameters across the different thresholds, randomization tests should be used since they do not need independence of the data.

We described two different approaches, which in a valid manner can indeed deal with the non-independency problem, namely, the *group-level-permutation-statistic-approach* and the *single-subject-connectivity-matrices-approach*. For intra-subject connectivity measures, like correlations between time series of resting-state fMRI, coherence measures of EEG or measures dependency obtained by fibre tracking in diffusion tensor imaging both suggested approaches are applicable. Whether the *group-level-permutation-statistic-approach* or the *single-subject-connectivity-matrices-approach* should be employed depends on the available data and the deployed research question. The advantages of the randomisation procedure are that permutation statistics can be applied when the assumptions of classical inferential statistics are untenable or distribution of the data is unknown and sample size is small (Langer, et al., 2011). An additional advantage is that an exact p-value (or a marginally exact p-value when Monte-Carlo procedure is used) can be calculated. The disadvantages of permutation tests are that the computation time could be very extensive, and that they also tend to be conservative. Further advantages and disadvantages could be found in: (Nichols and Holmes, 2002) and (Berger, 2000). Nevertheless, the *group –level-permutations-statistics-approach* is to our knowledge the only valid approach for using connectivity measures obtained on the basis of inter-subject correlations (i.e. structural MRI and DTI, when only using FA-values). The advantage of the *single-subject-connectivity-matrices-approach* is that it permits the use of single

subject variance for statistical analysis (e.g. regression analysis). The disadvantage of this approach is that it is only available for intra-subject data (e.g., times-series data in fMRI, MEG or EEG, as well as DTI, when fibre tracking is used).

There is currently no definitive and generally accepted strategy for applying particular thresholds in graph-theoretical networks analyses. How large should the threshold steps be? What are the smallest or largest thresholds that one can use? There are currently no concrete answers to these questions. Nonetheless, we present here and in our previous studies (Jancke and Langer, 2011; Jancke, et al., 2012; Nichols and Holmes, 2002) several possibilities to proceed if the connectivity measures are obtained by means of group level dependency. Probably the best way to circumvent the problem is to threshold the connectivity matrix over a wide range of thresholds and to then conduct the permutation analysis for each threshold individually as described above and in the supplementary data section. However, one has to face a problem with these approaches, which is the tremendous computation time for these analyses. For example, to perform a randomization test as described in the context of our *single-subject-connectivity-matrices-approach* with 84 nodes six days of computation time is needed for a standard workstation. When using more nodes, computation time exponentially increases to weeks or even months for the same workstation.

Using unthresholded weighted connectivity matrices (as it was demonstrated above) is another possibility to statistically test the network parameters, but this approach can also generate long computation times. In addition, thresholded networks exhibit a clearer small-world topology, because the noise of the data is

reduced by the thresholding procedure (Langer, et al., 2011). In our previous study, we presented a further possibility (Bullmore and Bassett, 2011; Jancke and Langer, 2011). We first determined the threshold, which exhibited the best small-world topology and then used this threshold. This is only one of several possibilities to choose a particular threshold. Most studies use thresholds over a predefined range that are defined a priori. This approach is adequate if these differently thresholded matrices are not used as independent measures or for parametric statistical tests.

Taken together there are several valid possibilities of dealing with thresholding in network analysis. The choice of the applied approach should be decided based on the particular hypothesis, the amount of data, the methods used for network analysis, and the resources that are available for the computations. We suggest that if there is the possibility to calculate a connectivity matrix for each individual subject, then one should *not* create mean connectivity matrices for a whole group and compare this mean connectivity between different groups.

4.3.5. References

Berger VW. Pros and cons of permutation tests in clinical trials. *Statistics in Medicine,* 19: 1319-1328, 2000.

Bullmore E and Sporns O. Complex brain networks: Graph theoretical analysis of structural and functional systems. *Nat Rev Neurosci,* 10: 186-98, 2009.

Bullmore ET and Bassett DS. Brain graphs: Graphical models of the human brain connectome. *Annu Rev Clin Psychol,* 7: 113-40, 2011.

Cohen J. *Statistical power analysis for the behavioral sciences*. New York: Academic Press, 1969.

Edgington ES. *Randomization tests*. New York: Marcel Dekker, 1995.

Fisher RA. *The design of experiment*. New York: Hafner, 1935.

Gong G, Rosa-Neto P, Carbonell F, Chen ZJ, He Y, and Evans AC. Age- and gender-related differences in the cortical anatomical network. *J Neurosci,* 29: 15684-93, 2009.

Hanggi J, Wotruba D, and Jancke L. Globally altered structural brain network topology in grapheme-color synesthesia. *J Neurosci,* 31: 5816-28, 2011.

He Y, Chen Z, and Evans A. Structural insights into aberrant topological patterns of large-scale cortical networks in alzheimer's disease. *J Neurosci,* 28: 4756-66, 2008.

He Y, Chen ZJ, and Evans AC. Small-world anatomical networks in the human brain revealed by cortical thickness from mri. *Cereb Cortex,* 17: 2407-19, 2007.

http://www.mathworks.ch/products/matlab/. *Secondary Titl*.

Jancke L and Langer N. A strong parietal hub in the small-world network of coloured-hearing synaesthetes during resting state eeg. *J Neuropsychol,* 5: 178-202, 2011.

Jancke L, Langer N, and Hanggi J. Diminished whole-brain but enhanced peri-sylvian connectivity in absolute pitch musicians. *J Cogn Neurosci,* 24: 1447-61, 2012.

Langer N, Beeli G, and Jancke L. When the sun prickles your nose: An eeg study identifying neural bases of photic sneezing. *PLoS One,* 5: e9208, 2010.

Langer N, Pedroni A, Gianotti LR, Hanggi J, Knoch D, and Jancke L. Functional brain network efficiency predicts intelligence. *Hum Brain Mapp*, 2011.

Li Y, Liu Y, Li J, Qin W, Li K, Yu C, and Jiang T. Brain anatomical network and intelligence. *PLoS Comput Biol,* 5: e1000395, 2009.

Manly BFJ. *Randomization, bootstrap, and monte-carlo methods in biology*. London: Chapman and Hall, 1997.

Meunier D, Achard S, Morcom A, and Bullmore E. Age-related changes in modular organization of human brain functional networks. *Neuroimage,* 44: 715-23, 2009.

Micheloyannis S, Pachou E, Stam CJ, Breakspear M, Bitsios P, Vourkas M, Erimaki S, and Zervakis M. Small-world networks and disturbed functional connectivity in schizophrenia. *Schizophr Res,* 87: 60-6, 2006.

Micheloyannis S, Vourkas M, Tsirka V, Karakonstantaki E, Kanatsouli K, and Stam CJ. The influence of ageing on complex brain networks: A graph theoretical analysis. *Hum Brain Mapp,* 30: 200-8, 2009.

Nichols TE and Holmes AP. Nonparametric permutation tests for functional neuroimaging: A primer with examples. *Human Brain Mapping,* 15: 1-25, 2002.

Opsahl T. *Structure and evolution of weighted networks*. *Secondary Titl*. London: University of London (Queen Mary College), 2009.

Opsahl T, Colizza V, Panzarasa P, and Ramasco JJ. Prominence and control: The weighted rich-club effect. *Physical Review Letters,* 101: -, 2008.

Opsahl T and Panzarasa P. Clustering in weighted networks. *Social Networks,* 31: 155-163, 2009.

Pitman EJG. Significance tests which may be applied to samples form any population. *Royal Statistical Society Supplement,* 4: 119-130 & 225-232, 1937.

Pitman EJG. Significance tests which may be applied to samples from any populations. *Biometrika,* 30: 322-335, 1938.

Raven J, Raven, J.C., Court, J.H. *Manual for raven's progressive matrices and vocabulary scales. Section1: General overview*. San Antonia: Harcourt Assessment, 2003.

Rubinov M, Knock SA, Stam CJ, Micheloyannis S, Harris AW, Williams LM, and Breakspear M. Small-world properties of nonlinear brain activity in schizophrenia. *Hum Brain Mapp,* 30: 403-16, 2009.

Rubinov M and Sporns O. Complex network measures of brain connectivity: Uses and interpretations. *Neuroimage,* 52: 1059-69, 2010.

Salvador R, Suckling J, Coleman MR, Pickard JD, Menon D, and Bullmore E. Neurophysiological architecture of functional magnetic resonance images of human brain. *Cereb Cortex,* 15: 1332-42, 2005.

Smit DJ, Stam CJ, Posthuma D, Boomsma DI, and de Geus EJ. Heritability of "Small-world" Networks in the brain: A graph theoretical analysis of resting-state eeg functional connectivity. *Hum Brain Mapp,* 29: 1368-78, 2008.

Sporns O. *Networks of the brain*: MIT Press, 2010.

Stam CJ. Use of magnetoencephalography (meg) to study functional brain networks in neurodegenerative disorders. *J Neurol Sci,* 289: 128-34, 2010.

van den Heuvel MP, Stam CJ, Kahn RS, and Hulshoff Pol HE. Efficiency of functional brain networks and intellectual performance. *J. Neurosci.,* 29: 7619-7624, 2009.

Watts DJ and Strogatz SH. Collective dynamics of 'small-world' networks. *Nature,* 393: 440-2, 1998.

4.3.6. Supplementary Information

Method: Group-level-permutation-statistics

Example 1 – real data

Table S1. Listed are the p-values for each small-world parameter of the permutation statistics of the first example (EEG data) of all thresholds. We compared the difference of the real EEG data to 1000 randomly generated group pairs. All threshold showed an increased small-worldness for the high IQ group.

		Nr. Edges	Clustering Coefficient	Path Length
threshhold 0.95	p	0.001	0.003	0.003
threshhold 0.90	p	0.003	0.003	0.004
threshhold 0.85	p	<0.001	<0.001	0.004
threshhold 0.80	p	0.002	0.001	0.003
threshhold 0.75	p	0.001	<0.001	0.003
threshhold 0.70	p	0.002	0.001	0.004
threshhold 0.65	p	0.006	0.001	0.007

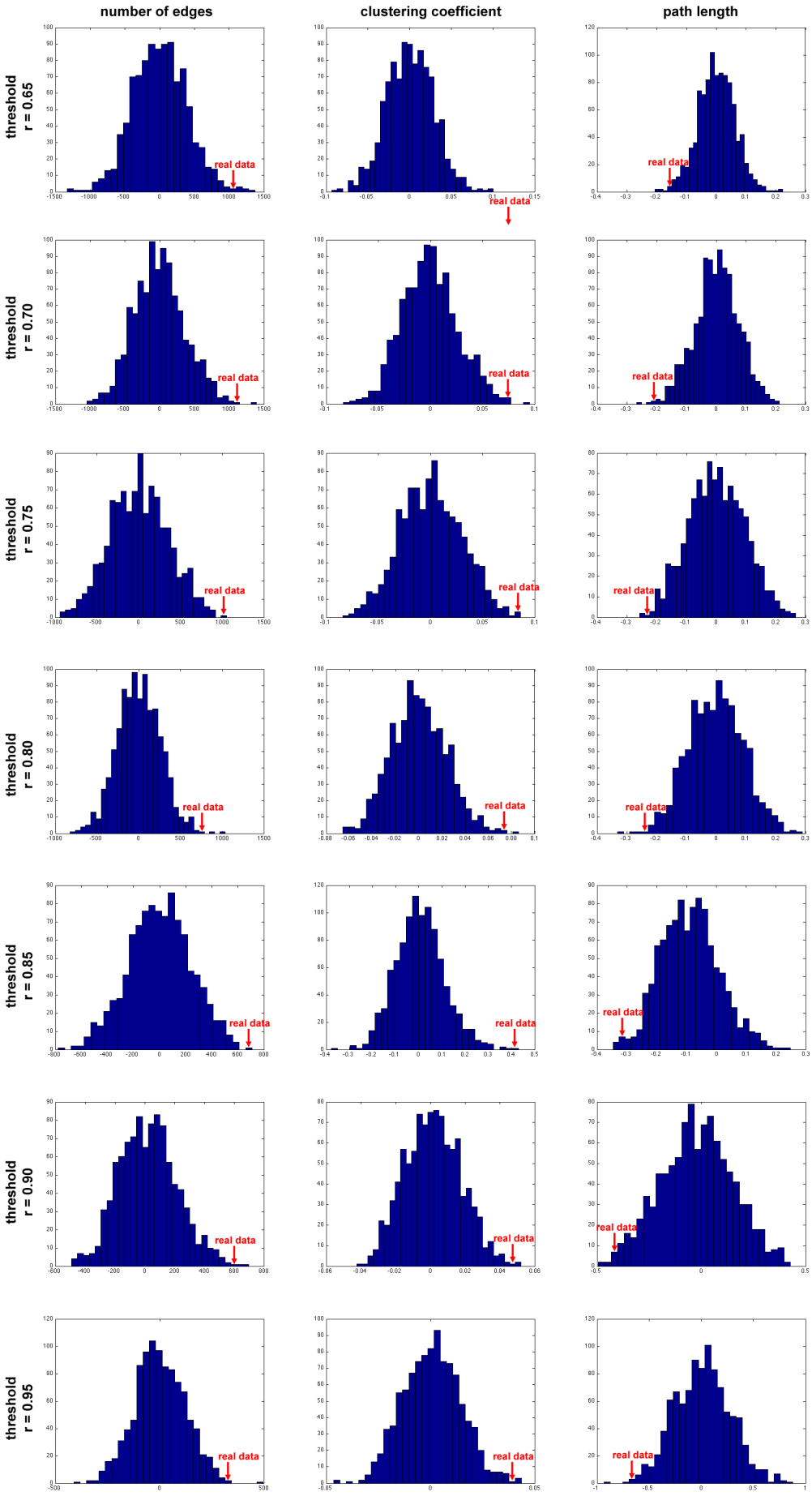
number of edges
clustering coefficient
path length
threshold r = 0.65
threshold r = 0.70
threshold r = 0.75
threshold r = 0.80
threshold r = 0.85
threshold r = 0.90
threshold r = 0.95
real data

Figure S1: Displayed are the distributions of the randomly generated group pair differences for all thresholds. The red arrow indicates where the differences of the real EEG data are located within the distribution. The results of all thresholds show, that the high IQ group revealed increases small-worldness.

Method: Single-subject-connectivity-matrices-approach

Example 1 –real data

Table S2. Listed are the t-values and p-values for each small-world parameter of the single subject method of the first example (EEG data) for all thresholds. We compared the small-world parameters between the high and the low IQ group for each threshold separately. All threshold showed an increased small-worldness for the high IQ group.

		Clustering Coefficient	Path Length	Nr. Edges
threshhold	t	3.43	-2.61	2.69
0.95	p	0.001	0.011	0.01
threshhold	t	3.51	-2.83	2.72
0.90	p	0.001	0.006	0.009
threshhold	t	3.54	-2.70	2.83
0.85	p	0.001	0.009	0.006
threshhold	t	3.28	-2.58	2.69
0.80	p	0.002	0.013	0.01
threshhold	t	3.28	-2.61	2.73
0.75	p	0.002	0.012	0.008
threshhold	t	3.26	-2.66	2.76
0.70	p	0.0019	0.01	0.008
threshhold	t	3.28	-2.72	2.80
0.65	p	0.002	0.008	0.007

5. General Discussion

The main purpose of experiment 1 was to identify whether individual differences in cognitive functions such as intelligence are associated with differences in small-world characteristics of functional networks based on resting-state EEG data. Small-world topology in the context of intelligence was previously investigated with resting fMRI (Langer, et al., 2011) and DTI data (van den Heuvel, et al., 2009), but only once with EEG data (Li, et al., 2009), which revealed contrary results to the former two studies. While the cause of this discrepancy is not yet clear, there are methodological issues of concern, such as the limited set of surface electrodes and the network analysis on scalp level, which suffers from the volume conductivity problem. To circumvent these methodological issues, we re-addressed our study by using high-density EEG in association with a valid method to estimate the intracortical sources of surface EEG standardized low resolution brain electromagnetic tomography (sLORETA) (Micheloyannis, et al., 2006b). In fact our results revealed increased small-world topology in the alpha2 frequency band, which is predictive to the performance in the intelligence task. This was also shown by the fMRI and DTI data mentioned above. This findings assured us that we are able to investigate functional brain networks with EEG data, which we later adopted to different context, as investigating differences between synesthetes and controls (Pascual-Marqui, 2002), during cycling exercise (Jancke and Langer, 2011) or in pianist (in preparation). Motivated by a study, which could demonstrate a high reproducibility of functional brain networks of the resting-state (Hilty, et al., 2011), the aim of experiment 2 was to investigate, if the resting-state of the brain could be changed due to intensive

working memory training. In particular we hypothesized to shift the functional brain network more toward small-world topology. In fact, we first identified that a more efficient functional network in the theta band is associated with an increased working memory performance (by analyzing only the pre-training data) and subsequently a significant increase of small-worldness induced by the working memory training. So far as we know, this is the first investigation of plasticity of functional brain networks based on resting-state EEG data. Since graph theoretical analyses are relatively new in neuroscience, there are some methodological considerations. The problem of thresholding was illustrated in experiment 3, where we demonstrated based on EEG and artificial data that the number of thresholded networks is arbitrary. Moreover, the obtained thresholded networks are not independent samples. We revealed in experiment 3 the potential consequences of the number of thresholds and non-independency of samples in two examples. However, the problem of thresholding in network analyses is only one of the methodological considerations. In the next section some additional methodological considerations will be presented.

5.1. Methodological Considerations

Functional brain network analyses with EEG data provide a powerful method to investigate cognitive processes in the brain, but one have to be aware of potential methodological flaws, which will be discussed here. The precision of the EEG-source localization is limited. Nevertheless, the areas found in the first two experiments are typically showed by other research groups studying intelligence (Deuker, et al., 2009) and working memory (Jung and Haier, 2007). For example (Hampson, et al., 2006), could demonstrate in their fMRI connectivity analysis

during working memory performance a very similar connectivity pattern as revealed in experiment 2. At a more general level, the source reconstruction technique is fundamental for the entire network analysis. The source reconstruction, as was used in our studies (Hampson, et al., 2006; Pascual-Marqui, 2002), has been experimentally validated in various studies and under diverse conditions (Khateb, et al., 2001; Langer, et al., 2010; Pascual-Marqui, 2007b) and cross-validated with fMRI (Pizzagalli, et al., 2000; Seeck, et al., 1998). Nevertheless, further studies using graph-theoretical analysis at an intracortical level could be improved by referring to the individual brain anatomy, which creates less uncertainty for inverse modelling than an average brain. In addition, one of the unsolved problems in connectivity analysis based on EEG data is the volume conduction, although to a lesser extent in the intracortical space than at sensor level, which could even be improved by using only the lagged coherence. In our studies, we used instantaneous coherence measures, because we were not able to detect small-world topology in lagged data. Probably lagged coherence is more useful in an event-related design and studying effective connectivity, which is not plausible in resting state data. We used the coherence measure, but there is also an other valid connectivity measure, phase synchrony as used by Singer and Gray (Worrell, et al., 2000). Another issue in experiment 1 is the influence of age. We found a strong correlation between age and IQ and thus use age as a covariate to statistically eliminate age effects on the EEG data. However, the implicit assumption here is that age is linearly related to alpha2 activity. However, it might be that there are also non-linear associations, which we did not detect in our analyses of experiment 1.

In summary, this thesis has emphasized the appealing data reductionistic

straightforwardness, generalizability and clinical significance of brain graphs, but graph analysis of neuroimaging data is not “plug and play.” It is a model-based approach, demanding arbitrary assumptions and decisions, which can have significant effects on the outcomes of the analysis. Moreover, there is no best way how to compare topological metrics between graphs and it is in general not a trivial question. In addition to these relatively specific issues about construction and comparison of brain networks, any procedure to graph theoretical analysis of neuroimaging data also put up a number of inquires about data acquisition, preprocessing, statistical tests, multiple comparisons and visualization.

5.2. No transfer effects to intelligence: Why?

However, in contrast to previous studies (Singer and Gray, 1995) no far transfer effects to other cognitive domains was found in experiment 2. We could only speculate about the reasons. One possibility is the different working memory training. In our study the working memory had more (verbal) memory proportion, whereas the working memory training of the Jaeggi study involved a dual n-back tasks with a visuo-spatial and a auditory component, which might be more similar to the RAPM intelligence test. A feasible reason also could be the speed factor, because the time to solve the intelligence test was to short in the Jaeggi study, which was criticized by other scientists (Jaeggi, et al., 2008). A last possible explanation could be conjectured by the fact, that in our previous functional brain network study of intelligence the alpha2 frequency is crucial for the RAPM intelligence task, whereas the literature about working memory and the present study revealed a theta band involvement in working memory tasks

and training. Although the identified brain regions underlying intelligence and working memory in experiment 1 and 2 overlap in a considerable amount, the related brain oscillations to the particular cognitive processes are different in our experiments. To draw an analogy to language: assuming a multilingual human, which mother tongue is German and the subject knows in addition English and Chinese. When the subject trains the English vocabulary the Chinese vocabulary will consequently not improve. A similar mechanism could underlie in the brain network. Brain oscillations might be a kind of language within the brain network. While the efficiency of one oscillation might be enhanced by an intervention, the other oscillations will not automatically benefit of this improvement, although the underlying brain anatomy is equivalent.

5.3. Brain Plasticity after Training

The detection that the human brain has the capacity to adapt rapidly to changing demands, which can take place from a synaptic to a cortical level throughout the life, has caused an alteration in the perspective of cognitive neuroscience (Jäncke, 2009). The antecedent believe was that the adult brain is hard-wired and resistant to change (Moody, 2009). Animal and human studies has proved that the configuration of the adult cerebral cortex can change considerably as a product of experience and practice (Draganski, et al., 2004; Draganski and May, 2008; Driemeyer, et al., 2008; Jäncke, 2009; Jancke, et al., 2009; Kolb and Whishaw, 1998; Maguire, et al., 2000; Merzenich, et al., 1983). Brain plasticity can take place at several levels of the central nervous system, from the molecular or synaptic level of cortical maps and large-scale neural networks (Pascual-Leone, et al., 2005). “If the neuroanatomic, neurochemical and functional changes that

occur in response to practice also underlie the recovery of function following damage to the brain, then this knowledge will aid in the understanding of the mechanisms of repair and recovery in damaged or malfunctioning brains" (Buonomano and Merzenich, 1998). Finding training effects, as in experiment 2, raise the question, whether an increase or decrease in the same areas is prominent as before the training or if a neural distribution to new areas has taken place. Experience-dependent activation decreases is suggested to reflect sharpening of the response in a specific brain area so that less neurons fire in response to a particular stimulus or task (Kelly, et al., 2006). Such activation decreases reflect increased efficient neural assemblies and cognitive processes as was proposed by the neural efficiency theory (Poldrack, 2000). In contrast activation increases is suggested to correspond expansions in the spatial extent of cortical representations and increases in the strength or amplitude of activations (Neubauer, et al., 2004). The distinction between these two possibilities is practically difficult, for the reason that expanded representations may be undetectable at the spatial resolution of most neuroimaging studies (Kelly, et al., 2006). From a microscopic viewpoint activation increases could reflect recruitment of additional neurons with practice, which is seen by neuroimaging methods as an increase in the spatial extent of activation or as a strengthening of the response within a particular region (Kelly, et al., 2006). A reorganization of functional activations as a result of practice is a commonly observed pattern. There are two types of practice-related reorganization, which could be distinguished. Redistribution of functional activation reflects more a quantitative change. It constitutes the above-mentioned combination of increases and decreases in functional activations, whereas functional reorganization of

activation results of a qualitative shift in the cognitive processes underlying task performance and a change in the location of activations as a result of practice (Poldrack, 2000).

Previous studies could show arguments for both possibilities, although no study investigated functional brain networks in this context (Jonides, 2004; Kelly, et al., 2006; Petersen, et al., 1998; Schneiders, et al., 2011). Taking a closer inspection of the hubs and nodes of experiment 2, the identified network revealed very similar brain regions, which were associated with working memory performance und those brain regions, which were changed by the working memory training. Although this finding argues more for the theory of efficient processing instead of a neural reorganization (or scaffolding storage framework), we additionally also find regions which were significant only in the training effects analysis, which could be taken as an indicator for activity redistribution. Probably both mechanisms are prominent in the present study, as been also proposed by Buschkuehl et al. (Dux, et al., 2009). Chein and Schneider proposed a dual process theory, where they described discrete states of learning, such as a controlled task performance emerging in to a automatic task performance, which is associated with a decrease in general control centers but an increase in task specific regions (Buschkuehl, et al., 2011). In early learning a support of a control processing center (domain-general) is more required. Such domain-general processing centers could be assigned to the prefrontal areas of the brain, whereas task specific regions are located more in the parietal regions (Chein and Schneider, 2005). Analog training effects in a parieto-frontal network could be observed in experiment 2.

5.4. Future directions

Graph-theoretical networks analyses in neuroscience open up numerous new investigation possibilities. Previous studies on small-world networks focused almost exclusively on functional connectivity in the resting-state of the subjects. Future studies investigating small-world networks should also consider effective connectivity, since causal relationships provide more information about cognitive processes and enable enhanced possibilities for modification of behavior. Furthermore, it is still unclear how structural and functional networks are related to each other. Although there are some studies about the relationship between structural networks, obtained by structural MRI or DTI, compared to functional networks with fMRI, future studies should also examine the link between structural networks on the basis of cortical thickness data and the functional networks measured by EEG data. This relationship is of particular importance, since EEG signal is depending on structural properties of the brain. Therefore information about this specific relationship between structural and functional networks could further improve comprehension and application of EEG in neuroscience. Simultaneous fMRI and EEG measurements with subsequent network analyses could provide information's about the relationship between functional neural networks based on different neuroscientific measurement methods, although one should be careful, since cleaning the EEG recorded inside the MR scanner involves several filtering steps, which could in principle induce long-range dependency. A further implementation of graph-theoretical network analysis has been shown by Ray and colleagues. In their study, a classification of epileptic patient or healthy subject, based on EEG data, has been improved with small-world network analysis (Ray et al., 2010). I think network analyses has

potential to be adopted to a clinical practice, such as composition of network biomarkers for psychiatric and neurological diseases. As mentioned in the beginning, previous studies on small-world networks have focused on the resting state of the brain. Although this thesis and other studies showed that similar brain regions are connected in the resting-state as during task performance, future studies should also examine the small-world networks during an active condition. Such analyses could help to understand the cognitive processes, strategies to solve the tasks and possible reasons for success or failure. Taken together, graph-theoretical network analysis in neuroscience is a rapidly emerging field and the study of brain connectivity will open new experimental and theoretical concepts in neuroscience.

6. References

Achard S, Bullmore E (2007): Efficiency and cost of economical brain functional networks. PLoS Comput Biol 3(2):e17.

Achard S, Salvador R, Whitcher B, Suckling J, Bullmore E (2006): A resilient, low-frequency, small-world human brain functional network with highly connected association cortical hubs. J Neurosci 26(1):63-72.

Andersen RA, Cui H (2009): Intention, action planning, and decision making in parietal-frontal circuits. Neuron 63(5):568-83.

Annett M (1970): A classification of hand preference by association analysis. Br J Psychol 61(3):303-21.

Anokhin A, Vogel F (1996): EEG alpha rhythm frequency and intelligence in normal adults. Intelligence 23(1):1-14.

Asada H, Fukuda Y, Tsunoda S, Yamaguchi M, Tonoike M (1999): Frontal midline theta rhythms reflect alternative activation of prefrontal cortex and anterior cingulate cortex in humans. Neurosci Lett 274(1):29-32.

Awh E, Jonides J, Smith EE, Schumacher EH, Koeppe RA, Katz S (1996): Dissociation of storage and rehearsal in verbal working memory: Evidence from positron emission tomography. Psychological Science 7(1):25-31.

Babiloni C, Binetti G, Cassetta E, Cerboneschi D, Dal Forno G, Del Percio C, Ferreri F, Ferri R, Lanuzza B, Miniussi C, Moretti DV, Nobili F, Pascual-Marqui RD, Rodriguez G, Romani GL, Salinari S, Tecchio F, Vitali P, Zanetti O, Zappasodi F, Rossini PM (2004a): Mapping distributed sources of cortical rhythms in mild Alzheimer's disease. A multicentric EEG study. Neuroimage 22(1):57-67.

Babiloni C, Ferri R, Moretti DV, Strambi A, Binetti G, Dal Forno G, Ferreri F, Lanuzza B, Bonato C, Nobili F, Rodriguez G, Salinari S, Passero S, Rocchi R, Stam CJ, Rossini PM (2004b): Abnormal fronto-parietal coupling of brain rhythms in mild Alzheimer's disease: a multicentric EEG study. Eur J Neurosci 19(9):2583-90.

Babiloni F, De Vico Fallani F, Cincotti F (2011): Multimodal Integration of EEG, MEG, and Functional MRI in the Study Of Human Brain Activity. In: Cerutti S, Marchesi C, editors. Advanced Methods of Biomedical Signal Processing. Hoboken: John Wiley & Sons, Inc.

Baddeley A (2000): The episodic buffer: a new component of working memory? Trends Cogn Sci 4(11):417-423.

Baddeley A (2003): Working memory: Looking back and looking forward. Nature Reviews Neuroscience 4(10):829-839.

Baddeley AD (2002): Is working memory still working? European Psychologist 7(2):85-97.

Baddeley AD, Hitch GJ (1974): Working Memory. In: Bower GA, editor. The psychology of learning and motivation: advances in research and theory. New York: Academic Press.

Barabasi AL (2009): Scale-Free Networks: A Decade and Beyond. Science 325(5939):412-413.

Barrat A, Barthelemy M, Pastor-Satorras R, Vespignani A (2004): The architecture of complex weighted networks. Proc Natl Acad Sci U S A 101(11):3747-52.

Bartolomei F, Bosma I, Klein M, Baayen JC, Reijneveld JC, Postma TJ, Heimans JJ, van Dijk BW, de Munck JC, de Jongh A, Cover KS, Stam CJ (2006): Disturbed functional connectivity in brain tumour patients: evaluation by graph analysis of synchronization matrices. Clin Neurophysiol 117(9):2039-49.

Bassett DS, Bullmore E (2006): Small-world brain networks. Neuroscientist 12(6):512-23.

Bassett DS, Bullmore E, Verchinski BA, Mattay VS, Weinberger DR, Meyer-Lindenberg A (2008): Hierarchical organization of human cortical networks in health and schizophrenia. J Neurosci 28(37):9239-48.

Bassett DS, Bullmore ET (2009): Human brain networks in health and disease. Curr Opin Neurol 22(4):340-7.

Bassett DS, Meyer-Lindenberg A, Achard S, Duke T, Bullmore E (2006): Adaptive reconfiguration of fractal small-world human brain functional networks. Proc Natl Acad Sci U S A 103(51):19518-23.

Berger VW (2000): Pros and cons of permutation tests in clinical trials. Statistics in Medicine 19(10):1319-1328.

Birbaumer N, Elbert T, Canavan AG, Rockstroh B (1990): Slow potentials of the cerebral cortex and behavior. Physiol Rev 70(1):1-41.

Brett M, Johnsrude IS, Owen AM (2002): The problem of functional localization in the human brain. Nature Reviews Neuroscience 3(3):243-249.

Britz J, Landis T, Michel CM (2009): Right parietal brain activity precedes perceptual alternation of bistable stimuli. Cereb Cortex 19(1):55-65.

Brodal A, Walberg F (1982): A re-evaluation of the question of ascending fibers in the pyramidal tract. Brain Res 232(2):271-81.

Brodmann K. (1909). Vergleichende Lokalisationslehre der Grosshirnrinde in ihren Prinzipien dargestellt auf Grund des Zellenbaues. Leipzig: Barth.

Bullmore E, Fadili J, Maxim V, Sendur L, Whitcher B, Suckling J, Brammer M, Breakspear M (2004): Wavelets and functional magnetic resonance imaging of the human brain. Neuroimage 23 Suppl 1:S234-49.

Bullmore E, Sporns O (2009): Complex brain networks: graph theoretical analysis of structural and functional systems. Nat Rev Neurosci 10(3):186-98.

Bullmore ET, Bassett DS (2011): Brain graphs: graphical models of the human brain connectome. Annu Rev Clin Psychol 7:113-40.

Buonomano DV, Merzenich MM (1998): Cortical plasticity: From synapses to maps. Annual Review of Neuroscience 21:149-186.

Buschkuehl M, Jaeggi SM, Jonides J (2011): Neuronal effects following working memory training. Developmental Cognitive Neuroscience.

Butts CT (2009): Revisiting the foundations of network analysis. Science 325(5939):414-6.

Cajal SR. (1995). Histology of Nervous System of Man and Vertebrates. New York: Oxford University Press.

Canals S, Beyerlein M, Merkle H, Logothetis NK (2009): Functional MRI evidence for LTP-induced neural network reorganization. Curr Biol 19(5):398-403.

Canolty RT, Edwards E, Dalal SS, Soltani M, Nagarajan SS, Kirsch HE, Berger MS, Barbaro NM, Knight RT (2006): High gamma power is phase-locked to theta oscillations in human neocortex. Science 313(5793):1626-8.

Carpenter PA, Just MA, Shell P (1990): What one intelligence test measures: a theoretical account of the processing in the Raven Progressive Matrices Test. Psychol Rev 97(3):404-31.

Catani M, ffytche DH (2005): The rises and falls of disconnection syndromes. Brain 128(Pt 10):2224-39.

Chein JM, Schneider W (2005): Neuroimaging studies of practice-related change: fMRI and meta-analytic evidence of a domain-general control network for learning. Brain Res Cogn Brain Res 25(3):607-23.

Cheyne D, Bakhtazad L, Gaetz W (2006): Spatiotemporal mapping of cortical activity accompanying voluntary movements using an event-related beamforming approach. Hum Brain Mapp 27(3):213-29.

Cohen J. (1969). Statistical power analysis for the behavioral sciences. New York: Academic Press.

Conway ARA, Kane MJ, Engle RW (2003): Working memory capacity and its relation to general intelligence. Trends in Cognitive Sciences 7(12):547-552.

Courchesne E, Pierce K (2005): Why the frontal cortex in autism might be talking only to itself: local over-connectivity but long-distance disconnection. Curr Opin Neurobiol 15(2):225-30.

Damoiseaux JS, Greicius MD (2009): Greater than the sum of its parts: a review of studies combining structural connectivity and resting-state functional connectivity. Brain Struct Funct 213(6):525-33.

Daneman M, Carpenter PA (1980): Individual differences in working memory and reading. Journal of Verbal Learning & Verbal Behavior 19:450-466.

Danon L, Diaz-Guilera A, Duch J, Arenas A (2005): Comparing community structure identification. Journal of Statistical Mechanics-Theory and Experiment.

de Araujo DB, Baffa O, Wakai RT (2002): Theta oscillations and human navigation: a magnetoencephalography study. J Cogn Neurosci 14(1):70-8.

de Haan W, Pijnenburg YA, Strijers RL, van der Made Y, van der Flier WM, Scheltens P, Stam CJ (2009): Functional neural network analysis in frontotemporal dementia and Alzheimer's disease using EEG and graph theory. BMC Neurosci 10:101.

de Vico Fallani F, Astolfi L, Cincotti F, Mattia D, la Rocca D, Maksuti E, Salinari S, Babiloni F, Vegso B, Kozmann G, Nagy Z (2009): Evaluation of the brain network organization from EEG signals: a preliminary evidence in stroke patient. Anat Rec (Hoboken) 292(12):2023-31.

De Vico Fallani F, Maglione A, Babiloni F, Mattia D, Astolfi L, Vecchiato G, De Rinaldis A, Salinari S, Pachou E, Micheloyannis S (2010): Cortical network analysis in patients affected by schizophrenia. Brain Topogr 23(2):214-20.

Deary IJ, Penke L, Johnson W (2010): The neuroscience of human intelligence differences. Nat Rev Neurosci 11(3):201-11.

deJonge P, deJong PF (1996): Working memory, intelligence and reading ability in children. Personality and Individual Differences 21(6):1007-1020.

Deuker L, Bullmore ET, Smith M, Christensen S, Nathan PJ, Rockstroh B, Bassett DS (2009): Reproducibility of graph metrics of human brain functional networks. Neuroimage 47(4):1460-8.

Dietz V, Grillner S, Trepp A, Hubli M, Bolliger M (2009): Changes in spinal reflex and locomotor activity after a complete spinal cord injury: a common mechanism? Brain 132(Pt 8):2196-205.

Doppelmayr M, Klimesch W, Hodlmoser K, Sauseng P, Gruber W (2005): Intelligence related upper alpha desynchronization in a semantic memory task. Brain Res Bull 66(2):171-7.

Draganski B, Gaser C, Busch V, Schuierer G, Bogdahn U, May A (2004): Neuroplasticity: changes in grey matter induced by training. Nature 427(6972):311-2.

Draganski B, May A (2008): Training-induced structural changes in the adult human brain. Behav Brain Res 192(1):137-42.

Driemeyer J, Boyke J, Gaser C, Buchel C, May A (2008): Changes in gray matter induced by learning--revisited. PLoS One 3(7):e2669.

Dux PE, Tombu MN, Harrison S, Rogers BP, Tong F, Marois R (2009): Training improves multitasking performance by increasing the speed of information processing in human prefrontal cortex. Neuron 63(1):127-38.

Edgington ES. (1995). Randomization tests. New York: Marcel Dekker.

Engvig A, Fjell AM, Westlye LT, Moberget T, Sundseth O, Larsen VA, Walhovd KB (2010): Effects of memory training on cortical thickness in the elderly. Neuroimage 52(4):1667-76.

Erdös P, Rényi A (1959): On random graphs. Publicationes Mathematicae 6:290-297.

Euler L (1736): Solutio problematis ad geometriam situs pertinentis. Commentarii Academiae Scientiarum Imperialis Petropolitanae 8:128-140.

Evans AC, Collins DL, Mills SR, Brwon ED, Kelly RL, Pters TM. (1993): 3d statistical neuroanatomical models from 305 MRI volumes. In: Processings IEEE Nuclear Science Symposium and Medical Imaging Conference. San Francisco CA. p 1813-1817.

Fisher RA. (1935). The Design of Experiment. New York: Hafner.

Ford JM, Mathalon DH, Whitfield S, Faustman WO, Roth WT (2002): Reduced communication between frontal and temporal lobes during talking in schizophrenia. Biol Psychiatry 51(6):485-92.

Freeman LC (1978): Centrality in social networks: Conceptual clarification. Social Networks 1:215-239.

Fries P (2005): A mechanism for cognitive dynamics: neuronal communication through neuronal coherence. Trends Cogn Sci 9(10):474-80.

Friston KJ (1994): Functional and Effective Connectivity in Neuroimaging: A Synthesis. Human Brain Mapping 2:56-78.

Friston KJ, Frith CD (1995): Schizophrenia: a disconnection syndrome? Clin Neurosci 3(2):89-97.

Friston KJ, Frith CD, Liddle PF, Frackowiak RS (1993): Functional connectivity: the principal-component analysis of large (PET) data sets. J Cereb Blood Flow Metab 13(1):5-14.

Fuchs M, Kastner J, Wagner M, Hawes S, Ebersole JS (2002): A standardized boundary element method volume conductor model. Clinical Neurophysiology 113(5):702-712.

Gerstein GL, Perkel DH (1969): Simultaneously recorded trains of action potentials: analysis and functional interpretation. Science 164(3881):828-30.

Geweke J (1982): Measurement of Linear-Dependence and Feedback between Multiple Time-Series. Journal of the American Statistical Association 77(378):304-313.

Girvan M, Newman ME (2002): Community structure in social and biological networks. Proc Natl Acad Sci U S A 99(12):7821-6.

Golubeva EA. (1980). Individual characteristics of human memory: A psychophysiological study. Moscow.

Gong G, Rosa-Neto P, Carbonell F, Chen ZJ, He Y, Evans AC (2009): Age- and gender-related differences in the cortical anatomical network. J Neurosci 29(50):15684-93.

Gray JR, Chabris CF, Braver TS (2003): Neural mechanisms of general fluid intelligence. Nat Neurosci 6(3):316-22.

Gray JR, Thompson PM (2004): Neurobiology of intelligence: science and ethics. Nat Rev Neurosci 5(6):471-82.

Hagmann P, Cammoun L, Gigandet X, Meuli R, Honey CJ, Wedeen VJ, Sporns O (2008): Mapping the structural core of human cerebral cortex. PLoS Biol 6(7):e159.

Haier RJ, Siegel B, Tang C, Abel L, Buchsbaum MS (1992a): Intelligence and Changes in Regional Cerebral Glucose Metabolic-Rate Following Learning. Intelligence 16(3-4):415-426.

Haier RJ, Siegel BV, Maclachlan A, Soderling E, Lottenberg S, Buchsbaum MS (1992b): Regional Glucose Metabolic Changes after Learning a Complex Visuospatial Motor Task - a Positron Emission Tomographic Study. Brain Research 570(1-2):134-143.

Haier RJ, Siegel BV, Nuechterlein KH, Hazlett E, Wu JC, Paek J, Browning HL, Buchsbaum MS (1988): Cortical Glucose Metabolic-Rate Correlates of

Abstract Reasoning and Attention Studied with Positron Emission Tomography. Intelligence 12(2):199-217.

Haier RJ, White NS, Alkire MT (2003): Individual differences in general intelligence correlate with brain function during nonreasoning tasks. Intelligence 31(5):429-441.

Halford GS, Cowan N, Andrews G (2007): Separating cognitive capacity from knowledge: a new hypothesis. Trends Cogn Sci 11(6):236-42.

Hampson M, Driesen NR, Skudlarski P, Gore JC, Constable RT (2006): Brain connectivity related to working memory performance. J Neurosci 26(51):13338-43.

Hanggi J, Wotruba D, Jancke L (2011): Globally altered structural brain network topology in grapheme-color synesthesia. J Neurosci 31(15):5816-28.

He Y, Chen Z, Evans A (2008): Structural insights into aberrant topological patterns of large-scale cortical networks in Alzheimer's disease. J Neurosci 28(18):4756-66.

He Y, Chen ZJ, Evans AC (2007): Small-world anatomical networks in the human brain revealed by cortical thickness from MRI. Cereb Cortex 17(10):2407-19.

Hebb DO. (1949). The organization of behavior. New York: Wiley & Sons.

Herculano-Houzel S (2009): The human brain in numbers: a linearly scaled-up primate brain. Frontiers in human neuroscience 3:31.

Hilty L, Langer N, Pascual-Marqui R, Boutellier U, Lutz K (2011): Fatigue-induced increase in intracortical communication between mid/anterior insular and motor cortex during cycling exercise. Eur J Neurosci 34(12):2035-42.

Hogan MJ, Swanwick GR, Kaiser J, Rowan M, Lawlor B (2003): Memory-related EEG power and coherence reductions in mild Alzheimer's disease. Int J Psychophysiol 49(2):147-63.

Holm S (1979): A simple sequentially rejective multiple test procedure Scandinavian Journal of Statistics(6):65-70.

Honey CJ, Kotter R, Breakspear M, Sporns O (2007): Network structure of cerebral cortex shapes functional connectivity on multiple time scales. Proc Natl Acad Sci U S A 104(24):10240-5.

Honey CJ, Sporns O, Cammoun L, Gigandet X, Thiran JP, Meuli R, Hagmann P (2009): Predicting human resting-state functional connectivity from structural connectivity. Proc Natl Acad Sci U S A 106(6):2035-40.

Honey CJ, Thivierge JP, Sporns O (2010): Can structure predict function in the human brain? Neuroimage 52(3):766-76.

Horstmann MT, Bialonski S, Noennig N, Mai H, Prusseit J, Wellmer J, Hinrichs H, Lehnertz K (2010): State dependent properties of epileptic brain networks: comparative graph-theoretical analyses of simultaneously recorded EEG and MEG. Clin Neurophysiol 121(2):172-85.

Hsieh LT, Ekstrom AD, Ranganath C (2011): Neural oscillations associated with item and temporal order maintenance in working memory. J Neurosci 31(30):10803-10.

http://www.mathworks.ch/products/matlab/.

Humphries MD, Gurney K (2008): Network 'small-world-ness': a quantitative method for determining canonical network equivalence. PLoS One 3(4):e0002051.

Humphries MD, Gurney K, Prescott TJ (2006): The brainstem reticular formation is a small-world, not scale-free, network. Proc Biol Sci 273(1585):503-11.

Imfeld A, Oechslin MS, Meyer M, Loenneker T, Jancke L (2009): White matter plasticity in the corticospinal tract of musicians: a diffusion tensor imaging study. Neuroimage 46(3):600-7.

Ishai A, Ungerleider LG, Haxby JV (2000): Distributed neural systems for the generation of visual images. Neuron 28(3):979-90.

Ishii R, Shinosaki K, Ukai S, Inouye T, Ishihara T, Yoshimine T, Hirabuki N, Asada H, Kihara T, Robinson SE, Takeda M (1999): Medial prefrontal cortex generates frontal midline theta rhythm. Neuroreport 10(4):675-9.

Jaeggi SM, Buschkuehl M, Jonides J, Perrig WJ (2008): Improving fluid intelligence with training on working memory. Proc Natl Acad Sci U S A 105(19):6829-33.

Jäncke L (2009): The plastic human brain. Restor Neurol Neurosci 27(5):521-38.

Jancke L, Koeneke S, Hoppe A, Rominger C, Hanggi J (2009): The architecture of the golfer's brain. PLoS One 4(3):e4785.

Jancke L, Langer N (2011): A strong parietal hub in the small-world network of coloured-hearing synaesthetes during resting state EEG. J Neuropsychol 5(2):178-202.

Jancke L, Langer N, Hanggi J (2012): Diminished whole-brain but enhanced peri-sylvian connectivity in absolute pitch musicians. J Cogn Neurosci 24(6):1447-61.

Jann K, Koenig T, Dierks T, Boesch C, Federspiel A (2010): Association of individual resting state EEG alpha frequency and cerebral blood flow. Neuroimage 51(1):365-72.

Jausovec N, Jausovec K (2000): Differences in resting EEG related to ability. Brain Topogr 12(3):229-40.

Jausovec N, Jausovec K (2004): Differences in induced brain activity during the performance of learning and working-memory tasks related to intelligence. Brain Cogn 54(1):65-74.

Jausovec N, Jausovec K (2009): Do women see things differently than men do? Neuroimage 45(1):198-207.

Jensen O, Tesche CD (2002): Frontal theta activity in humans increases with memory load in a working memory task. Eur J Neurosci 15(8):1395-9.

Jolles DD, van Buchem MA, Crone EA, Rombouts SA (2011): Functional brain connectivity at rest changes after working memory training. Hum Brain Mapp.

Jonides J (2004): How does practice makes perfect? Nat Neurosci 7(1):10-1.

Jonides J, Lewis RL, Nee DE, Lustig C, Berman MG, Moore KS (2008): The mind and brain of short-term memory. Annual Review of Psychology 59:193-224.

Jonides J, Smith EE, Koeppe RA, Awh E, Minoshima S, Mintun MA (1993): Spatial working memory in humans as revealed by PET. Nature 363(6430):623-5.

Jung RE, Haier RJ (2007): The Parieto-Frontal Integration Theory (P-FIT) of intelligence: converging neuroimaging evidence. Behav Brain Sci 30(2):135-54; discussion 154-87.

Jung RE, Segall JM, Jeremy Bockholt H, Flores RA, Smith SM, Chavez RS, Haier RJ (2009): Neuroanatomy of creativity. Hum Brain Mapp.

Jurcak V, Tsuzuki D, Dan I (2007): 10/20, 10/10, and 10/5 systems revisited: Their validity as relative head-surface-based positioning systems. Neuroimage 34(4):1600-1611.

Kahana MJ, Sekuler R, Caplan JB, Kirschen M, Madsen JR (1999): Human theta oscillations exhibit task dependence during virtual maze navigation. Nature 399(6738):781-4.

Kaiser M, Hilgetag CC (2006): Nonoptimal component placement, but short processing paths, due to long-distance projections in neural systems. PLoS Comput Biol 2(7):e95.

Kaminski MJ, Blinowska KJ (1991): A new method of the description of the information flow in the brain structures. Biological Cybernetics 65:203-210.

Kelly C, Foxe JJ, Garavan H (2006): Patterns of normal human brain plasticity after practice and their implications for neurorehabilitation. Arch Phys Med Rehabil 87(12 Suppl 2):S20-9.

Khateb A, Michel CM, Pegna AJ, Thut G, Landis T, Annoni JM (2001): The time course of semantic category processing in the cerebral hemispheres: an electrophysiological study. Brain Res Cogn Brain Res 10(3):251-64.

Klimesch W (1999): EEG alpha and theta oscillations reflect cognitive and memory performance: a review and analysis. Brain Res Brain Res Rev 29(2-3):169-95.

Klimesch W, Doppelmayr M, Pachinger T, Russegger H (1997a): Event-related desynchronization in the alpha band and the processing of semantic information. Brain Res Cogn Brain Res 6(2):83-94.

Klimesch W, Doppelmayr M, Russegger H, Pachinger T (1996): Theta band power in the human scalp EEG and the encoding of new information. Neuroreport 7(7):1235-40.

Klimesch W, Doppelmayr M, Schimke H, Ripper B (1997b): Theta synchronization and alpha desynchronization in a memory task. Psychophysiology 34(2):169-76.

Klimesch W, Doppelmayr M, Stadler W, Pollhuber D, Sauseng P, Rohm D (2001): Episodic retrieval is reflected by a process specific increase in human electroencephalographic theta activity. Neurosci Lett 302(1):49-52.

Kolb BW, Whishaw IQ (1998): Brain plasticity and behavior. Annual Review of Psychology 49:43-64.

Kondacs A, Szabó M (1999): Long-term intra-individual variability of the background EEG in normals. Clinical neurophysiology : official journal of the International Federation of Clinical Neurophysiology 110(10):1708-16.

Kubicki S, Herrmann WM, Fichte K, Freund G (1979): Reflections on the topics: EEG frequency bands and regulation of vigilance. Pharmakopsychiatr Neuropsychopharmakol 12(2):237-45.

Lancaster JL, Woldorff MG, Parsons LM, Liotti M, Freitas ES, Rainey L, Kochunov PV, Nickerson D, Mikiten SA, Fox PT (2000): Automated Talairach Atlas labels for functional brain mapping. Human Brain Mapping 10(3):120-131.

Langer N, Beeli G, Jancke L (2010): When the sun prickles your nose: an EEG study identifying neural bases of photic sneezing. PLoS One 5(2):e9208.

Langer N, Hanggi J, Muller NA, Simmen HP, Jancke L (2012): Effects of limb immobilization on brain plasticity. Neurology 78(3):182-8.

Langer N, Pedroni A, Gianotti LR, Hanggi J, Knoch D, Jancke L (2011): Functional brain network efficiency predicts intelligence. Hum Brain Mapp.

Laufs H (2008): Endogenous brain oscillations and related networks detected by surface EEG-combined fMRI. Hum Brain Mapp 29(7):762-9.

Lehmann D, Faber PL, Gianotti LR, Kochi K, Pascual-Marqui RD (2006): Coherence and phase locking in the scalp EEG and between LORETA model sources, and microstates as putative mechanisms of brain temporo-spatial functional organization. J Physiol Paris 99(1):29-36.

Li Y, Liu Y, Li J, Qin W, Li K, Yu C, Jiang T (2009): Brain anatomical network and intelligence. PLoS Comput Biol 5(5):e1000395.

Lisman JE, Idiart MA (1995): Storage of 7 +/- 2 short-term memories in oscillatory subcycles. Science 267(5203):1512-5.

Maguire EA, Gadian DG, Johnsrude IS, Good CD, Ashburner J, Frackowiak RS, Frith CD (2000): Navigation-related structural change in the hippocampi of taxi drivers. Proc Natl Acad Sci U S A 97(8):4398-403.

Manly BFJ. (1997). Randomization, bootstrap, and Monte-Carlo methods in biology. London: Chapman and Hall.

Martin A, Wiggs CL, Ungerleider LG, Haxby JV (1996): Neural correlates of category-specific knowledge. Nature 379(6566):649-52.

Maslov S, Sneppen K (2002): Specificity and stability in topology of protein networks. Science 296(5569):910-3.

Mazziotta J, Toga A, Evans A, Fox P, Lancaster J, Zilles K, Woods R, Paus T, Simpson G, Pike B, Holmes C, Collins L, Thompson P, MacDonald D, Iacoboni M, Schormann T, Amunts K, Palomero-Gallagher N, Geyer S, Parsons L, Narr K, Kabani N, Le Goualher G, Boomsma D, Cannon T, Kawashima R, Mazoyer B (2001): A probabilistic atlas and reference system for the human brain: International Consortium for Brain Mapping (ICBM). Philosophical Transactions of the Royal Society B-Biological Sciences 356(1412):1293-1322.

McIntosh AR, Rajah MN, Lobaugh NJ (2003): Functional connectivity of the medial temporal lobe relates to learning and awareness. J Neurosci 23(16):6520-8.

Meltzer JA, Zaveri HP, Goncharova, II, Distasio MM, Papademetris X, Spencer SS, Spencer DD, Constable RT (2008): Effects of working memory load on oscillatory power in human intracranial EEG. Cereb Cortex 18(8):1843-55.

Merzenich MM, Kaas JH, Wall J, Nelson RJ, Sur M, Felleman D (1983): Topographic reorganization of somatosensory cortical areas 3b and 1 in adult monkeys following restricted deafferentation. Neuroscience 8(1):33-55.

Meunier D, Achard S, Morcom A, Bullmore E (2009): Age-related changes in modular organization of human brain functional networks. Neuroimage 44(3):715-23.

Michel CM, Koenig T, Brandeis D, Gianotti LR, Wackermann J. (2009). Electrical Neuroimaging. Cambridge: Cambridge University Press.

Micheloyannis S, Pachou E, Stam CJ, Breakspear M, Bitsios P, Vourkas M, Erimaki S, Zervakis M (2006a): Small-world networks and disturbed functional connectivity in schizophrenia. Schizophr Res 87(1-3):60-6.

Micheloyannis S, Pachou E, Stam CJ, Vourkas M, Erimaki S, Tsirka V (2006b): Using graph theoretical analysis of multi channel EEG to evaluate the neural efficiency hypothesis. Neurosci Lett 402(3):273-7.

Micheloyannis S, Vourkas M, Tsirka V, Karakonstantaki E, Kanatsouli K, Stam CJ (2009): The influence of ageing on complex brain networks: a graph theoretical analysis. Hum Brain Mapp 30(1):200-8.

Miller EK, Cohen JD (2001): An integrative theory of prefrontal cortex function. Annu Rev Neurosci 24:167-202.

Miller GA, Galanter E, Pribram KH. (1960). Plans and the Structure of Behavior. New York: Holt, Rinehart & Winston.

Miller R. (1991). Cortico-Hipocampal Interplay and the Representation of Contexts in the Brain. Berlin: Springer.

Monsell S (2003): Task switching. Trends in Cognitive Sciences 7(3):134-140.

Moody DE (2009): Can intelligence be increased by training on a task of working memory? Intelligence 37(4):327-328.

Mulert C, Jager L, Schmitt R, Bussfeld P, Pogarell O, Moller HJ, Juckel G, Hegerl U (2004): Integration of fMRI and simultaneous EEG: towards a comprehensive understanding of localization and time-course of brain activity in target detection. Neuroimage 22(1):83-94.

Murias M, Webb SJ, Greenson J, Dawson G (2007): Resting state cortical connectivity reflected in EEG coherence in individuals with autism. Biol Psychiatry 62(3):270-3.

Näpflin M, Wildi M, Sarnthein J (2007): Test-retest reliability of resting EEG spectra validates a statistical signature of persons. Clinical neurophysiology : official journal of the International Federation of Clinical Neurophysiology 118(11):2519-24.

Neisser U, Boodoo G, Bouchard TJ, Boykin AW, Brody N, Ceci SJ, Halpern DF, Loehlin JC, Perloff R, Sternberg RJ, Urbina S (1996): Intelligence: Knowns and unknowns. American Psychologist 51(2):77-101.

Neubauer AC, Fink A (2009): Intelligence and neural efficiency. Neurosci Biobehav Rev 33(7):1004-23.

Neubauer AC, Fink A, Schrausser DG (2002): Intelligence and neural efficiency: The influence of task content and sex on the brain-IQ relationship. Intelligence 30(6):515-536.

Neubauer AC, Grabner RH, Freudenthaler HH, Beckmann JF, Guthke H (2004): Intelligence and individual differences in becoming neurally efficient. Acta Psychologica 116(1):55-74.

Newman ME (2004): Analysis of weighted networks. Phys Rev E Stat Nonlin Soft Matter Phys 70(5 Pt 2):056131.

Newman ME (2006): Modularity and community structure in networks. Proc Natl Acad Sci U S A 103(23):8577-82.

Nichols TE, Holmes AP (2002): Nonparametric permutation tests for functional neuroimaging: A primer with examples. Human Brain Mapping 15(1):1-25.

Oberauer K, Süss H-M, Wilhelm O, Sander N (2007): Individual differences in working memory capacity and reasoning ability. In: Conway C, Jarrold MJ, Kane J, Miyake A, Towse N, editors. Variation in working memory. New York: Oxford University Press.

Oberauer K, Suss HM, Schulze R, Wilhelm O, Wittmann WW (2000): Working memory capacity - facets of a cognitive ability construct. Personality and Individual Differences 29(6):1017-1045.

Oberauer K, Suss HM, Wilhelm O, Wittman WW (2003): The multiple faces of working memory: Storage, processing, supervision, and coordination. Intelligence 31(2):167-193.

Oken BS, Flegal K, Zajdel D, Kishiyama S, Haas M, Peters D (2008): Expectancy effect: Impact of pill administration on cognitive performance in healthy seniors. Journal of Clinical and Experimental Neuropsychology 30(1):7-17.

Olesen PJ, Westerberg H, Klingberg T (2004): Increased prefrontal and parietal activity after training of working memory. Nat Neurosci 7(1):75-9.

Oliveri M, Turriziani P, Carlesimo GA, Koch G, Tomaiuolo F, Panella M, Caltagirone C (2001): Parieto-frontal interactions in visual-object and visual-spatial working memory: evidence from transcranial magnetic stimulation. Cereb Cortex 11(7):606-18.

Onton J, Delorme A, Makeig S (2005): Frontal midline EEG dynamics during working memory. Neuroimage 27(2):341-56.

Oostenveld R, Praamstra P (2001): The five percent electrode system for high-resolution EEG and ERP measurements. Clinical Neurophysiology 112(4):713-719.

Opsahl T. (2009): Structure and evolution of weighted networks. London: University of London (Queen Mary College).

Opsahl T, Colizza V, Panzarasa P, Ramasco JJ (2008): Prominence and Control: The Weighted Rich-Club Effect. Physical Review Letters 101(16):-.

Opsahl T, Panzarasa P (2009): Clustering in weighted networks. Social Networks 31(2):155-163.

Owen AM, Evans AC, Petrides M (1996): Evidence for a two-stage model of spatial working memory processing within the lateral frontal cortex: a positron emission tomography study. Cereb Cortex 6(1):31-8.

Owen AM, McMillan KM, Laird AR, Bullmore E (2005): N-back working memory paradigm: a meta-analysis of normative functional neuroimaging studies. Hum Brain Mapp 25(1):46-59.

Palva JM, Monto S, Kulashekhar S, Palva S (2010a): Neuronal synchrony reveals working memory networks and predicts individual memory capacity. Proc Natl Acad Sci U S A 107(16):7580-5.

Palva S, Monto S, Palva JM (2010b): Graph properties of synchronized cortical networks during visual working memory maintenance. Neuroimage 49(4):3257-68.

Pascual-Leone A, Amedi A, Fregni F, Merabet LB (2005): The plastic human brain cortex. Annu Rev Neurosci 28:377-401.

Pascual-Marqui RD (2002): Standardized low-resolution brain electromagnetic tomography (sLORETA): technical details. Methods Find Exp Clin Pharmacol 24 Suppl D:5-12.

Pascual-Marqui RD. (2007a): Discrete, 3D distributed, linear imaging methods of electrical neuronal activity. Part 1: exact, zerror error localization. .

Pascual-Marqui RD. (2007b): Instantaneous and lagged measurements of linear and nonlinear dependence between groups of multivariate times series: frequency decomposition. arXiv:0711.1455[stat.ME].

Perrin F, Pernier J, Bertrand O, Giard MH, Echallier JF (1987): Mapping of scalp potentials by surface spline interpolation. Electroencephalogr Clin Neurophysiol 66(1):75-81.

Petersen SE, van Mier H, Fiez JA, Raichle ME (1998): The effects of practice on the functional anatomy of task performance. Proc Natl Acad Sci U S A 95(3):853-60.

Pickering SJ. (2006). Working Memory and Education. Oxford: Elsevier.

Pitman EJG (1937): Significance tests which may be applied to samples form any population. Royal Statistical Society Supplement 4:119-130 & 225-232.

Pitman EJG (1938): Significance tests which may be applied to samples from any populations. Biometrika 30:322-335.

Pizzagalli D, Lehmann D, Koenig T, Regard M, Pascual-Marqui RD (2000): Face-elicited ERPs and affective attitude: brain electric microstate and tomography analyses. Clin Neurophysiol 111(3):521-31.

Polania R, Paulus W, Nitsche MA (2011): Noninvasively Decoding the Contents of Visual Working Memory in the Human Prefrontal Cortex within High-gamma Oscillatory Patterns. J Cogn Neurosci 24(2):304-14.

Poldrack RA (2000): Imaging brain plasticity: conceptual and methodological issues--a theoretical review. Neuroimage 12(1):1-13.

Raghavachari S, Kahana MJ, Rizzuto DS, Caplan JB, Kirschen MP, Bourgeois B, Madsen JR, Lisman JE (2001): Gating of human theta oscillations by a working memory task. J Neurosci 21(9):3175-83.

Raghavachari S, Lisman JE, Tully M, Madsen JR, Bromfield EB, Kahana MJ (2006): Theta oscillations in human cortex during a working-memory task: evidence for local generators. J Neurophysiol 95(3):1630-8.

Raj A, Mueller SG, Young K, Laxer KD, Weiner M (2010): Network-level analysis of cortical thickness of the epileptic brain. Neuroimage 52(4):1302-13.

Raven J, Raven, J.C., Court, J.H. (2003). Manual for Raven's Progressive Matrices and Vocabulary Scales. Section1: General Overview. San Antonia: Harcourt Assessment.

Ravizza SM, Delgado MR, Chein JM, Becker JT, Fiez JA (2004): Functional dissociations within the inferior parietal cortex in verbal working memory. Neuroimage 22(2):562-73.

Reijneveld JC, Ponten SC, Berendse HW, Stam CJ (2007): The application of graph theoretical analysis to complex networks in the brain. Clinical neurophysiology : official journal of the International Federation of Clinical Neurophysiology 118(11):2317-31.

Rounis E, Stephan KE, Lee L, Siebner HR, Pesenti A, Friston KJ, Rothwell JC, Frackowiak RS (2006): Acute changes in frontoparietal activity after

repetitive transcranial magnetic stimulation over the dorsolateral prefrontal cortex in a cued reaction time task. J Neurosci 26(38):9629-38.

Rubinov M, Knock SA, Stam CJ, Micheloyannis S, Harris AW, Williams LM, Breakspear M (2009): Small-world properties of nonlinear brain activity in schizophrenia. Hum Brain Mapp 30(2):403-16.

Rubinov M, Sporns O (2010): Complex network measures of brain connectivity: uses and interpretations. Neuroimage 52(3):1059-69.

Rykhlevskaia E, Uddin LQ, Kondos L, Menon V (2009): Neuroanatomical correlates of developmental dyscalculia: combined evidence from morphometry and tractography. Front Hum Neurosci 3:51.

Rypma B, Berger JS, Prabhakaran V, Bly BM, Kimberg DY, Biswal BB, D'Esposito M (2006): Neural correlates of cognitive efficiency. Neuroimage 33(3):969-79.

Salvador R, Suckling J, Coleman MR, Pickard JD, Menon D, Bullmore E (2005): Neurophysiological architecture of functional magnetic resonance images of human brain. Cereb Cortex 15(9):1332-42.

Sammer G, Blecker C, Gebhardt H, Bischoff M, Stark R, Morgen K, Vaitl D (2007): Relationship between regional hemodynamic activity and simultaneously recorded EEG-theta associated with mental arithmetic-induced workload. Hum Brain Mapp 28(8):793-803.

Sarnthein J, Petsche H, Rappelsberger P, Shaw GL, von Stein A (1998): Synchronization between prefrontal and posterior association cortex during human working memory. Proc Natl Acad Sci U S A 95(12):7092-6.

Sauseng P, Griesmayr B, Freunberger R, Klimesch W (2010): Control mechanisms in working memory: a possible function of EEG theta oscillations. Neurosci Biobehav Rev 34(7):1015-22.

Sauseng P, Klimesch W, Schabus M, Doppelmayr M (2005): Fronto-parietal EEG coherence in theta and upper alpha reflect central executive functions of working memory. Int J Psychophysiol 57(2):97-103.

Schlaug G, Marchina S, Norton A (2009): Evidence for plasticity in white-matter tracts of patients with chronic Broca's aphasia undergoing intense intonation-based speech therapy. Ann N Y Acad Sci 1169:385-94.

Schneiders JA, Opitz B, Krick CM, Mecklinger A (2011): Separating intra-modal and across-modal training effects in visual working memory: an fMRI investigation. Cereb Cortex 21(11):2555-64.

Scholz J, Klein MC, Behrens TE, Johansen-Berg H (2009): Training induces changes in white-matter architecture. Nat Neurosci 12(11):1370-1.

Seeck M, Lazeyras F, Michel CM, Blanke O, Gericke CA, Ives J, Delavelle J, Golay X, Haenggeli CA, de Tribolet N, Landis T (1998): Non-invasive epileptic focus localization using EEG-triggered functional MRI and electromagnetic tomography. Electroencephalogr Clin Neurophysiol 106(6):508-12.

Shaffer JP (1995): Mutiple hypothesis testing. Annual Review of Psychology(46):561-584.

Shah P, Miyake A (1999): Models of working memory: an introduction. Models of Working Memory: mechanism of Active Maintenance and Executive Control. New York: Cambridge University Press.

Sinai A, Pratt H (2003): High-resolution time course of hemispheric dominance revealed by low-resolution electromagnetic tomography. Clin Neurophysiol 114(7):1181-8.

Singer W (1999): Neuronal synchrony: a versatile code for the definition of relations? Neuron 24(1):49-65, 111-25.

Singer W, Gray CM (1995): Visual feature integration and the temporal correlation hypothesis. Annu Rev Neurosci 18:555-86.

Skudlarski P, Jagannathan K, Calhoun VD, Hampson M, Skudlarska BA, Pearlson G (2008): Measuring brain connectivity: diffusion tensor imaging validates resting state temporal correlations. Neuroimage 43(3):554-61.

Smit DJ, Stam CJ, Posthuma D, Boomsma DI, de Geus EJ (2008): Heritability of "small-world" networks in the brain: a graph theoretical analysis of resting-state EEG functional connectivity. Hum Brain Mapp 29(12):1368-78.

Smith EE, Jonides J (1998): Neuroimaging analyses of human working memory. Proc Natl Acad Sci U S A 95(20):12061-8.

Smith SM, Miller KL, Salimi-Khorshidi G, Webster M, Beckmann CF, Nichols TE, Ramsey JD, Woolrich MW (2011): Network modelling methods for FMRI. Neuroimage 54(2):875-891.

Spearman C (1904): General intelligence, objectively determined and measured. American Journal of Psychology 15:201-293.

Sporns O. (2010). Networks of the Brain: MIT Press.

Sporns O, Chialvo DR, Kaiser M, Hilgetag CC (2004): Organization, development and function of complex brain networks. Trends Cogn Sci 8(9):418-25.

Sporns O, Kotter R (2004): Motifs in brain networks. PLoS Biol 2(11):e369.

Sporns O, Zwi JD (2004): The small world of the cerebral cortex. Neuroinformatics 2(2):145-62.

Stam CJ (2004): Functional connectivity patterns of human magnetoencephalographic recordings: a 'small-world' network? Neurosci Lett 355(1-2):25-8.

Stam CJ (2010): Use of magnetoencephalography (MEG) to study functional brain networks in neurodegenerative disorders. J Neurol Sci 289(1-2):128-34.

Stam CJ, de Haan W, Daffertshofer A, Jones BF, Manshanden I, van Cappellen van Walsum AM, Montez T, Verbunt JP, de Munck JC, van Dijk BW, Berendse HW, Scheltens P (2009): Graph theoretical analysis of magnetoencephalographic functional connectivity in Alzheimer's disease. Brain 132(Pt 1):213-24.

Stam CJ, Jones BF, Nolte G, Breakspear M, Scheltens P (2007a): Small-world networks and functional connectivity in Alzheimer's disease. Cereb Cortex 17(1):92-9.

Stam CJ, Nolte G, Daffertshofer A (2007b): Phase lag index: assessment of functional connectivity from multi channel EEG and MEG with diminished bias from common sources. Hum Brain Mapp 28(11):1178-93.

Stam CJ, Reijneveld JC (2007): Graph theoretical analysis of complex networks in the brain. Nonlinear Biomed Phys 1(1):3.

Steriade M, Jones E, Llinas RR. (1990). Thalamic Oscillations and Signaling. New York: Wiley.

Strogatz SH (2001): Exploring complex networks. Nature 410(6825):268-76.

Supekar K, Menon V, Rubin D, Musen M, Greicius MD (2008): Network analysis of intrinsic functional brain connectivity in Alzheimer's disease. PLoS Comput Biol 4(6):e1000100.

Swanson LW. (2003). Brain Architecture. Oxford: Oxford University Press.

Tachibana K, Suzuki K, Mori E, Miura N, Kawashima R, Horie K, Sato S, Tanji J, Mushiake H (2009): Neural activity in the human brain signals logical rule identification. J Neurophysiol 102(3):1526-37.

Takahashi T, Murata T, Hamada T, Omori M, Kosaka H, Kikuchi M, Yoshida H, Wada Y (2005): Changes in EEG and autonomic nervous activity during meditation and their association with personality traits. Int J Psychophysiol 55(2):199-207.

Takeuchi H, Taki Y, Hashizume H, Sassa Y, Nagase T, Nouchi R, Kawashima R (2011): Effects of training of processing speed on neural systems. J Neurosci 31(34):12139-48.

Thatcher RW, North D, Biver C (2007): Intelligence and EEG current density using low-resolution electromagnetic tomography (LORETA). Hum Brain Mapp 28(2):118-33.

Thatcher RW, North DM, Biver CJ (2008): Intelligence and EEG phase reset: a two compartmental model of phase shift and lock. Neuroimage 42(4):1639-53.

Thorndike EL (1921): Intelligence and its measurement: A symposium. Journal of Educational Psychology 12:124-127.

Tsapkini K, Rapp B (2009): The orthography-specific functions of the left fusiform gyrus: Evidence of modality and category specificity. Cortex.

Uchida S, Maehara T, Hirai N, Kawai K, Shimizu H (2003): Theta oscillation in the anterior cingulate and beta-1 oscillation in the medial temporal cortices: a human case report. J Clin Neurosci 10(3):371-4.

Uhlhaas PJ, Singer W (2006): Neural synchrony in brain disorders: relevance for cognitive dysfunctions and pathophysiology. Neuron 52(1):155-68.

van den Heuvel MP, Stam CJ, Kahn RS, Hulshoff Pol HE (2009): Efficiency of Functional Brain Networks and Intellectual Performance. J. Neurosci. 29(23):7619-7624.

Varela F, Lachaux JP, Rodriguez E, Martinerie J (2001): The brainweb: phase synchronization and large-scale integration. Nat Rev Neurosci 2(4):229-39.

Wang C, Ulbert I, Schomer DL, Marinkovic K, Halgren E (2005): Responses of human anterior cingulate cortex microdomains to error detection, conflict monitoring, stimulus-response mapping, familiarity, and orienting. J Neurosci 25(3):604-13.

Wasserman S, Faust K. (1994). Social Network Analysis. Cambridge, MA: Cambridge University Press.

Watts DJ, Strogatz SH (1998): Collective dynamics of 'small-world' networks. Nature 393(6684):440-2.

Wechsler D. (1939). The Measurement of Adult Intelligence. Baltimore (MD): Williams & Witkins.

Winterer G, Coppola R, Egan MF, Goldberg TE, Weinberger DR (2003): Functional and effective frontotemporal connectivity and genetic risk for schizophrenia. Biol Psychiatry 54(11):1181-92.

Womelsdorf T, Schoffelen JM, Oostenveld R, Singer W, Desimone R, Engel AK, Fries P (2007): Modulation of neuronal interactions through neuronal synchronization. Science 316(5831):1609-12.

Wong ACN, Palmeri TJ, Rogers BP, Gore JC, Gauthier I (2009): Beyond Shape: How You Learn about Objects Affects How They Are Represented in Visual Cortex. PLoS One 4(12):e8405.

Worrell GA, Lagerlund TD, Sharbrough FW, Brinkmann BH, Busacker NE, Cicora KM, O'Brien TJ (2000): Localization of the epileptic focus by low-resolution electromagnetic tomography in patients with a lesion demonstrated by MRI. Brain Topogr 12(4):273-82.

Yu S, Huang D, Singer W, Nikolic D (2008): A small world of neuronal synchrony. Cereb Cortex 18(12):2891-901.

Zaehle T, Frund I, Schadow J, Tharig S, Schoenfeld MA, Herrmann CS (2009): Inter- and intra-individual covariations of hemodynamic and oscillatory gamma responses in the human cortex. Front Hum Neurosci 3:8.

Zalesky A, Fornito A, Harding IH, Cocchi L, Yucel M, Pantelis C, Bullmore ET (2010): Whole-brain anatomical networks: does the choice of nodes matter? Neuroimage 50(3):970-83.

Zarei M, Johansen-Berg H, Jenkinson M, Ciccarelli O, Thompson AJ, Matthews PM (2007): Two-dimensional population map of cortical connections in the human internal capsule. J Magn Reson Imaging 25(1):48-54.

7. Curriculum Vitae

Curriculum Vitae
Nicolas Langer

PERSONAL

Address	Bäckerstrasse 30, 8004 Zürich, Switzerland
Date and place of birth	16. November 1983 in Zurich (CH)
Nationality	Swiss

CURRENT POSITION

Position	Research Assistant
Address	Division of Neuropsychology, Institute of Psychology University of Zurich (Prof. Dr. rer. nat. Lutz Jäncke) Binzmuehlestrasse 14/25. CH-8050 Zurich, Switzerland Tel: +41 (0)44 635 73 96 Fax: +41 (0)44 635 73 96 Email: n.langer@psychologie.uzh.ch

EDUCATION

08/2008 – 02/2012	Ph.D. studies in Neuropsychology and Neuroscience (University of Zurich)
03/2006 – 05/2008	MSc in Science (University of Zurich) Master thesis: »Neural Plasticity in Sports« (summa cum laude) Supervision: Prof. Lutz Jäncke

10/2002 – 02/2006	Bsc in Science (University of Zurich)
08/2008 – 02/2012	International Ph.D. Program in Neuroscience (www.neuroscience.ethz.ch)
08/2007 – 08/2008	University of Zurich, Psychological Institute Department Neuropsychology Research Assistant
06/2006 – 11/2006	Charité Berlin Clinical Internship at the Department of Neurology and Psychosomatic Medicine
08/2004 – 05/2005	University of Zurich, Psychological Institute Department Clinical Psychology, Prof. Heinrichs Research Assistant
05/2002 – 01/2008	Bildkom GmbH Zurich statistics and data analysis

PUBLICATIONS

Articles with peer-review

Langer, N., Hänggi, J., Müller, A., Simmen, H.P., Jäncke, L. (2012). The effects of limb immobilization on brain plasticity. *Neurology*. 78 (3): 182-188.

Langer, N., Pedroni, A., Gianotti, L.R.R., Knoch, D., Hänggi, J., Jäncke, L. (2011). Functional Brain Network Efficiency Predicts Intelligence. *Human Brain Mapping*. doi: 10.1002/hbm.21297.

Langer, N., Beeli, G., Jäncke, L. (2010). When the Sun Prickles your Nose: An EEG Study. *PLoS ONE*. 5(2): e9208.

Pedroni, A., Langer, N., König, T., Allemand, M., Jäncke, L. (2011). Electroencephalographic Topography-Measures of Experienced Utility. *Journal of Neuroscience*. 31 (29): 10474-10480.

Jäncke, L., Langer, N. (2011) A strong parietal hub in the small-wolrd network of coloured-hearing synaesthetes during resting state EEG. *Journal of Neuropsychology*. 5 (2): 178-202.

Ott, C., Langer, N., Jäncke, L., Meyer, M. (2011). Processing of voiced and unvoiced acoustic stimuli in musicians. *Frontiers Psychology*. 2: 195.

Hilty, L., Langer, N., Pascual-Marqui, R., Boutellier, U., Lutz, K. (2011). Fatigue-induced increase in intracortical communication between mid/anterior insular and motor cortex during cycling exercise. *European Journal of Neuroscience*. 34 (12): 2035-2042.

Hänggi, J., Langer, N., Jäncke, L. (2012). Small-world topology in musicians with absolute pitch. *Journal of Cognitive Neuroscience* (in review)

Langer, N., von Bastian, C., Oberauer, K., Jäncke, L. (2012). Training of Small-World Networks in the Human Brain. In preparation.

Langer, N., Jäncke, L. (2012). Duration and Transition of resting state EEG microstates in synesthesia. In preparation.

Langer, N., Pedroni, A., Jäncke, L. (2012). The problem of thresholding in small-world network analysis. In preparation.

Abstracts

Langer, N., von Bastian, C., Oberauer, K., Jäncke, L. (2012). Training of Small-World Networks in the Human Brain. Alpine Brain Imaging Meeting, Champery, Switzerland.

Langer, N., Pedroni, A., Gianotti, L., Hänggi, J., Knoch, D., Jäncke, L. (2010). Functional Brain Network Efficiency Predicts Intelligence. Human Brain Mapping, Quebec, Canada.

Langer, N., Pedroni, A., Jäncke, L. (2011). The Problem of Thresholding in Small-World Network Analysis. Alpine Brain Imaging Meeting, Champery, Switzerland.

Langer, N., Pedroni, A., Gianotti, L., Hänggi, J., Knoch, D., Jäncke, L. (2010). Functional Brain Network Efficiency Predicts Intelligence. ZNZ Symposium, Zurich, Switzerland.

Langer, N., Pedroni, A., Gianotti, L., Hänggi, J., Knoch, D., Jäncke, L. (2010). Functional Brain Network Efficiency Predicts Intelligence. Alpine Brain Imaging Meeting, Champery, Switzerland.

Langer, N., Hänggi, J., Gianotti, L., Knoch, D., Jäncke, L. (2009). Neural correlates of visuo-spatial abilities (general fluid intelligence). ZNZ Symposium, Zurich, Switzerland.

Langer, N., Hänggi, J., Köneke, S., Brütsch, K., Jäncke, L. (2008). Brain Plasticity in Sports. ZNZ Symposium, Zurich, Switzerland.

Langer, N., Hänggi, J., Köneke, S., Brütsch, K., Jäncke, L. (2007). Training induced structural plasticity in professional handball players. (LiDoKo), Zurich, Switzerland.

Langer, N., Beeli, G., Jäncke, L. (2007). ACHOO syndrome- The Photic Sneeze Reflex (LiDoKo), Zurich, Switzerland.

RESEARCH SKILLS

Extensive knowledge in:

Matlab, SPSS, SPM, Freesurfer, FSL, Brainvision Analyzer, sLORETA, Cartool, tnet-software, Brain Connectivity Toolbox, Electrical Geodesics EEG recording hardware, MRI acquisition on Philips MR-Scanner.

Knowledge of Presentation, E-Prime, EEGlab, R-statistics.

SKILLS

Computer Skills	Microsoft Office (Word, Excel, PowerPoint), Photoshop, Illustrator, Final Cut Pro, adept to Mac & PC hard- and software.
Languages	German, English, French, Czech

LECTURES

Seminar: Affective Neuroscience

Workshop: Imaging methods in neuropsychology
Workshop: Implications of resting-state EEG

Supervision of M.Sc. theses:

“How EEG-signal changes as a function of speech perception” (Gmür, Cornel)

“Speech processing in musicians with and without absolute pitch” (Spirig, Nadine)

“Neural Correlates of Tinnitus. An Investigation with EEG” (Lüthi, Mathias)

“Alpha and Theta differences in older adults during prospective memory” (Fallegger, Irene)

“Spatio-temporal correlates of visual perception. A EEG study” (Grämiger, Linus)

"Training of Small-World Networks in the Human Brain" (Wirz, Helen)

FURTHER EXPERIENCES

08/2010 – 05/2011	Charity work in supervised residential group for homeless people
01/2002 – 08/2006	Part-time tennis and snowboard instructor for children
02/2003 – present	Member of the ice hockey team of the University Zurich
10/1990 – 3/2001	Member of competitive ice hockey team (Kloten Flyers)

REFERENCES

Lutz Jäncke	Prof. Dr. rer. nat. Lutz Jäncke University of Zurich, Department Neuropsychology Tel.: +41 44 635 74 01 l.jaencke@psychologie.uzh.ch
Christoph Michel	Prof. Dr. rer. nat. Christoph Michel University of Geneva, Functional Brain Mapping Lab Tel.: +41 22 379 54 57 christoph.michel@unige.ch
Andreas Pedroni	Andreas Pedroni, Ph.D. in Neuropsychology University of Basel, Social and Affective Neuroscience Tel.: +41 61 267 02 84 andreas.pedroni@unibas.ch

8. Appendix

Measure	Binary and undirected definitions	Weighted definitions
Basic concepts and measures	N is the set of all nodes in the network, and n is the number of nodes. L is the set of all links in the network, and l is the number of links. (i,j) is a link between nodes i and j (i,j ∈ N) aij is the connection status between i and j: aij = 1 when link (i, j) exists (when i and j are neighbors); aij = 0 otherwise (aii = 0 for all i). The number of links is computed as l =Σi,j∈N aij (to avoid ambiguity with directed links each undirected link is counted twice, as aij and as aji).	Links (i, j) are associated with connection weights w_{ij} Henceforth, we assume that weights are normalized, such that $0 \le w_{ij} \le 1$ for all i and j. l^w is the sum of all weights in the network, computed as $l^w = \sum_{i,j \in N} wij$. Directed links (i,j) are ordered from i to j. Consequently, in directed networks a_{ij} does not necessarily equal a_{ji}.
Degree: number of links connected a node	Degree of a node i, $k_i = \sum_{j \in N} aij$.	Weighted degree of i, $k_i^w = \sum_{j \in N} wij$.
Shortest path length: a basic measure for integration	Shortest path length (distance) between nodes i and j, $dij = \sum_{a_{uv} \in g_{i \leftrightarrow j}} a_{uv}$, where $g_{i \leftrightarrow j}$ is the shortest path (geodesic) between i and j. Note that $d_{ij} = \infty$ for all disconnected pairs i,j.	Shortest weighted path length between i and j, $d_{ij}^w = \sum_{a_{uv} \in g_{i \leftrightarrow j}^w} f(w_{uv})$, where f is a map (e.g. an inverse) from weighted to length and is the shortest weighted path between i and j
Number of triangles: a basic measure for segregation	Number of triangles around a node i, $t_i = \frac{1}{2} \sum_{j,h \in N} a_{ij} a_{ih} a_{jh}$.	Weighted geometric mean of triangles around i, $t_i^w = \frac{1}{2} \sum_{j,h \in N} (w_{ij} w_{ih} w_{jh})^{1/3}$.
Measure of integration Characteristic path length	Characteristic path length of the network (Watts and Strogatz, 1998), $L = \frac{1}{n} \sum_{i \in N} L_i = \frac{1}{n} \sum_{i \in N} \frac{\sum_{j \in N, j \neq i} d_{ij}}{n-1}$, where L_i is the average distance between node i and all other nodes.	Weighted characteristic path length $L^w = \frac{1}{n} \sum_{i \in N} \frac{\sum_{j \in N, j \neq i} d_{ij}^w}{n-1}$.
Measure of segregation Clustering coefficient	Clustering Coefficient of the network (Watts and Strogatz, 1998) $C = \frac{1}{n} \sum_{i \in N} C_i = \frac{1}{n} \sum_{i \in N} \frac{2t_i}{k_i(k_i-1)}$, where C_i is the clustering coefficient of node i ($C_i = 0$ for $k_i<2$).	Weigthed clustering coefficient (Onnela et al., 2005), $C^w = \frac{1}{n} \sum_{i \in N} \frac{2t_i^w}{k_i(k_i-1)}$, see Saramaki et al., (2007) for other variants
Transitivity	Transitivity of the network (e.g., Newman, 2003) $T = \frac{\sum_{i \in N} 2t_i}{\sum_{i \in N} k_i(k_i-1)}$. Note that transitivity is not defined for individual nodes.	Weighted transitivity $T^w = \frac{\sum_{i \in N} 2t_i^w}{\sum_{i \in N} k_i(k_i-1)}$.
Modularity	Modularity of the network (Newman, 2004), $Q = \sum_{u \in M} \left[e_{uu} - \left(\sum_{v \in M} e_{uv} \right)^2 \right]$,	Weighted modularity (Newman, 2004), $Q^w = \frac{1}{l^w} \sum_{i,j \in M} \left[w_{ij} - \frac{k_i^w k_j^w}{l^w} \right] \delta_{m_i, m_j}$,
Measures of centrality Closeness centrality	Closeness centrality of node i (Freemann, 1978) $L_i^{-1} = \frac{n-1}{\sum_{j \in N, j \neq i} d_{ij}}$.	Weighted closeness centrality $\left(L_i^w\right)^{-1} = \frac{n-1}{\sum_{j \in N, j \neq i} d_{ij}^w}$.
Betweenness centrality	Betweenness centrality of node i (Freemann, 1978) $b_i = \frac{1}{(n-1)(n-2)} \sum_{h,j \in N, h \neq j, h \neq i, j \neq i} \frac{\rho_{hj}(i)}{\rho_{hj}}$, where ρ_{hj} is the number of shortest paths between h and j, and $\rho_{hj}(i)$ is the number of shortest paths between h and j that pass through i	Betweenness centrality is computed equivalently on weighted networks provided that path lengths are computed on respective weighted paths.
Measure of network Small-worldness	Network small-worldness (Humphries and Gurney, 2009) $S = \frac{C / C_{rand}}{L / L_{rand}}$, where C and C rand are the clustering coefficients, and L and L rand are the characteristic path length of the respective tested network and a random network. Small World networks often have S >> 1.	Weighted network small-worldness, $S_w = \frac{C^w / C^w_{rand}}{L^w / L^w_{rand}}$,